REGIONAL GEOLOGY, GROUNDWATER FLOW SYSTEMS AND SLOPE STABILITY

by

ROBERT A.L. HODGE
B.A.Sc., University of British Columbia, 1972

A THESIS SUBMITTED IN PARTIAL FULFILLMENT OF
THE REQUIREMENTS FOR THE DEGREE OF
MASTER OF APPLIED SCIENCE

in

THE FACULTY OF GRADUATE STUDIES
Department of Geological Sciences
The University of British Columbia

We accept this thesis as conforming
to the required standard

THE UNIVERSITY OF BRITISH COLUMBIA
June, 1976

© Robert A.L. Hodge, 1976

In presenting this thesis in partial fulfilment of the requirements for an advanced degree at the University of British Columbia, I agree that the Library shall make it freely available for reference and study. I further agree that permission for extensive copying of this thesis for scholarly purposes may be granted by the Head of my Department or by his representatives. It is understood that copying or publication of this thesis for financial gain shall not be allowed without my written permission.

Department of Geological Sciences

The University of British Columbia
2075 Wesbrook Place
Vancouver, Canada
V6T 1W5

Date June 25, 1976

R 74-446 C

ABSTRACT

The purpose of this thesis is to show, using computer simulation of flow systems in a variety of hypothetical slopes, how different geological environments affect the groundwater flow regime, which in turn is fundamental to the stability of a slope. Galerkin's method is used to derive a finite element program to model two dimensional, saturated, steady state flow through anisotropic and heterogeneous rigid porous media.

An understanding of the regional geology is required in order to understand the regional flow system. The following points are illustrated.

a. In anisotropic media, the most adverse groundwater condition for slope stability occurs when the major axis of conductivity lies down the dip of the slope.

b. Depending on their characteristics, faults, contacts and dykes can be either detrimental or favourable in their effect on the flow system. Careful field investigation is required to establish that effect.

c. Deep weathering commonly causes a confining zone of low conductivity, a situation very detrimental to stability.

d. Stress relief fractures on valley walls can adversely influence the effect of groundwater on stability.

e. A regional aquifer can cause high pore pressure development beneath a valley.

f. Fluctuations in the regional groundwater system can cause instability in Pleistocene terraces.

g. The presence of an underlying less conductive zone or unit

can have an adverse effect on the flow system. Conductivity contrasts of less than two orders of magnitude can cause pore pressure development critical to stability.

Three other points are demonstrated which have direct application to slope stability analysis and control.

1. The pressure head distribution on rock wedges can be non-linear rather than the commonly assumed linear distribution.
2. The introduction of a reservoir at the toe of a slope can influence the groundwater regime well above the reservoir surface; even a low reservoir can cause the change required to cause instability.
3. Piezometric measurements and drainage systems must penetrate through any less conductive unit that might be acting as a slide plane.

CONTENTS

CONTENTS (Cont'd)

TABLES

ILLUSTRATIONS

ILLUSTRATIONS (Cont'd)

* APPENDIX II - IS IN Map Cabinet 3

ACKNOWLEDGMENTS

A number of people have given much needed help and advice throughout this project. Katsayuki Fujinawa, visiting graduate student from Kyoto University, Japan, spent many hours with me patiently discussing the numerical and computer techniques. Peter Byrne, Department of Civil Engineering, U.B.C. reviewed my work on slope stability analyses. Hardy Bunn, C.B.A. Engineering Ltd., and Julie Wytrwal, Department of Mathematics, U.B.C., managed to wade through my hieroglyphic writing and produce a neatly typed manuscript.

Two people in particular have influenced and guided me during the past few years: F.D. Patton, Consultant Engineering Geologist, and my supervisor, R.A. Freeze, Department of Geological Sciences, U.B.C. Without the technical and moral assistance they have provided, this thesis would not have been possible.

CHAPTER ONE: INTRODUCTION

The critical role that groundwater plays in the stability of slopes has long been recognized. However, for many years the mechanism that related porewater pressures to the strength of the soil or rock was not understood. In 1923 Terzaghi provided that link with his effective stress law. Using the concept of effective stress, a number of techniques have been developed to quantitatively analyze the stresses in a slope to provide an estimate of stability. All of these methods assume that porewater pressures are a known quantity. In practice, these are usually obtained by field measurement with piezometers. Unfortunately, such measurements are both difficult to obtain and sometimes inaccurate.

In 1940, Hubbert proposed the exact mathematical equations that govern steady-state groundwater flow. However, it was not until Toth (1962, 1963) introduced the method of mathematically modelling a groundwater flow system by solving a formal boundary value problem, that it became possible to obtain an estimate of the groundwater flow system by a means other than with direct measurement of the pore pressure distribution. With an understanding of conductivity contrasts and a knowledge of the water table configuration, flow systems could be readily modelled and an estimate of the complete pore pressure distribution obtained. The power of this technique was demonstrated by Freeze and Witherspoon (1966, 1967) who discussed in detail the theoretical analysis of regional groundwater flow systems. It is now possible to model three-dimensional, transient groundwater flow through a porous media that includes both saturated and unsaturated zones (Freeze, 1971a).

Mathematical models can provide an independent check on measured pore pressures. When anomalies arise, models can point to field conditions not previously expected and modifications to field investigations can result.

Deere and Patton (1967, 1971) and Patton and Hendron (1974) have discussed the implications to slope stability of groundwater flow in a number of different slope environments. Despite the recognition of these implications, the versatile modelling techniques now available have not been applied to accurately illustrating flow systems in the complex geologic environments often associated with unstable slopes.

The purpose of this thesis is to show, using computer simulations of flow conditions in a variety of hypothetical slopes, how different geologic environments affect the groundwater flow regime which in turn is fundamental to the stability of a slope. It will be shown that to understand the distribution of pore pressures in a given slope, it is necessary to understand the regional flow system in which the slope is located.

To familiarize myself with the mechanics of slope stability analyses and to establish how the effects of groundwater were factored into the analyses, a review was undertaken of all the available literature pertaining to the techniques of slope stability analysis. The results of this review are reported in Chapter Two. In Chapter Three, the theory underlying the computerized mathematical models is given in detail and a simplified example is presented which illustrates the numerical technique. In any practical application of mathematical

models it is critical that underlying assumptions are understood. These are presented in Chapter Four. The results of the modelling and discussion of their implications is found in Chapter Five and in Chapter Six the project is summarized.

CHAPTER TWO: A REVIEW OF SLOPE STABILITY ANALYSES

Introduction

To completely document all the developments which have led to the presently used techniques of analyzing slope stability would require a lengthy volume. The purpose of this review is twofold. Firstly, a brief description is given of the three categories of analysis: methods based on limit equilibrium, elastic solutions of the finite element type, and Cundall's method based on discrete particle mechanics. Following this initial discussion, a more detailed account is presented of the various steps which have led to the present-day form of the limit equilibrium method. Three distinct aspects of this development can be isolated: identifying all the stresses acting, understanding the mechanics which relate the stresses, and determining the natural properties which govern the material behaviour when the stresses are acting.

The initial intent of this review was to gain insight into the assumptions that various investigators have made regarding the role of groundwater. This underlying motivation remains. For this reason, the chapter concludes with a brief discussion of the concept of effective stress followed by a summary of different ways of handling groundwater in limit equilibrium techniques.

Categories of Slope Stability Analysis

The three categories of slope stability analysis are summarized in Table 2-1. As well as descriptions, also listed are advantages, disadvantages, and the ability of each to account for groundwater.

Limit Equilibrium Methods

Limit equilibrium methods assume a failure plane, consider forces acting on the failing mass, and further assume that a critical limit occurs after which resisting forces are no longer greater than forces causing instability. Failure then occurs simultaneously everywhere along the failure surface. For a given slope, a factor of safety is calculated by considering the ratio of the materials shear strength (forces resisting failure) to the shear stress (forces causing failure). The critical limit referred to above is equivalent to a factor of safety of one.

In relating shear strength to normal stress, materials are assumed to follow either Coulomb's Law (Coulomb, 1776):

$$\tau = c + \sigma_t \tan\phi \qquad (2.1)$$

or the Revised Coulomb Equation (Terzaghi, 1923, 1936):

$$\tau = c' + (\sigma_t - u)\tan\phi' \qquad (2.2)$$

where τ = shear strength

c and c' = cohesion and effective cohesion

σ_t = total normal stress

u = porewater pressure

CATEGORY OF ANALYSIS	ADVANTAGES	DISADVANTAGES	GROUNDWATER
LIMIT EQUILIBRIUM The equilibrium condition of a rigid body or a system of rigid bodies is considered. A factor of safety is calculated by comparing the shear strength to the shear stress.	1. Results in a single factor of safety (within confidence limits) which is easily understandable. 2. Readily handles heterogeneous material properties. 3. Readily handles any porewater pressure distribution. 4. When a pre-existing, known discontinuity controls the failure, exact modelling is possible.	1. If the failure surface has not been located, the worst case must be found by trial and error. 2. No measure of strain on displacement is obtained. 3. Because only static equilibrium conditions are considered, dynamic situations such as a progressive failure cannot be modelled. 4. Is indeterminate due to an inadequate understanding of the normal stress distribution on the base and the normal and shear stress distribution on the sides of slices. Depending on the method, different assumptions are made to render the problem determinate.	Any groundwater flow system can be readily handled.
ELASTIC SOLUTIONS OF THE FINITE ELEMENT TYPE The stress-strain condition of a continuous body is developed, based on the theory of elasticity.	1. Results in a complete stress picture for the body. Stresses, strains, and displacements can be obtained. 2. A failure plane need not be assumed. 3. All the laws of mechanics are satisfied: equilibrium, compatibility, and boundary conditions. 4. Fairly easy to handle a quasi-dynamic situation.	1. Limited to small strain by the theory of elasticity. (This does not preclude large displacements.) 2. Because the body must remain a continuum, discontinuities cannot be truly modelled although approximations can be made by using highly elastic joint elements. 3. The correct stress-strain relationship for each element must be known. 4. Cannot handle a progressive failure.	Groundwater can be handled in terms of porewater pressures at nodes or seepage forces. However, the effect of groundwater on a materials modulus of elasticity is not generally agreed upon.
DISCRETE PARTICLE ANALYSIS A slope is modelled as a collection of discrete rigid blocks. The equilibrium of each block is considered. Uses an explicit time integration by considering a series of static equilibrium analyses (quasi-dynamic). Motion is calculated as a function of time.	1. Results in a dynamic illustration of the slope which stands if stable or falls if unstable. 2. Does not require the preselection of a failure surface. 3. Systems of fractures can be modelled exactly. 4. Allows for unlimited displacements and rotations. 5. Can describe a progressive failure.	1. Is written in terms of total stresses, not effective stresses. 2. Applies only to slopes which can be modelled as systems of rigid blocks.	Cannot at present handle porewater pressures.

Table 2-1. Categories of Slope Stability Analysis

ϕ and ϕ' = angle and effective angle of internal friction

Depending on which law is used, analyses are said to be in terms of total or effective stresses.

Most stability analyses involve an experimental calculation of c and ϕ or c' and ϕ' These values are then used in the analysis, in essence replacing the real by an ideal material. Terzaghi and Peck (1967, p. 104) point out that this replacement involves the assumption that both c and ϕ or c' and ϕ' are independent of strain and only when the shearing stress at every point along the continuous failure surface overcomes the shear strength is a failure generated.

In fact, with the exception of ideal plastic materials, strength is dependent on strain. After an initial peak is overcome, strength decreases with further strain until a constant residual value is attained. Figure 2-1 shows schematically the stress-strain curves for an ideal plastic material (peak strength not strain dependent) and a more realistic material (strength is strain dependent).

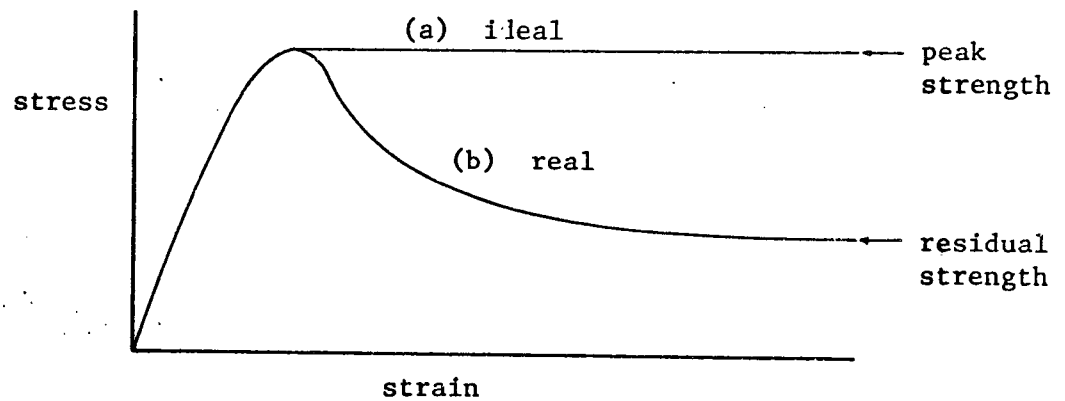

Figure 2-1. Schematic stress-strain curves for ideal and real materials

For any natural material characterized by curve (b) in Figure 2-1, the assumption of a simultaneous failure will be violated because strains along a potential failure surface will not be uniform. As a consequence, material along parts of the failure surface will be exerting peak strength and the remainder, something less. Failure will then start at one point and propagate along the failure surface causing a "progressive failure". Progressive failures invalidate the assumptions on which limit equilibrium techniques are based.

A review of all the ideas pertaining to progressive failure is beyond the scope of this project. However, for further background, the reader is referred to Bishop (1967, 1971), Bjerrum (1967), Christian and Whitman (1969), Haefeli (1965), Lo (1972), Lo and Lee (1973), Lutton (1971), Romani et al (1972), Turnbull and Hvorslev (1967), and Manfredini et al (1975).

Despite the above limitations, limit equilibrium techniques remain a powerful tool. Heterogeneous material properties cause no difficulty. Any porewater pressure distribution can easily be included. The geometry of failure planes controlled by discontinuities can be modelled exactly. And finally, provided one is aware of the limitations and assumptions underlying its calculation, the resulting factor of safety is understandable and useful for both design purposes and decision-making.

Because of an inadequate understanding of the normal stress distribution along the base of the slide and the normal and shear stress distribution on the sides of slices (in the case of methods involving slices), limit equilibrium methods are indeterminate. To

render the problem determinate, an assumption must be made regarding either the side or base forces. The various techniques of limit equilibrium analysis are differentiated by the assumption used to overcome this mechanics problem.

Elastic Solutions of the Finite Element Type

An alternate approach to the limit equilibrium methods is to use the stress-strain relationships of the theories of elasticity and model a slope as a continuous elastic medium. Commonly, such analyses are solved numerically using the finite element technique. The result is an understanding of the stress-strain condition of the slope. No factor of safety is generated but the method is ideal for identifying zones of stress concentration. An underlying and limiting assumption required by the theory of elasticity is that strains are small, less than one percent. To overcome this difficulty and to approximate discontinuities, Goodman et al (1968) proposed the use of joint elements with properties much different than the surrounding rock. The medium is still, however, modelled as a continuum.

Another limitation is that most stress-strain analyses are in terms of total stresses. Although porewater pressures can be introduced as an external force on any node, it is not clear what effect the water has on the stress-strain relationships which must be assumed for every element. (P. Byrne, personal communication).

Nevertheless, this approach is used for both soil and rock and is particularly useful in developing the stress-strain situation that exists around excavations such as open pits and underground openings. One advantage is that in obtaining the stress-strain picture, actual displacements can be measured and predicted. Examples in the literature are numerous but for a start the reader is referred to Desai (1972).

Discrete Particle Analysis

Cundall (1971, 1974) and Cundall et al (1975) describe another approach to slope stability utilizing the concepts of discrete particle mechanics. A computer program has been developed which models a rock slope as an assemblage of discrete and rigid blocks. Presumably if the computer capacity and data were available, smaller and smaller rock blocks could be considered until, in fact, a soil was being modelled. The program is similar to limit equilibrium analyses in that all displacements occur along joints and discontinuities, but different in that displacements, rotations, and interactions of the blocks are calculated as a function of time with failure surfaces being generated as instabilities develop. The program differs from finite element analysis in that as an instability develops the rock blocks are free to undergo large displacements and rotations.

The analysis is not truly dynamic: an explicit time integration is used by considering a series of static equilibrium analyses. In each step the equilibrium of each block is considered. Resultant

forces are used with Newton's second law to calculate an acceleration. Thus, motion is calculated as a function of time. Interaction with the program is via a graphics terminal. The geometry of a slope, complete with discontinuities, is drawn on the terminal and, with program execution, instabilities can be seen to develop and failures occur.

Unfortunately, Cundall's work is entirely in terms of total stresses. Because the effects of water are almost always critical to slope stability in soil or rock, it is apparent that this method has severe limitations until it can be modified to work in terms of effective stress.

Historic Development of Limit Equilibrium Methods

Without question, the first significant contribution was Coulomb's (1776) memoir presented to the Academy of Science in Paris. Heyman (1972) gives not only a copy of the original memoir but also an English translation with discussion of the principal features.

In his paper, Coulomb first presented the law that now bears his name (2.1). Although since refined, this basic empirical law remains the backbone of many aspects of Applied Science. Modified to allow for effective stress (2.2), it underlies almost all presently used techniques for analyzing slope stability.

In considering potential failures behind retaining walls, Coulomb used, for the "simplicity of the results obtained, the ease of their application in practice, and the wish to be useful to and understood

by workmen" a planar failure surface. However, he did go on to briefly describe a method to handle curved surfaces. In this technique he broke his region into vertical slices. The credit for first using curved failure surfaces and slices is usually given to much more recent investigators.

Coulomb also recognized the critical role of water. He suggested that the pressure of water reduced the angle of internal friction. His reasoning was perhaps incomplete; he attributed the problem to "replacing soil forces by the frictionless pressure of a fluid" (Heyman, 1972; p. 57), but his astute observation is nevertheless worth noting.

Leggett (1962, p. 430) describes the contribution of Alexandre Collin, a little known French engineer. Collin's book (1846) describes the first shear tests on clay. These were completed to determine the mechanical properties of the soil which he might then apply in the mathematical analysis of the stability of an unsupported slope. Collin also recognized the dependence of all theoretical studies of slope stability upon the local geologic structure and conditions.

In 1860, Rankine put forward his theory of earth pressure. Like Coulomb, he dealt with potential failures and forces behind retaining walls. Both Coulomb and Rankine considered "active and passive pressures and thrusts caused by a cohesionless soil not subject to seepage forces" (Taylor, 1948, p. 488).

Culmann (1866) described plane failure through the toe of a slope. Forces acting on the failing wedge included only the weight of

the wedge and a resisting force resulting from a cohesion that was constant along the failure surface.

During the early 1900's much work was conducted in Sweden because of numerous slope failures that had occurred along the Swedish railroads. A major commission on slope stability was established and several important contributions resulted. From observing many failure surfaces that approximated circular areas, several "circular arc" methods were developed, including the method of slices, ϕ-circle method and the log spiral method.

The method of slices was developed by Fellenius (1927, 1936). The mass above an assumed failure surface is divided into vertical slices (Figure 2-2). The forces acting on each slice include the weight "W", the cohesion "c" and a third force "P" due to the materials angle of internal friction. Figure 2-3 shows how c and P are directly related to Coulomb's law. Letting c be the resisting force due to cohesion, the total resisting force is

$$F_R = c + W_N \tan\phi \qquad (2.3)$$

The frictional component of the resisting force is $W_N \tan\phi$ and can be represented vectorially by $\overline{W}_N + \overline{P}$ where $\overline{P}$ is inclined at an angle ϕ to the normal component of the weight ($\overline{W}_N$). Because only moments are being considered, the use of $\overline{P}$ is equivalent to the use of $W_N \tan\phi$ because $\overline{W}_N$ itself causes no moment.

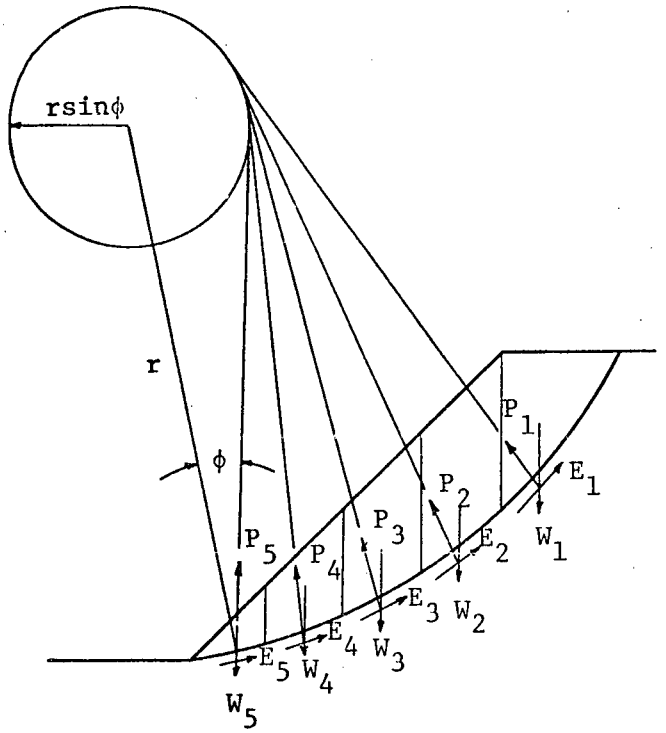

Figure 2-2. Fellenius' method of slices for a curved sliding surface through the toe of a slope (after Fellenius, 1936, p. 450)

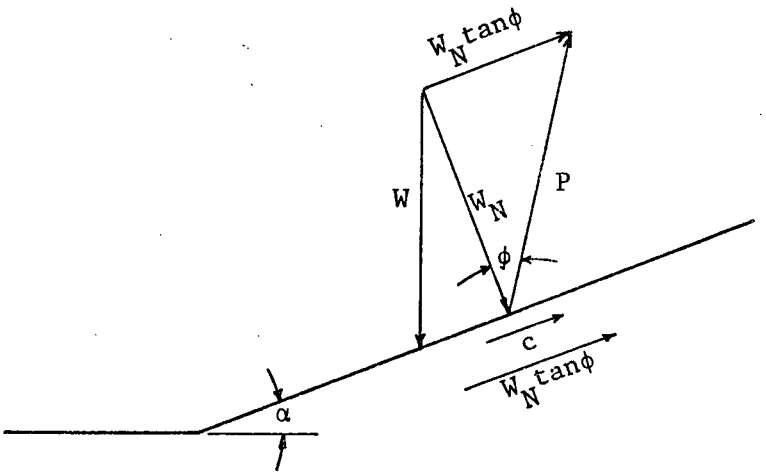

Figure 2-3. Force diagram showing a weight W acting on a slope inclined at an angle α

For each slice, P is tangent to a small circle with centre the same as that of the sliding surface and radius rsinϕ (Figure 2-2). The basic equilibrium equation used in the derivation of the factor of safety is the summation of moments about the centre of rotation. Interslice forces are assumed to act parallel to the base of the slide and therefore cancel out in the summation. The worse case is found by trial and error after a large number of failure surfaces have been considered.

The ϕ-circle method was described by Taylor (1937) although he attributed an earlier origin to Professors Glennon Gilboy and Arthur Casagrande. Taylor considered both failures passing through and below the toe. The region above the failure surface is assumed to be a single free body (Figure 2-4). The forces acting on the mass are the weight "W", a cohesion "c" acting parallel to the chord joining the two ends of the failure surface, and "P" a "resultant force transmitted from grain to grain of the soil across" the failure surface (Taylor, 1937, p. 345). "P", as before, is assumed to act at an angle ϕ to the failure circle, making it tangent to a small circle (the ϕ-circle) with centre at the origin of the failure circle. Moments of the mass about the origin are considered. A special case for $\phi = 0$ results when the material in question (for example, saturated undrained clay) can be considered purely cohesive. This case is thoroughly reviewed by Skempton (1948). As with Fellenius' method of slices, a large number of assumed failure surfaces must be considered in order to find the most critical case.

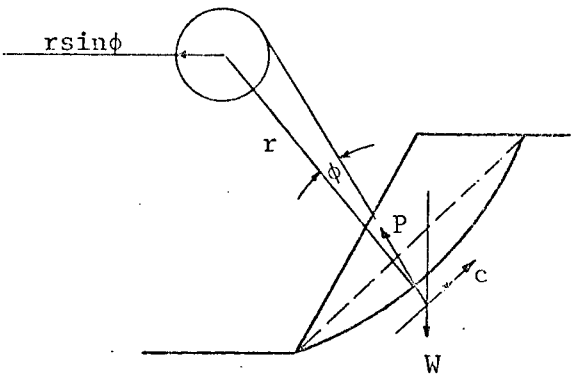

Figure 2-4. The ϕ-circle method for toe failures (Taylor, 1937, p. 344)

Rendulic (1935) proposed a slight variation from the ϕ-circle method based on assuming the failure circle to be a log spiral. Using this assumption he avoided the basic assumption of the ϕ-circle method as all radius vectors can be shown to intersect the failure curve at an angle of ϕ (Figure 2-5). Again, trial and error must be used to find the critical failure surface.

All of the three "circular arc" methods initially assumed dry, homogeneous and isotropic materials. After the introduction of the concept of effective stress they were extended to account for porewater pressures.

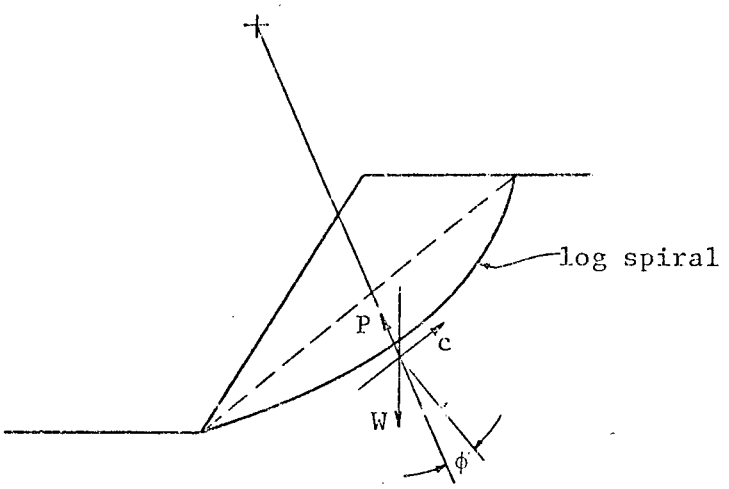

Figure 2-5. Rendulic's log-spiral method

Terzaghi's development of this concept stands with Coulomb's law in importance to the understanding of slope stability. Although first suggested in his work of 1923, it was not until he published his 1936 paper, in English, that the full impact of his empirical law could be felt. His effective stress law is

$$\sigma_e = \sigma_t - u \tag{2.4}$$

where

σ_e = effective stress

σ_t = total stress

u = porewater pressure

Coulomb's law (2.1) could then be restated in terms of effective stress (2.2).

Although commonly used in practice, the validity of Terzaghi's empirical effective stress law has been the subject of some controversy. Some of the debated ideas will be presented in a later section.

Following the introduction of his effective stress law, Terzaghi (1936(c)) went on to show how Fellenius' and Rendulic's methods could be modified for water pressures if part of the failing mass was below a static water table. For the submerged portion he simply used buoyant unit weights. He also noted that "percolating water" could be represented by flow nets. Using the porewater pressures he obtained from his flow net, he was able to use Fellenius' method for the case of steady seepage.

Taylor (1937) expanded Terzaghi's discussion in considering four cases using the ϕ-circle method: complete submergence (Figure 2-6), sudden drawdown, steady seepage, and capillary saturation (Figure 2-7).

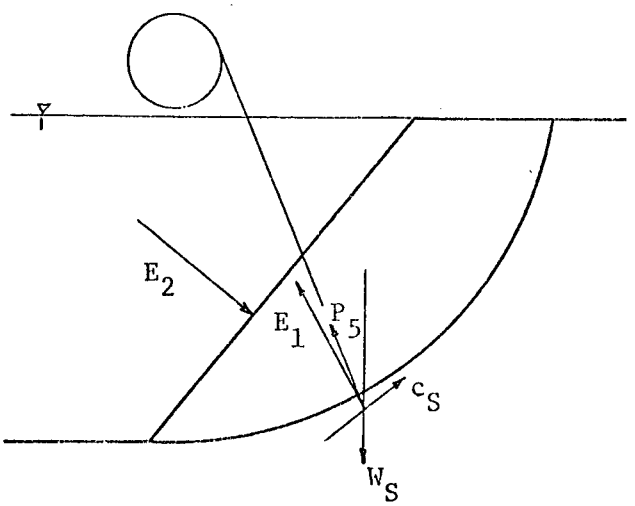

Figure 2-6. Taylor's ϕ-circle analysis for complete submergence

For complete submergence (Figure 2-6), Taylor used the "effective" weight, W_S, defined by

$$W_S = (\gamma_T - \gamma_{water}) \times \text{volume} \qquad (2.5)$$

where

γ_T = total unit weight

γ_{water} = unit weight of water .

Using W_S causes a redefinition of P because of their interdependence. Two additional water forces are introduced, E , the resultant of water forces acting everywhere normal to the failure circle; and E_2, the resulting "supporting" force due to the water above the failing mass. E_1 will not cause a moment. The moments of the entire mass are then considered as before.

The sudden drawdown case was simply calculated by removing the force E_2 .

For steady seepage, Taylor commented that, although flow nets could be sketched and used to obtain solutions, the work involved was long and tedious. The true solution for steady seepage would lie somewhere in between complete submergence and sudden drawdown. He recommended that the sudden drawdown calculation be used for the steady seepage case. Although his approach was conservative, he doubted that "the accuracy which can be attached to stability computations was great enough to warrant the drawing of a flow net and the involved procedure that must follow" (Taylor, 1937, p. 373).

Taylor considered one other case, capillary saturation (Figure 2-7).

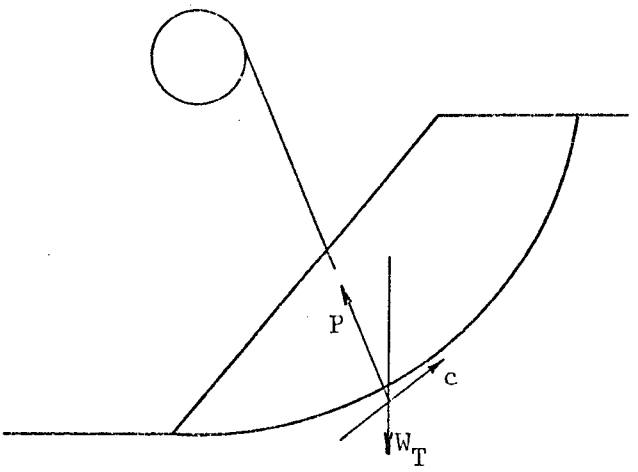

Figure 2-7. Taylor's ϕ-circle analysis for capillary saturation

For this case he used a total weight which consisted of the weight of the soil plus the weight of water retained by capillary action. This condition, he explained, could be attained by shutting off the supply of seepage water and thus eliminating seepage forces. Essentially, this would require draining to lower the water table below the failing slope.

The various circular arc methods discussed so far are theoretically incorrect, satisfying only one of the three aspects of static equilibrium, moment equilibrium; leaving unsatisfied the question of horizontal and vertical force equilibrium.

In 1954, Janbu (1954, 1957, 1973) first presented his Generalized Procedure of Slices. His work included the first attempt to consider all the three aspects of equilibrium as well as providing a method that could handle failure surfaces of any shape. The forces he considered are shown in Figure 2-8, where

dP = external load

dW = slice weight

E and E + dE = horizontal interslice forces

T and T + dT = vertical interslice forces

dS = resisting forces along the base

dN = normal force along the base.

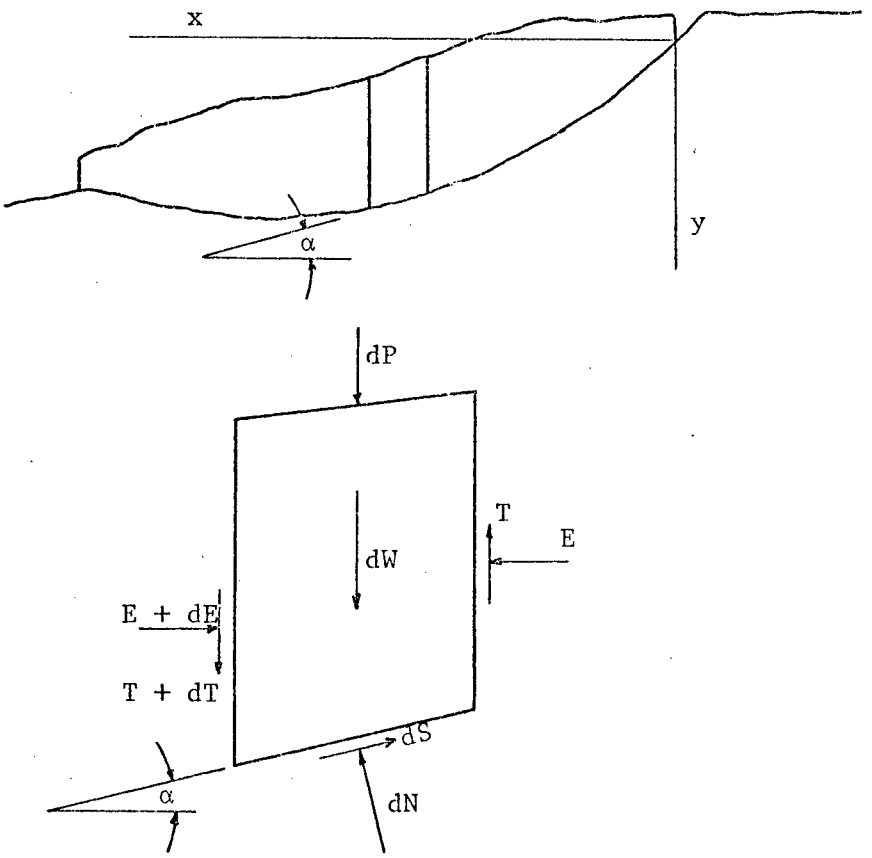

Figure 2-8. Forces used by Janbu
in his Generalized Procedure of Slices

For each slice he considered vertical, horizontal, and moment equilibrium. Integrating the vertical and horizontal forces for the entire body, he was able to consider vertical and horizontal equilibrium

for the mass as a whole. For stability criteria he used the horizontal condition of equilibrium. The resulting expression for safety factor was indeterminate without assuming a line of thrust for the interslice forces. These were then obtained by successive approximations and re-introduced into his safety factor expression. Terzaghi and Peck (1967, p. 253) suggest that with Janbu's method, moment equilibrium for individual slices is not satisfied by the forces derived from the solution. However, more recent summaries (for example, Wright et al, 1973; Duncan, 1975) include Janbu's method with those that satisfy all conditions of equilibrium.

Bishop (1955) put Fellenius' circular arc method of slices on a more correct foundation from a statistics point of view. Figure 2-9 shows the forces he considered, where

w = weight of slice

X_n, X_{n+1} = vertical shear forces

E_n, E_{n+1} = resultant horizontal interslice forces

S = shear force acting on the slice base

P = normal force acting on the slice base

By considering the moments about the origin "0" he developed an expression for the factor of safety which included the interslice forces. The terms involving these interslice forces had been previously shown by Krey (1926) and Terzaghi (1929) to cause only minor changes if neglected. The resulting simple expression meant an easy calculation of the safety factor but was in general conservative and could lead to unenconomical design. For this reason, Bishop went on to describe a

method that by successive approximations ensured that the vertical shear forces should sum to zero. Like Janbu, he had to assume a reasonable line of thrust. He also gave an expression that if satisfied would ensure that horizontal interslice forces would be in equilibrium as well.

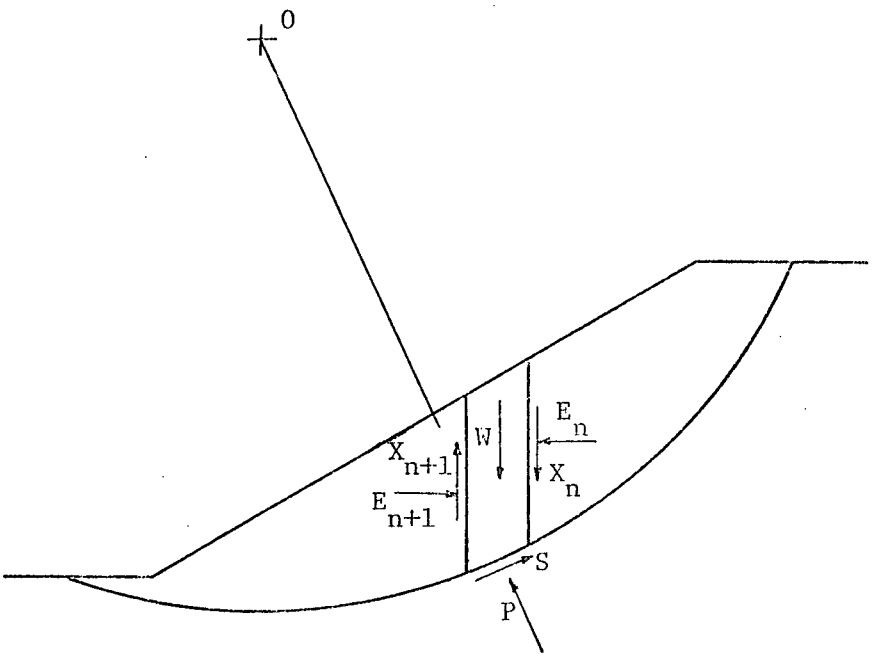

Figure 2-9. Forces used in Bishop's method

However, he added that, although the gain in accuracy obtained by ensuring vertical shear forces summed to zero was significant, the same could not be said of ensuring horizontal interslice force equilibrium. Bishop's simplified method which involves satisfying overall moment equilibrium and vertical shear force equilibrium but not horizontal interslice force equilibrium is commonly used and has been shown

(Duncan, 1975; Morgenstern and Price, 1965; Wright et al, 1973) to give accurate results for most cases.

Lowe and Karafiath (1960) proposed a graphical, modified method of slices which satisfied horizontal and vertical force equilibrium but not moment equilibrium. After calculating the magnitude and direction of weight and water forces, they assumed a "reasonable" direction for lateral earth forces. For a trial factor of safety, "a series of force polygons were constructed, one for each slice. By plotting the force polygons contiguous with each other and in sequence, a closure polygon is obtained" (Lowe and Karafiath, 1960, p. 542). If closure is not obtained, a new factor of safety is assumed and the exercise is repeated until the appropriate factor of safety is obtained.

The introduction of the computer into common usage in the 1950's revolutionized procedures for analyzing slope stability. Clearly many time-consuming and repetitive operations became simple and quick. Little and Price (1958), Horn (1960), and Whitman and Bailey (1967) discuss the application of the computer to slope stability.

Until the introduction of the computer, techniques were developed to give fast, reasonably accurate answers even though Laws of Mechanics were not always satisfied. Because of the indeterminate nature of Limit Equilibrium methods, techniques which satisfied the Laws of Mechanics commonly required successive approximations to reach a solution. Without the computer such solutions were unwieldy and time-consuming. However, with the computer, this difficulty was removed and iterative methods which ensured all the Laws of Mechanics were satisfied, replaced the earlier approximate methods.

Such a method was proposed by Morgenstern and Price (1965). The forces they considered are shown in Figure 2-10 where

x, $x + dx$ = vertical interslice shear forces

E', $E' + dE'$ = lateral effective side thrusts

P_W, $P_W + dP_W$ = resultant side water pressure

dP_b = water pressure acting on the base

dN' = effective normal pressure

dS = shear force acting on the base

α = inclination of the base

dW = weight of the slice

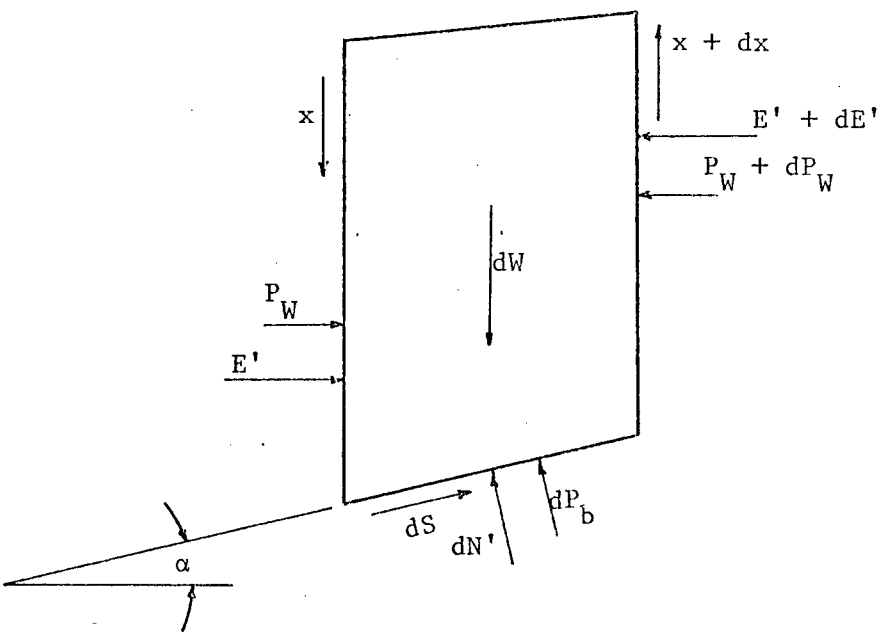

Figure 2-10. Forces used in the Morgenstern-Price Method

By taking moments about the centre of the base of the slice, summing forces perpendicular and parallel to the failure surface and subsequently simplifying, two governing differential equations in three

unknowns remain, a statically indeterminate problem. The remaining unknowns are the lateral side thrust E', its position of action, and the vertical interslice shear force x. A number of assumptions are possible to reduce the problem to a solvable case including assuming the position of the line of thrust or assuming a relationship between E and x. Morgenstern and Price use a form of this latter assumption by relating the total horizontal stress E ($= E' + P_w$) and x by

$$x = \lambda f(z)E \tag{2.6}$$

where λ is a constant which depends on reasonable boundary conditions and $f(z)$ is an arbitrary function of z, the vertical coordinate. $f(z)$ can be estimated from available elasticity solutions or (Morgenstern and Price, 1965, pp. 87 and 88):

> Specified on the basis of the intuitive assumption that for most cross-sections the higher the rate of curvature of the slip surface, the greater the ratio between the shear and horizontal forces at the slip interface ... Ultimately reliable field measurements of internal stress will provide the best guide.

Starting with guessed values of λ and $f(z)$ they integrate across all the slices to obtain values of E_n, the total horizontal stress and M_n, the moment; which in general will not both be zero. By modifying λ and $f(z)$ and systematically iterating, values are finally found for which E_n and M_n are zero.

Morgenstern and Price (1965) introduce porewater pressure data in the form of a coefficient "r_u" as defined by Bishop and Morgenstern (1960):

$$r_u = \frac{u}{\gamma h} \tag{2.7}$$

where

u = pore pressure

γ = specific weight of the slide material

h = depth below slide surface

Although r_u can be varied from slice to slice, it would seem more reasonable to develop a flow net solution and introduce directly the appropriate values of the pore pressure. (This approach is used by Fredlund (1974).) The use of r_u will be discussed more thoroughly in a later section.

Since Morgenstern and Price published their paper, several others have described solutions which depend on different assumptions used to eliminate the indeterminacy of the problem. Spencer (1967) assumed parallel interslice forces; i.e., a constant interslice force inclination. Bell (1968) made an assumption about the variation of the normal stress acting on the potential slip surface. Interslice forces, however, did not enter into his equation of equilibrium as he considered them internal to the free body being examined. Janbu (1973) restated his method which assumes a line of thrust of interslice forces. The various methods are summarized by Duncan (1975).

Thus far in this discussion, no comment has been given on the relationship between analyses for rock slope stability and soil slope stability. The first concepts and methods for analyzing slope stability originated within what is now considered the science of Soil Mechanics. The closely related science of Rock Mechanics developed some time later but is based on many of the same principles. Limit equilibrium techniques are used for the analysis of both soil and rock slope stability.

If a rock slope is so highly fractured or weathered that it can be considered to act like a soil, then the techniques of soil mechanics are applicable. More commonly, the strength of a rock slope is controlled by discontinuities, faults, and fractures, and is better modelled as a system of rock blocks and wedges. In some cases, individual blocks and wedges must be considered. Techniques for handling these cases are described by Goodman and Taylor (1967), John (1968), Londe et al (1969, 1970), and Hendron et al (1971). Obviously, scale and the nature and spacing of discontinuities are critical in deciding on the most appropriate model.

In summarizing the development of limit equilibrium techniques, three distinct aspects can be isolated: identifying the different stresses acting; understanding the mechanics which relate the stresses; and determining the natural properties that govern the material behaviour when the stresses are acting.

The recognition of different stresses, one due to overburden load and the other due to fluid pressures, led Terzaghi to his effective stress law. His recognition of this concept was a major step forward. A further stress problem is the role of residual tectonic stresses due to past and present geologic processes. These can be grouped into local or regional residual stresses. Local stresses are often due to stress relief and rebound after removal of materials. This removal can be a result of natural processes such as rivers and glaciers or man-made excavations. Regional stresses are related to large geologic structures resulting from regional tectonic activity. The exact role of residual tectonic stresses is not completely understood and certainly at the

present time is not included in limit equilibrium slope stability calculations. Although the magnitude of these stresses is probably small, in some cases it may be significant.

A second aspect of the development of limit equilibrium techniques was arriving at a full understanding of the mechanics which relate the stresses being considered. Given the problem in terms of effective stresses and a computer to eliminate repetitive and time-consuming operations, the task was then to properly relate all the forces acting. This was achieved by application of all the laws of static equilibrium. The problem, however, is still indeterminate and the various assumptions used for solutions, result in the different methods.

The final aspect is a large subject in itself and a thorough treatment is well beyond the scope of this review. However, for completeness I mention it here. The usefulness of any method depends on the understanding and the accurate measurement of the natural properties used in the various equations. Such properties include cohesion, internal friction angle, specific weight, permeability, porosity, and compressibility. To obtain a meaningful value or distribution of values which describe each of these properties is a difficult task. Laboratory measurements, field measurements, and back calculations can all be used but it remains a difficult problem. It is this aspect, more than the others, which limits the accuracy and usefulness of the techniques themselves.

The Concept of Effective Stress

The concept of effective stress may not be as simple as suggested by Terzaghi's empirical law (2-3). In fact, Terzaghi (1923) originally proposed the law in a slightly different form:

$$\sigma_e = \sigma_t - \alpha u \tag{2.8}$$

where α is a parameter, the exact value of which is controversial. Terzaghi (1923) suggested that α should equal the porosity but found experimentally that $\alpha \simeq 1$. These conclusions were repeated in his 1936(a) paper where he called α a reduction factor. Hubbert and Rubey (1959, 1960) attempted to show theoretically that $\alpha = 1$ but the validity of their proof has been questioned by Laubscher (1960). Skempton (1961) proposed that more correct expressions for effective stress in fully saturated material are

for shear strength $\sigma_e = \sigma_t - (1 - \frac{a\tan\psi}{\tan\phi'})u$ (2.9)

for volume change $\sigma_e = \sigma_t - (1 - \frac{c_s}{c})u$ (2.10)

where

a = the area of contact between particles per unit gross area of the material

ψ = intrinsic angle of internal friction

ϕ' = effective angle of internal friction

c_s = compressibility of the solid particles

c = compressibility of the overall material

and the other symbols are as defined previously.

For fully saturated soils, at pressures normally encountered in engineering practice, both "a" and "c_s/c" are very small and

(2.9) and (2.10) will degenerate to Terzaghi's empirial relationship (2.3). However for saturated rock and concrete relationships (2.9) and (2.10) should be used.

Nur and Byerlee (1971) give both experimental evidence and a theoretical proof of (2.10). However, they note that "when the compressibility of the aggregate is sufficiently greater than that of the grains," Terzaghi's empirical law is an excellent approximation regardless of porosity. For mechanically isotropic, elastically linear aggregates, the law (2.10) holds. They further suggest that one can determine "accurately the strain in a porous solid with pore pressure from the measured elastic modulii of the material without pore pressure."

In practice, Terzaghi's empirical law is commonly used. It would appear from the above discussion that under certain circumstances Terzaghi's law gives an adequate approximation but in other cases more accurate relationships should be used.

The problem of effective stress in unsaturated materials is discussed by Jennings (1960), Blight (1967), and Skempton (1961), who point out that above the saturated zone Terzaghi's empirical law does not hold. They proposed alternate forms of the effective stress law and the reader is referred to those papers for details.

Groundwater and Limit Equilibrium Methods

Fredlund (1974) summarized the different procedures for handling groundwater in limit equilibrium methods. He listed the following five alternatives:

1. total stress analysis, no porewater pressure
2. use of the coefficient r_u
3. pore pressures are expressed as a ratio of overburden pressure
4. pore pressures are expressed as x and y coordinates of a peizometric line
5. pore pressures are evaluated by interpolation between grid of known pore pressures

Except under very special circumstances (for example clays with strength due only to cohesion), a total stress analysis in which strength is not considered to be a function of pore pressures, is not appropriate for slope stability analysis. In fact, the presence of water is commonly the cause of stability problems and an effective stress analysis is best.

As previously mentioned, Bishop and Morgenstern (1960) introduced the porewater pressure coefficient r_u defined by (2.7) or

$$u = r_u \gamma h \tag{2.11}$$

The pore pressure can be seen by (2.11) to be expressed as a simple function of the depth h. Although r_u can be made to vary from slice to slice, it results in an approximation that can be markedly different from the actual case. In reality, porewater pressures are rarely a simple linear function of depth. The exception is the case of a saturated static water table where r_u would simply indicate the ratio of the specific weight of water to that of the overburden. Such a condition is not common in nature. Because techniques are now available to accurately model field conditions with relative ease, it no longer makes sense to use an approximation like r_u and its use should be discouraged.

Expressing pore pressures as a ratio of overburden pressure was suggested by Hilf (1948) as a means of estimating construction pore pressures in rolled earth dams. As with the use of r_u, means are now available to accurately establish conditions by numerical modelling and the use of this approximation is also no longer justified.

In a situation where field measurements have established the piezometric surface, expressing pore pressures as x and y coordinates of a piezometric line may be the best way to handle groundwater.

Evaluating pore pressures by interpolation between a grid of known pore pressures which have been obtained by field measurement and/or mathematical modelling is the best of the listed alternatives. Finite difference and finite element techniques are now commonly available to model complex groundwater flow regimes. Provided the boundary conditions have been correctly interpreted and reasonable estimates have been obtained of natural properties, these methods give accurate solutions of the groundwater flow problem.

CHAPTER THREE: GROUNDWATER FLOW, GALERKIN'S METHOD AND THE FINITE ELEMENT METHOD

Introduction

Fluid flow through porous media can be treated mathematically as a boundary value problem. For regions that are geometrically simple and that consist of homogeneous isotropic materials, one can obtain an exact analytic solution. For more complicated regions and materials, exact solutions are not possible and numerical approximations are necessary.

Galerkin's method is one of a number of procedures available for finding an approximate numerical solution to a differential equation. Others include the method of Kantorovich, Raleigh-Ritz, and Euler's Finite Difference technique (Crandall, 1956; Forray, 1968; Kantorovich and Krylov, 1964). All of these methods utilize an approximating function for the unknown quantity and involve minimizing the resulting error. The various methods are differentiated by their degree of generalization and technique of error minimization. In some cases, one method can be shown to reduce to another. For example, Crandall (1956, p 233), Kantorovich and Krylov (1964, pp 262-264) and Forray (1968, p 193) discuss the equivalence under certain condition, of the Raleigh-Ritz and Galerkin methods.

The following discussion is limited to solving the equation of flow for two dimensional, saturated, steady state flow through anisotropic

and heterogeneous porous media. Galerkin's approach and the finite element technique are used to develop a set of solvable linear equations. The works of Pinder and Frind (1972) and of Remson, Hornberger and Molz (1971) were particularly useful in synthesizing concepts.

Theory

Consider a region R in which we wish to compute the hydraulic head, $\phi(x,y)$, at certain points or nodes. Let these nodes form the vertices of small but finite triangular elements (Figure 3-1).

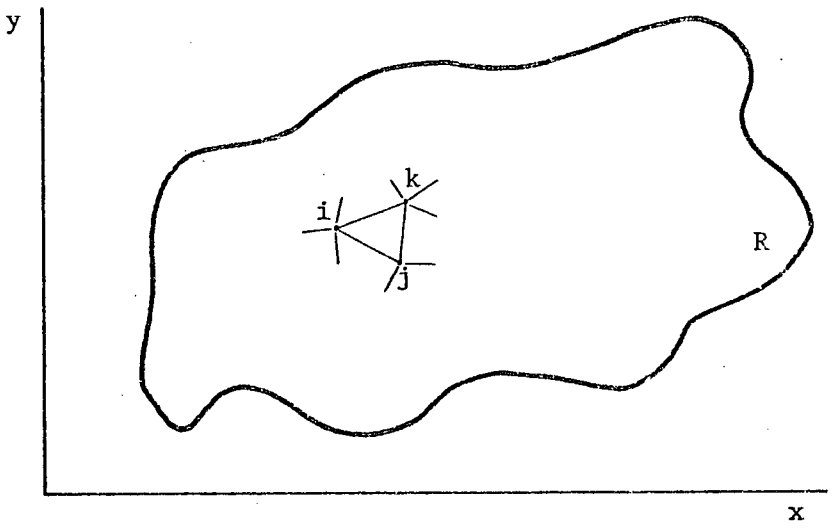

Figure 3-1 . Descritization of region into finite triangular elements.

Other more complex (higher order) elemental shapes are possible and are desirable for more accurate solutions to geometrically complex regions. For example, Zienkiewicz (1971) and Pinder and Frind (1972) discuss the curved isoparametric quadrilateral. However, for simplicity this discussion

will be limited to that of the triangle.

The solution $\phi(x,y)$ in R can be viewed as a surface with coordinates ϕ_i, ϕ_j, ϕ_k at the i^{th}, j^{th}, and k^{th} nodes respectively. The simplest approximation of this solution surface is a linear plane which for each element is of the form:

$$\phi = Ax + By + C \tag{3.1}$$

We want to solve for the nodal values of $\phi(x,y)$ therefore we solve for A, B and C knowing the plane used in approximating the element i, j, k must pass through all three points, thus:

$$\begin{aligned} \phi_i &= Ax_i + By_i + C \\ \phi_j &= Ax_j + By_j + C \\ \phi_k &= Ax_k + By_k + C \end{aligned} \tag{3.2}$$

Equations (3.2) can be used to solve for A, B and C . The resulting expressions for A, B and C can then be substituted into equation (3.1) so ϕ', the approximation within the triangular element, can be written in terms of the nodel values of ϕ at the vertices and three coefficients which are functions of the node positions:

$$\phi' = N_i\phi_i + N_j\phi_j + N_k\phi_k \tag{3.3}$$

where

$$N_i = [(x_j y_k - x_k y_j) + (y_j - y_k)x + (x_k - x_j)y]/2D$$

$$N_j = [(x_k y_i - x_i y_k) + (y_k - y_i)x + (x_i - x_k)y]/2D \qquad (3.4)$$

$$N_k = [(x_i y_j - x_j y_k) + (y_i - y_j)x + (x_j - x_i)y]/2D$$

and $2D$ = 2 × area of the elemental triangle i, j, k

= determinant $\begin{vmatrix} 1 & x_i & y_i \\ 1 & x_j & y_j \\ 1 & x_k & y_k \end{vmatrix}$

Equation (3.3) can be re-written as:

$$\phi \simeq \phi' = \sum_{i=1}^{n} N_i \phi_i \qquad (3.5)$$

where i labels the nodes contributing to that element, n is the total number of nodes contributing, ϕ_i are the heads at the nodes and N_i are defined by equation (3.4) and are called "shape" or "basis" functions. For more complicated elements, the basis functions are linear, quadratic or cubic polynomials, depending on the element shape (Pinder and Frind, 1972, p 110).

Equation (3.5) expresses the linear approximation to the real ϕ values. The basis functions, N_i, are chosen so that the boundary conditions imposed on the governing partial differential equation, (the equation of flow), are satisfied. Where Darcy's Law is assumed to be correct, the governing equation for two-dimensional steady-state flow through anisotropic porous media is:

$$L(\phi) = \frac{\partial}{\partial x}\left(K_{xx}\frac{\partial \phi}{\partial x}\right) + \frac{\partial}{\partial y}\left(K_{yy}\frac{\partial \phi}{\partial y}\right) = 0 \qquad (3.6)$$

where L is the differential operator and K_{xx} and K_{yy} are the hydraulic conductivities in the x and y directions. The x and y axes are chosen to correspond locally (i.e. for each element) with the principle directions of the hydraulic conductivity ellipse.

Equation (3.5) will be the exact solution to (3.6) if

$$L(\phi') = 0 \qquad (3.7)$$

This condition is equivalent to the requirement that $L(\phi')$ be orthogonal to all the shape functions (Kantorovich and Krylov, 1964 p. 262) or,

$$\iint_R L(\phi')\, N_j \, dx\, dy = 0 \qquad (3.8)$$

and substituting in equation (3.5):

$$\iint_R L\left(\sum_{i=1}^{n} N_i \phi_i\right) N_j \, dx\, dy = 0 \qquad j = 1 \ldots n \qquad (3.9)$$

Equation (3.9) results in n equations in n unknowns. Expanding equation (3.9):

$$\iint_R \left[\left(\frac{\partial}{\partial x} K_{xx} \frac{\partial}{\partial x} + \frac{\partial}{\partial y} K_{yy} \frac{\partial}{\partial y}\right)\left(\sum_{i=1}^{n} N_i \phi_i\right)_{j=1 \ldots n}\right] N_j \, dx\, dy = 0 \qquad (3.10)$$

Now, for a given triangular element, three equations will be generated, one for each node of that triangle. Assuming K_{xx} and K_{yy} are constant within the element in question, equation (3.10) can be re-written

$$\iint_R \left| \sum_{i=1} \phi_i \left(K_{xx} \frac{\partial^2 N_i}{\partial x^2} + K_{yy} \frac{\partial^2 N_i}{\partial y^2} \right) \right| N_j \, dx \, dy = 0 \qquad (3.11)$$

This equation includes second derivatives which are difficult to handle numerically. To eliminate then, Green's Theorem is applied in the following form (Weinstock, 1952, p 13):

$$\iint_R \psi \frac{\partial^2 \phi}{\partial x^2} + \psi \frac{\partial^2 \phi}{\partial y^2} \, dx \, dy = - \iint_R \left(\frac{\partial \phi}{\partial x} \cdot \frac{\partial \psi}{\partial x} + \frac{\partial \phi}{\partial y} \cdot \frac{\partial \psi}{\partial y} \right) dx \, dy + \int_c \psi \frac{\partial \phi}{\partial n} \, ds \qquad (3.12)$$

where c represents the boundary of R and $\frac{\partial \phi}{\partial n}$ is the outward normal derivative of the function $\phi(x,y)$:

$$\frac{\partial \phi}{\partial n} = \frac{\partial \phi}{\partial x} \ell_x + \frac{\partial \phi}{\partial y} \ell_y$$

ℓ_x and ℓ_y are direction cosines.

Comparing (3.11) and (3.12) we can write

$$\psi \equiv N_i$$

$$\phi \equiv N_i$$

and rewrite Green's Theorem as:

$$\iint \left(N_j \frac{\partial^2 N_i}{\partial x^2} + N_j \frac{\partial^2 N_i}{\partial y^2} \right) dx \, dy = - \iint_R \left(\frac{\partial N_i}{\partial x} \cdot \frac{\partial N_j}{\partial x} + \frac{\partial N_i}{\partial y} \cdot \frac{\partial N_j}{\partial y} \right) dx \, dy + \iint_c N_j \frac{\partial N_i}{\partial n} \, ds \qquad (3.13)$$

where $\frac{\partial N_i}{\partial n} = \frac{\partial N_i}{\partial x} \ell_x + \frac{\partial N_i}{\partial y} \ell_y$

Combining this result with equation (3.11) we can write the governing differential equation as:

$$-\iint_R \sum_{i=1}^{n} \phi_i \left(K_{xx} \frac{\partial N_i}{\partial x} \cdot \frac{\partial N_j}{\partial x} + K_{yy} \frac{\partial N_i}{\partial y} \frac{\partial N_j}{\partial y} \right) dx\, dy + \int_c N_j \sum_{i=1}^{n} \frac{\partial N_i}{\partial n} \phi_i \, ds = 0 \qquad j = 1 \ldots n \tag{3.14}$$

where $\frac{\partial N_i}{\partial n} = K_{xx} \frac{\partial N_i}{\partial x} \ell_x + K_{yy} \frac{\partial N_i}{\partial y} \ell_y$

Equation (3.14) represents the flow over a region which in our case is a triangular element. At any given node there will be contributions from the surrounding elements. We are interested in the value of the head at each nodal point. To write the equation for a given node we must sum the contributions from each of the adjacent elements. If there are "E" adjacent elements, we can write the equation for a given node as:

$$\sum_{e=1}^{E} \left| \iint \sum_{i=1}^{n} \phi_i \left(K^e_{xx} \frac{\partial N^e_i}{\partial x} \cdot \frac{\partial N^e_j}{\partial x} + K^e_{yy} \frac{\partial N^e_i}{\partial y} \cdot \frac{\partial N^e_j}{\partial y} \right) dx\, dy - \int_c N^e_j \sum_{i=1}^{n} \frac{\partial N^e_i}{\partial n} \phi_i \, ds \right| = 0 \qquad j = 1 \ldots n \tag{3.15}$$

where i labels the node in question and j identifies the nodes of the corners of the contributing elements.

The last term in equation (3.15) incorporates the Neuman boundary condition (constant flux):

$$K \frac{\partial \phi}{\partial n} = q \tag{3.16}$$

where q is the flux of water into the element per unit length of boundary. It is formed only when q is non zero in which case it takes the form (Pinder and Frind, 1972, p 112),

$$\int_c N_i \, q \, ds \tag{3.17}$$

According to Zienkiewicz and Cheung (1968, p 154) it reduces to

$$\frac{q \ell}{2} \tag{3.18}$$

where ℓ is the length of the element on the boundary.

At nodes where a Dirichlet boundary condition (constant head) is encountered, equation (3.15) is not generated as ϕ is a known quantity at such nodes.

Combining (3.15) and (3.18) we can rewrite the equation for a given node as:

$$\sum_{e=1}^{E} \left| \iint \sum_{i=1}^{n} \phi_i \left[K_{xx}^e \frac{\partial N_i^e}{\partial x} \cdot \frac{\partial N_j^e}{\partial x} + K_{yy}^e \frac{\partial N_i^e}{\partial y} \cdot \frac{\partial N_j^e}{\partial y} \right] dx \, dy - \frac{q^e \ell^e}{2} \right| = 0 \qquad j = 1 \ldots n \tag{3.19}$$

or in matrix form:

$$[P]\{\phi\} + \{F\} = 0 \tag{3.20}$$

where

$$P_{i,j} = \sum_{e=1}^{E} \left| \iint \sum_{i} K_{xx}^e \frac{\partial N_i^e}{\partial x} \cdot \frac{\partial N_j^e}{\partial x} + K_{yy}^e \frac{\partial N_i^e}{\partial y} \cdot \frac{\partial N_j^e}{\partial y} \right| dx \, dy \tag{3.21}$$

and

$$F_i = \sum_{e=1}^{E} \frac{q^e \ell^e}{2} \tag{3.22}$$

$[P]$ and $\{F\}$ can be evaluated, and using standard techniques of matrix algebra we can solve for $\{\phi\}$. The matrix of coefficients $[P]$, which is often called the stiffness matrix by analogy to structural mechanics, will be mostly zeros. This results from contributions to a given nodal equation being only from those elements surrounding the node for which the equation is being written. $[P]$ can be described as sparse and banded.

The programmed solution, listed and documented in Appendix I, sweeps through the region element by element. For each element, three quantities are calculated corresponding to the contributions of that element to each of the equations of the three vertices. During program execution the equation for each node is generated as the computor sweeps all the contributing elements surrounding that node. A brief outline of the solution used in my program for the resulting matrix equation is given in a latter section of this chapter.

Example

To illustrate the numerical technique, an example follows. For simplicity of computation an isotropic material will be considered. We can then set $K = K_{xx} = K_{yy}$ and factor accordingly. The flow region is bounded by constant head boundaries and is illustrated in Figure 3-2 .

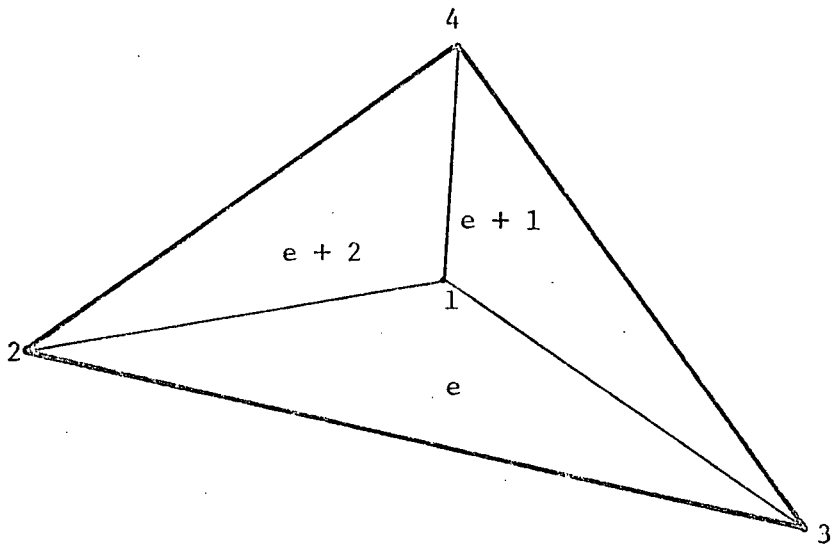

Figure 3-2 . Region of flow.

Consider node 1 in Figure 3-2 . The contribution from element e to the equation for node 1 is:

$$K^e\left|\phi_1\left(\frac{\partial N_1^e}{\partial x}\cdot\frac{\partial N_1^e}{\partial x}+\frac{\partial N_1^e}{\partial y}\cdot\frac{\partial N_1^e}{\partial y}\right)+\phi_2\left(\frac{\partial N_2^e}{\partial x}\cdot\frac{\partial N_1^e}{\partial x}+\frac{\partial N_2^e}{\partial y}\cdot\frac{\partial N_1^e}{\partial y}\right)\right.$$
$$\left.+\phi_3\left(\frac{\partial N_3^e}{\partial x}\cdot\frac{\partial N_1^e}{\partial x}+\frac{\partial N_3^e}{\partial y}\cdot\frac{\partial N_1^e}{\partial y}\right)\right|A^e=0 \qquad (3.23)$$

From element e + 1 we can write:

$$K^{e+1}\left|\phi_1\left(\frac{\partial N_1^{e+1}}{\partial x}\cdot\frac{\partial N_1^{e+1}}{\partial y}+\frac{\partial N_1^{e+1}}{\partial y}\cdot\frac{\partial N_1^{e+1}}{\partial y}\right)+\phi_3\left(\frac{\partial N_3^{e+1}}{\partial x}\cdot\frac{\partial N_1^{e+1}}{\partial x}+\frac{\partial N_3^{e+1}}{\partial y}\cdot\frac{\partial N_1^{e+1}}{\partial y}\right)\right.$$
$$\left.+\phi_4\left(\frac{\partial N_4^{e+1}}{\partial x}\cdot\frac{\partial N_1^{e+1}}{\partial x}\quad\frac{\partial N_4^{e+1}}{\partial y}\cdot\frac{\partial N_1^{e+1}}{\partial y}\right)\right|A^{e+1}=0 \qquad (3.24)$$

From element e + 2 we can write:

$$K^{e+2}\Bigg|\phi_1\left(\frac{\partial N_1^{e+2}}{\partial x}\cdot\frac{\partial N_1^{e+2}}{\partial x}+\frac{\partial N_1^{e+2}}{\partial y}\cdot\frac{\partial N_1^{e+2}}{\partial y}\right)+\phi_4\left(\frac{\partial N_4^{e+2}}{\partial x}\cdot\frac{\partial N_1^{e+2}}{\partial x}+\frac{\partial N_4^{e+2}}{\partial y}\cdot\frac{\partial N_1^{e+2}}{\partial y}\right)$$

$$+\phi_2\left(\frac{\partial N_2^{e+2}}{\partial x}\cdot\frac{\partial N_1^{e+2}}{\partial x}+\frac{\partial N_2^{e+2}}{\partial y}\cdot\frac{\partial N_1^{e+2}}{\partial y}\right)\Bigg|A^{e+2}=0 \qquad (3.25)$$

The equation for node 1 is obtained by summing the three contributions from the three surrounding elements. Combining appropriate terms, the following equation results:

$$\phi_1\Bigg\{K^eA^e\left|\frac{\partial N_1^e}{\partial x}\cdot\frac{\partial N_1^e}{\partial x}+\frac{\partial N_1^e}{\partial y}\cdot\frac{\partial N_1^e}{\partial y}\right|+K^{e+1}A^{e+1}\left(\frac{\partial N_1^{e+1}}{\partial x}\cdot\frac{\partial N_1^{e+1}}{\partial x}+\frac{\partial N_1^{e+1}}{\partial y}\cdot\frac{\partial N_1^{e+1}}{\partial y}\right)$$

$$+K^{e+2}A^{e+2}\left|\frac{\partial N_1^{e+2}}{\partial x}\cdot\frac{\partial N_1^{e+2}}{\partial x}\quad\frac{\partial N_1^{e+2}}{\partial y}\cdot\frac{\partial N_1^{e+2}}{\partial y}\right|\Bigg\}$$

$$+\phi_2\left\{K^eA^e\left|\frac{\partial N_2^e}{\partial x}\cdot\frac{\partial N_1^e}{\partial x}+\frac{\partial N_2^e}{\partial y}\cdot\frac{\partial N_1^e}{\partial y}\right|+K^{e+2}A^{e+2}\left|\frac{\partial N_2^{e+2}}{\partial x}\cdot\frac{\partial N_1^{e+2}}{\partial x}+\frac{\partial N_2^{e+2}}{\partial y}\cdot\frac{\partial N_1^{e+2}}{\partial y}\right|\right\}$$

$$+\phi_3\left\{K^eA^e\left|\frac{\partial N_3^e}{\partial x}\cdot\frac{\partial N_1^e}{\partial x}+\frac{\partial N_3^e}{\partial y}\cdot\frac{\partial N_1^e}{\partial y}\right|+K^{e+1}A^{e+1}\left|\frac{\partial N_3^{e+1}}{\partial x}\cdot\frac{\partial N_1^{e+1}}{\partial x}+\frac{\partial N_3^{e+1}}{\partial y}\cdot\frac{\partial N_1^{e+1}}{\partial y}\right|\right\}$$

$$+\phi_4\Bigg\{K^{e+1}A^{e+1}\left|\frac{\partial N_4^{e+1}}{\partial x}\cdot\frac{\partial N_1^{e+1}}{\partial x}+\frac{\partial N_4^{e+1}}{\partial y}\cdot\frac{\partial N_1^{e+1}}{\partial y}\right|$$

$$+K^{e+2}A^{e+2}\left|\frac{\partial N_4^{e+2}}{\partial x}\cdot\frac{\partial N_1^{e+2}}{\partial x}+\frac{\partial N_4^{e+2}}{\partial y}\cdot\frac{\partial N_1^{e+2}}{\partial y}\right|\Bigg\}$$

$$=0 \qquad (3.26)$$

For node 2 :

$$\phi_1\left\{K^e A^e\left|\frac{\partial N_1^e}{\partial x}\cdot\frac{\partial N_2^e}{\partial x}+\frac{\partial N_1^e}{\partial y}\cdot\frac{\partial N_2^e}{\partial y}\right|+K^{e+2}A^{e+2}\left|\frac{\partial N_1^{e+2}}{\partial x}\cdot\frac{\partial N_2^{e+2}}{\partial x}+\frac{\partial N_1^{e+2}}{\partial y}\cdot\frac{\partial N_2^{e+2}}{\partial y}\right|\right\}$$

$$+\phi_2\left\{K^e A^e\left|\frac{\partial N_2^e}{\partial x}\cdot\frac{\partial N_2^e}{\partial x}+\frac{\partial N_2^e}{\partial y}\cdot\frac{\partial N_2^e}{\partial y}\right|+K^{e+2}A^{e+2}\left|\frac{\partial N_2^{e+2}}{\partial x}\cdot\frac{\partial N_2^{e+2}}{\partial x}+\frac{\partial N_2^{e+2}}{\partial y}\cdot\frac{\partial N_2^{e+2}}{\partial y}\right|\right\}$$

$$+\phi_3\left\{K^e A^e\left|\frac{\partial N_3^e}{\partial x}\cdot\frac{\partial N_2^e}{\partial x}+\frac{\partial N_3^e}{\partial y}\cdot\frac{\partial N_2^e}{\partial y}\right|\right\}$$

$$+\phi_4\left\{K^{e+2}A^{e+2}\left|\frac{\partial N_4^{e+2}}{\partial x}\cdot\frac{\partial N_2^{e+2}}{\partial x}+\frac{\partial N_4^{e+2}}{\partial y}\cdot\frac{\partial N_2^{e+2}}{\partial y}\right|\right\}=0 \qquad (3.27)$$

For node 3 :

$$\phi_1\left\{K^e A^e\left|\frac{\partial N_1^e}{\partial x}\cdot\frac{\partial N_3^e}{\partial x}+\frac{\partial N_1^e}{\partial y}\cdot\frac{\partial N_3^e}{\partial y}\right|+K^{e+1}A^{e+1}\left|\frac{\partial N_1^{e+1}}{\partial x}\cdot\frac{\partial N_3^{e+1}}{\partial x}+\frac{\partial N_1^{e+1}}{\partial y}\cdot\frac{\partial N_3^{e+1}}{\partial y}\right|\right\}$$

$$+\phi_2\left\{K^e A^e\left|\frac{\partial N_2^e}{\partial x}\cdot\frac{\partial N_3^e}{\partial x}+\frac{\partial N_2^e}{\partial y}\cdot\frac{\partial N_3^e}{\partial y}\right|\right\}$$

$$+\phi_3\left\{K^e A^e\left|\frac{\partial N_3^e}{\partial x}\cdot\frac{\partial N_3^e}{\partial x}+\frac{\partial N_3^e}{\partial y}\cdot\frac{\partial N_3^e}{\partial y}\right|+K^{e+1}A^{e+1}\left|\frac{\partial N_3^{e+1}}{\partial x}\cdot\frac{\partial N_3^{e+1}}{\partial x}+\frac{\partial N_3^{e+1}}{\partial y}\cdot\frac{\partial N_3^{e+1}}{\partial y}\right|\right\}$$

$$+\phi_4\left\{K^{e+1}A^{e+1}\left|\frac{\partial N_4^{e+1}}{\partial x}\cdot\frac{\partial N_3^{e+1}}{\partial x}+\frac{\partial N_4^{e+1}}{\partial y}\cdot\frac{\partial N_3^{e+1}}{\partial y}\right|\right\}=0 \qquad (3.28)$$

For node 4 :

$$\phi_1\left\{K^{e+1}A^{e+1}\left[\frac{\partial N_1^{e+1}}{\partial x}\cdot\frac{\partial N_4^{e+1}}{\partial x}+\frac{\partial N_1^{e+1}}{\partial y}\cdot\frac{\partial N_4^{e+1}}{\partial y}\right]\right.$$

$$\left.+\,K^{e+2}A^{e+2}\left[\frac{\partial N_1^{e+2}}{\partial x}\cdot\frac{\partial N_4^{e+2}}{\partial x}+\frac{\partial N_1^{e+2}}{\partial y}\cdot\frac{\partial N_4^{e+2}}{\partial y}\right]\right\}$$

$$+\,\phi_2\left\{K^{e+2}A^{e+2}\left[\frac{\partial N_2^{e+2}}{\partial x}\cdot\frac{\partial N_4^{e+2}}{\partial x}+\frac{\partial N_2^{e+2}}{\partial y}\cdot\frac{\partial N_4^{e+2}}{\partial y}\right]\right\}$$

$$+\,\phi_3\left\{K^{e+1}A^{e+1}\left[\frac{\partial N_3^{e+1}}{\partial x}\cdot\frac{\partial N_4^{e+1}}{\partial x}+\frac{\partial N_3^{e+1}}{\partial y}\cdot\frac{\partial N_4^{e+1}}{\partial y}\right]\right\}$$

$$+\,\phi_4\left\{K^{e+1}A^{e+1}\left[\frac{\partial N_4^{e+1}}{\partial x}\cdot\frac{\partial N_4^{e+1}}{\partial x}+\frac{\partial N_4^{e+1}}{\partial y}\cdot\frac{\partial N_4^{e+1}}{\partial y}\right]\right.$$

$$\left.+\,K^{e+2}A^{e+2}\left[\frac{\partial N_4^{e+2}}{\partial x}\cdot\frac{\partial N_4^{e+2}}{\partial x}+\frac{\partial N_4^{e+2}}{\partial y}\cdot\frac{\partial N_4^{e+2}}{\partial y}\right]\right\}$$

$$=0 \qquad (3.29)$$

The four equations, one for each node can be put in matrix form as follows:

$$\begin{vmatrix} e,\ e+1,\ e+2 & e,\ e+2 & e,\ e+1 & e+1,\ e+2 \\ e,\ e+2 & e,\ e+2 & e & e+2 \\ e,\ e+1 & e & e,\ e+1 & e+1 \\ e+1,\ e+2 & e+2 & e+1 & e+1,\ e+2 \end{vmatrix} \begin{vmatrix} \phi_1 \\ \phi_2 \\ \phi_3 \\ \phi_4 \end{vmatrix} = \begin{vmatrix} 0 \\ 0 \\ 0 \\ 0 \end{vmatrix} \qquad (3.30)$$

where the e, $e + 1$, $e + 2$ represent a contribution from the element of the same label. The i^{th} row can be seen to represent the equation for the i^{th} node and the j^{th} column contains entries corresponding to the coefficient of the j^{th} head value.

Matrix Solution

Figure 3-3 illustrates the matrix form of equation (3.19).

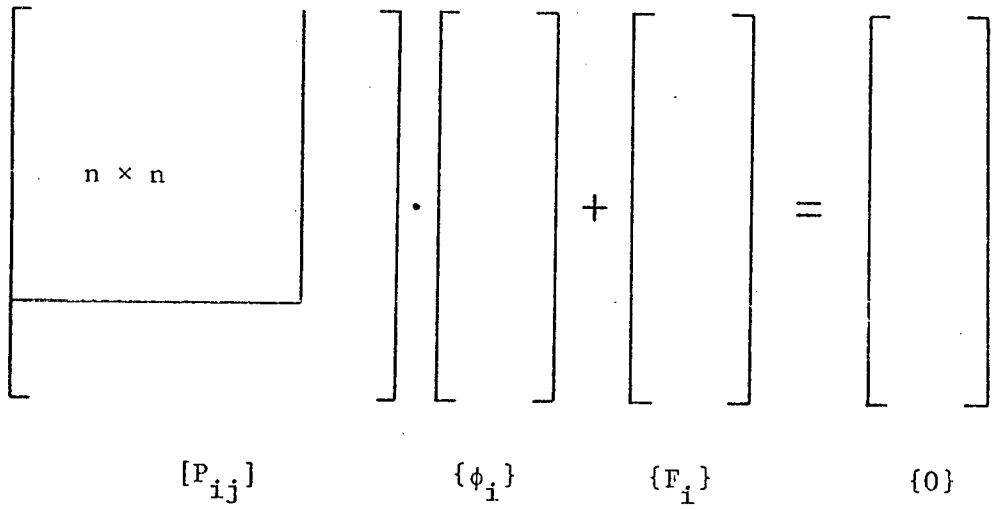

Figure 3-3 Matrix form of equation (3.19)

$[P]$, the matrix of coefficients is dimensioned $m \times m$ where m is the total number of nodes in the region. $\{\phi\}$ is a vector of mostly unknown head values and $\{F\}$ is a vector of constants which depend on the boundary conditions. $[P]$ can be partitioned into two parts of which one consists of a smaller $n \times n$ matrix where n is the toal number of unknowns. In numbering the nodes, the known values are numbered last.

It is then a simple matter of multiplying the known head values by the appropriate coefficients in the part of $[P_{ij}]$ where $0 < i \leq n$ and $n < j \leq m$. For each row "i" the resulting products can be summed, added to F_i and transferred to the right hand side of the equation. The resulting equation is of the form

$$[A] \cdot \{\phi\} = \{B\} \tag{3.31}$$

Where $[A]$ is an $n \times n$ matrix of coefficients, $\{\phi\}$ is a vector of n unknown head values and $\{B\}$ is a vector of known constants.

Standard computer programs can be used to solve for $\{\phi\}$. Such programs are commonly based on Cholesky Decomposition or Gaussian Elimination. The subroutine called by the program used in this study is based on Gaussian elimination (Bird, 1975, p. 42). Kreysig (1972) discusses the theory of the various numerical techniques.

Heterogeneity and Anisotropy

Within any element, physical properties are considered homogeneous (isotropic or anisotropic). However, from element to element, properties can vary widely allowing one to model heterogeneity.

If the principle directions of any given anisotropic element coincide with the global coordinates, equation (3.19) holds. If not, a coordinate transformation is required. Zienkiewicz (1971, p. 301) point out that an important difference arises here from the structural situation. As the matrix of coefficients [P] defines relationships between scalar

quantities, it is equally valid whatever the orientation of the local axes. Thus, use of local axes does not require a matrix transformation or a change in the assembly technique.

For any element, a local coordinate system can be defined, skewed appropriately from the global coordinate system. Within that element, equation (3.19) is valid relative to the local coordinate system and contributions to the nodal equations can be calculated and added in as before. Figure 3-4 illustrates the simple trigonometry used to define nodal coordinates relative to axes coincident with the local principal directions of hydraulic conductivity.

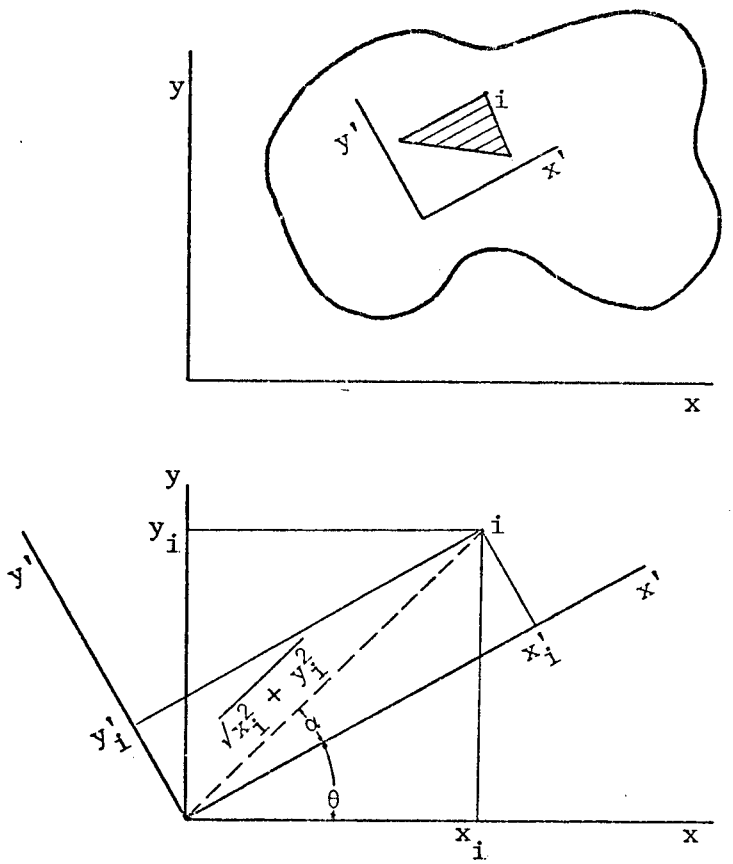

Figure 3-4 Trigonometry used in defining nodal coordinates in terms of a local coordinate system.

The origin at $(0,0)$ is kept fixed and the local coordinate axes are skewed an angle of θ from the global coordinates. The following relationships hold:

$$\alpha + \theta = \tan^{-1} \frac{y_i}{x_i} \tag{3.32}$$

$$\alpha = \tan^{-1} \frac{y_1}{x_1} - \theta_1 \tag{3.33}$$

$$x_i' = \sqrt{x_i^2 + y_i^2} \cos \alpha \tag{3.34}$$

$$y_i' = \sqrt{x_i^2 + y_i^2} \sin \alpha \tag{3.35}$$

Equation (3.19) is solved for the transformed element in terms of x_i', x_j', x_k' and y_i', y_j', y_k' where the subscripts i, j, and k label the three vertices. Such a transformation imposes the restriction on data that x and y coordinates must be greater than zero.

CHAPTER FOUR: LIMITING ASSUMPTIONS AND HYDRAULIC CONDUCTIVITY

Limiting Assumptions

A number of assumptions underlie the theory presented in the previous chapter. In creating models of groundwater flow systems for studies of engineering significance, it is essential to understand these limiting assumptions. In the following paragraphs, eight assumptions are stated, underlined, and briefly discussed.

The models are fully saturated with the top flow boundary corresponding to the water table. Freeze and Witherspoon (1966) point out that in the rigorous approach the entire saturated-unsaturated system should be considered as continuous and the ground surface should be used as the upper boundary of flow. Although possible for soils (Freeze, 1971a, 1971b), the approach requires knowing the rather complex relationship between permeability and soil moisture content in the unsaturated zone. Such data are difficult to obtain and not commonly available. Further, I know of no work that has investigated flow in unsaturated fractured rock. In any case, the assumption is often quite reasonable for regional studies because the thickness of the unsaturated zone is small compared to the total thickness of a groundwater basin and therefore the effects of the unsaturated flow are probably small.

The position of the water table must be known and in most cases is chosen as the ground surface. From an engineering point of

view, choosing the ground surface as the water table is valid because it represents the worst case. In fact, for many situations, this condition may also be the most reasonable one to assume as stability problems often occur after heavy rains or during snow-melt when saturation would extend to the ground surface.

The models are steady-state. This means that boundary conditions and therefore the potential distribution are assumed to be time-independent. Freeze and Witherspoon (1966) rationalize the approximation of transient by steady-state conditions on the following basis:

1. For the regional scale of most investigations, the differences of a few feet between high water and low water positions of the water table will have little effect on flow patterns.

2. The relative configuration of the water table usually remains the same throughout the cycle of fluctuations; that is, high points remain the highest and low points remain the lowest.

It may be that for some slope stability problems, transient effects of water table fluctuations are important, but again, by considering the steady, fully saturated condition, the worst case is covered.

The models are two-dimensional. This assumption is equivalent to assuming a negligible gradient in the third dimension. For the homogeneous isotropic case this requirement leads to the result that flow in the third dimension is also zero. However, for anisotropic media, having the gradient zero in the third dimension does not necessarily mean that flow is zero in the third dimension. Flow in the third dimension will vanish only if the plane of the model coincides with two of the principal axes. This restriction is discussed in detail by Bear (1972 p. 142). In complex geologies it will not always be possible to

fulfill this restriction and some error will be introduced into the models. I know of no sensitivity analysis which has established the magnitude of the error. The best that can be done at present is to minimize the error by taking the two-dimensional section perpendicular to the contours of the water table surface.

The model boundaries are either a specified constant head (Dirichlet condition) or constant flux (Neuman condition). A special case of the Neuman condition is when the flux equals zero, corresponding to an impermeable boundary. The top flow boundary is either the assumed constant head water table or assumed flux boundary. It can be chosen to reasonably approximate field conditions. By constant head, it is not meant that the head on the water table is everywhere the same but rather the head at any point on the water table is kept constant with time. The side and bottom model boundaries cannot be observed in the field and their choice requires some explanation.

The sides are usually chosen as vertical impermeable boundaries corresponding to groundwater divides. This is an application of image theory which is valid provided the groundwater divide is indeed straight and vertical. This suggests a symmetry rarely met by field conditions, particularly in regions of complex geology. In fact, the assumption holds only under mountains or valleys exhibiting symmetric topography and underlain by a homogeneous, isotropic, porous media. A number of examples of irregular and perhaps more realistic groundwater divides can be drawn for the models described in the next chapter (Figures 5-3 to 5-11).

The difficulty can be overcome in two ways. Firstly a person experienced in modelling real cases may, with a knowledge of geologic conditions and resulting hydraulic properties, be able to estimate a reasonable position for a groundwater divide. The resulting irregular boundary can be easily handled by the finite element program. However, in some cases such a guess could be inaccurate. A second way, used in this project, is to model a large enough region so that incorrect boundary effects will not be felt in the local area of interest.

The choice of a horizontal impermeable boundary at depth is discussed by Freeze and Witherspoon (1967). At some depth, permeabilities will be lower than in the near surface units and at this point equipotentials become vertical. The lower boundary of the higher permeability unit acts like an impermeable boundary and the addition or deletion of the lower, less permeable unit has a negligible effect on the potential pattern. In designing a model for a given basin, they suggest that

> preliminary studies should probably begin with a greater basin depth than would seem necessary ... if one finds vertical equipotentials as suggested above, the basin depth can be limited accordingly.

Many investigators (for example, Davis, 1969) have noted the apparent decrease in permeability of rock with depth. This observation certainly substantiates the above reasoning. However, assuming a decrease in permeability or hydraulic conductivity with depth may not always be a reasonable assumption. Snow (1968) and Brace and Martin (1968), amongst others, discuss the dependence of permeability on effective stress, especially in rock. Because effective stress does not

always decrease with depth, there may be some, perhaps many geologic situations where permeability increases rather than decreases with depth.

Such a situation, however, requires a deforming media. The models used in this study are based on the assumption that the continuous porous media is rigid. Of all the assumptions, this may be the most difficult to defend. The models described in the next chapter illustrate a number of cases that could lead to local developments of high pore pressures and subsequent slope failures. In fact, what may actually happen is that increases in pore pressure may be limited to the point at which the accompanying decrease in effective stress is enough to cause a small local failure. An instantaneous increase in permeability results, pressures are relieved and effective stress is increased, which in turn causes an increase in stability. Snow (1968) discusses the elasticity of fractured media in response to fluid pressure changes and gives evidence for "fracture breathing". This possibility does not invalidate the results of modelling rigid media, but it may be cause for modification of some of the results. The topic of flow in deformable media is presently an active area of research (for example, see Gale, 1975). With greater understanding it may be possible to modify regional groundwater models accordingly. For the present, one can rationalize the rigid media assumption, particularly for engineering studies, by stating that the worst situation is being modelled and in any case the problem areas are being identified.

One of the most fundamental assumptions is that groundwater flow through porous media can be described by Darcy's Law. Bear (1972,

p. 127) distinguishes three types of fluid flow: linear laminar flow, nonlinear laminar flow, and nonlinear turbulent flow. Darcy's Law holds only for low velocities and head gradients when flow of the first type exists. For groundwater flow systems associated with most geologic situations, this is a reasonable assumption. For nonlinear laminar and turbulent flow, a number of power-law relationships have been proposed. These are also discussed by Bear (1972, p. 182).

One final and important assumption remains to be discussed: the geologic case being modelled can be reasonably approximated by an equivalent, continuous porous media. It is clear that examples exist for which an equivalent porous media cannot be assumed and in modelling groundwater flow systems for slope stability analyses these must be recognized. Certainly models of large regions which include highly fractured or otherwise porous geologic units can be reasonably modelled as a continuous porous media, while a small slope of sound rock cut by a few fractures cannot. Louis is quoted by Londe (1971, p. 3) as suggesting that for a given cross-section of rock, an equivalent porous media can be assumed only if the number of fissures cut by the cross-section is of the order 10,000. Although principles of flow through porous media are well established, the principles governing flow through a fractured media that cannot be approximated by an equivalent porous media are not. The problem is discussed by many investigators including Castillo (1972), Gale (1975), Londe (1971), Louis (1969), Louis and Pernot (1972), Sharp and Maini (1972), Snow (1968, 1969, 1972), Wittke (1971), Wittke and Louis (1966) and Wittke et al (1972). It is not possible at the present time to make generalizations about the validity

of this assumption. Rather, each model must be judged independently on the basis of the geologic conditions encountered.

Hydraulic Conductivity

Under the set of assumptions described above, the only material property that requires specification is the hydraulic conductivity. The hydraulic conductivity "K" is the coefficient of proportionality which appears in Darcy's Law. It reflects both properties of the fluid and the solid matrix and is not to be confused with the intrinsic permeability, "k", which is a property of the matrix only. The two are related by

$$K = k \frac{\gamma}{\mu} \tag{4.1}$$

where γ is the specific weight of the fluid and μ is the viscosity. Confusion has arisen in the past because the term "coefficient of permeability" has been applied to the hydraulic conductivity.

Figure 4-1 gives approximate ranges of hydraulic conductivity for different rock types and unconsolidated materials. This figure was used to obtain a first estimate of relative conductivities between different geologic units. However, in some cases, hydraulic conductivities were assigned on a basis other than lithology. Davis (1969) has pointed out that in many cases weathering history and fracturing are more significant to hydraulic characteristics than lithologies.

Interestingly, it is not the absolute values of hydraulic conductivity that control the form of the potential nets described in

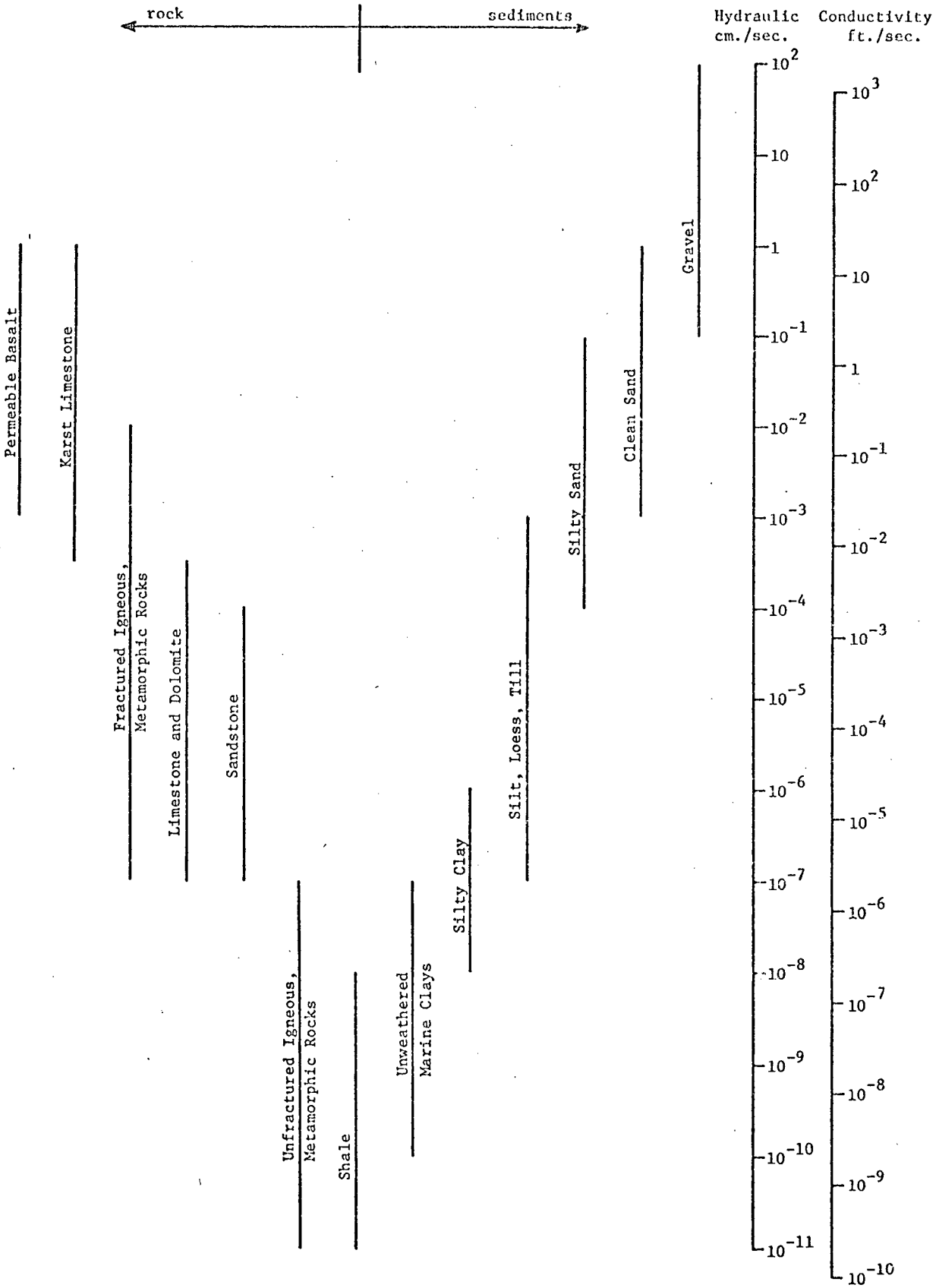

Figure 4-1. Approximate ranges of hydraulic conductivity (Freeze, 1976, personal communication).

the next chapter, but rather the relative conductivities between units. For practical application, it may be more accurate to estimate order-of-magnitude differences in hydraulic conductivity rather than exact values and be able to produce a reasonable model of the flow system even though exact hydraulic conductivities are not known.

CHAPTER FIVE: MODEL RESULTS AND DISCUSSION

Introduction

To model the complex geologies of interest, fairly large models were required. However, because of the time required in setting up element grids and tabulating element and nodal data, the number of elements were limited to 500 and the number of nodes to 275. This resulted in a storage requirement of 162 k. Execution times were between 6 and 13 seconds, depending on the number of iterations required to achieve the desired tolerance of .001 in calculating the nodal potentials. All models were run on the IBM 370/168 at the University of British Columbia.

Gillham and Farvolden (1974) reported solution instability in their finite element flow program using single precision variables for conductivity contrasts of over 500. This required their use of double precision variables. They also found that as the number of nodes in a cross-section was increased, the solution became unstable at lower conductivity ratios. Using the matrix solution SLIMP, programmed by the UBC Computing Centre, I encountered no such difficulties. Single precision variables were used with variations in conductivity of up to six orders of magnitude. For smaller computers the storage requirement of 162 k may at present cause difficulties but storage capabilities are rapidly increasing, rendering this a temporary problem, if one at all.

Six different topographic arrangements were modelled, each with a number of different geologies exhibiting different hydraulic conductivity contrasts. In all, over 75 models were run. Figure 5-1 summarizes the models and the various principles to be illustrated. Some of these hydrogeologic settings were suggested to me by the discussion of Deere and Patton (1967).

To show the effect of different flow systems on slope stability, use is made of piezometric lines which indicate hydraulic head at the base of an arbitrary plane, perhaps a slide surface. Water would rise to the piezometric line, in an open standpipe connected only to the slide surface.

The hydraulic head "ϕ" consists of two parts:

$$\phi = z + \Psi \tag{5.1}$$

where z is the elevation head and Ψ is the pressure head. Figure 5-2 illustrates the different parts of the hydraulic head.

The pore pressure "u" found in Terzaghi's effective stress law, (2.4), is related to the pressure head by

$$u = \gamma\Psi \tag{5.2}$$

where γ is the specific weight of water. Also shown on Figure 5-2 is a plot of pressure head at the base of the slide plane. In most slope stability analyses the slide is broken into vertical slices and the pressure head is used to calculate the pore pressure acting on each slice. In practice, it is not necessary to plot a separate pressure head diagram, as a measurement of the height of the piezometric line above the slide plane can be taken directly from the numerically simulated hydraulic

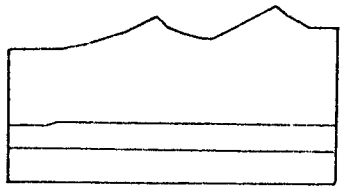

The effects of anisotropy. Figure 5-3

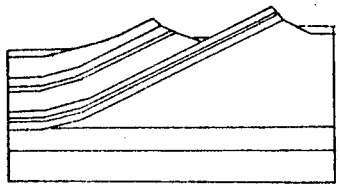

Thrusts and interbedded sedimentry rocks. Figure 5-5

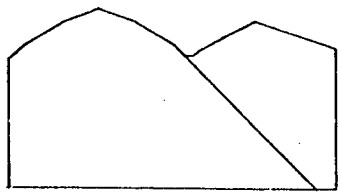

Faults, contacts, dykes and weathering profiles. Figure 5-6

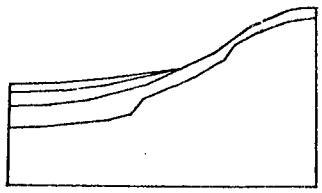

Layered colluvium and weathering profiles. Figure 5-8

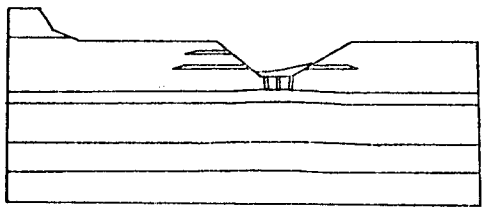

Flat lying weak rocks, fractures due to stress relief, and the effects of a regional aquifer. Figure 5-9

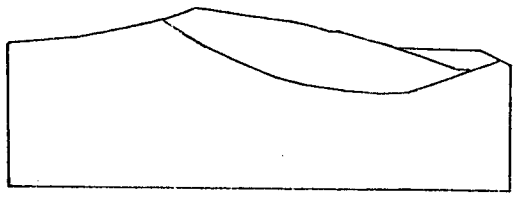

Pleistocene Terraces. Figure 5-10

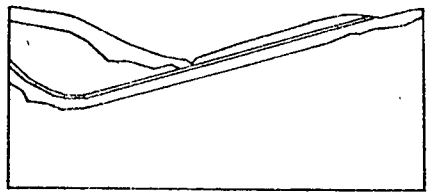

Deformed metamorphic rocks, and the effect of a reservoir on a deep rock slide. Figure 5-11

Figure 5-1. Summary of Models

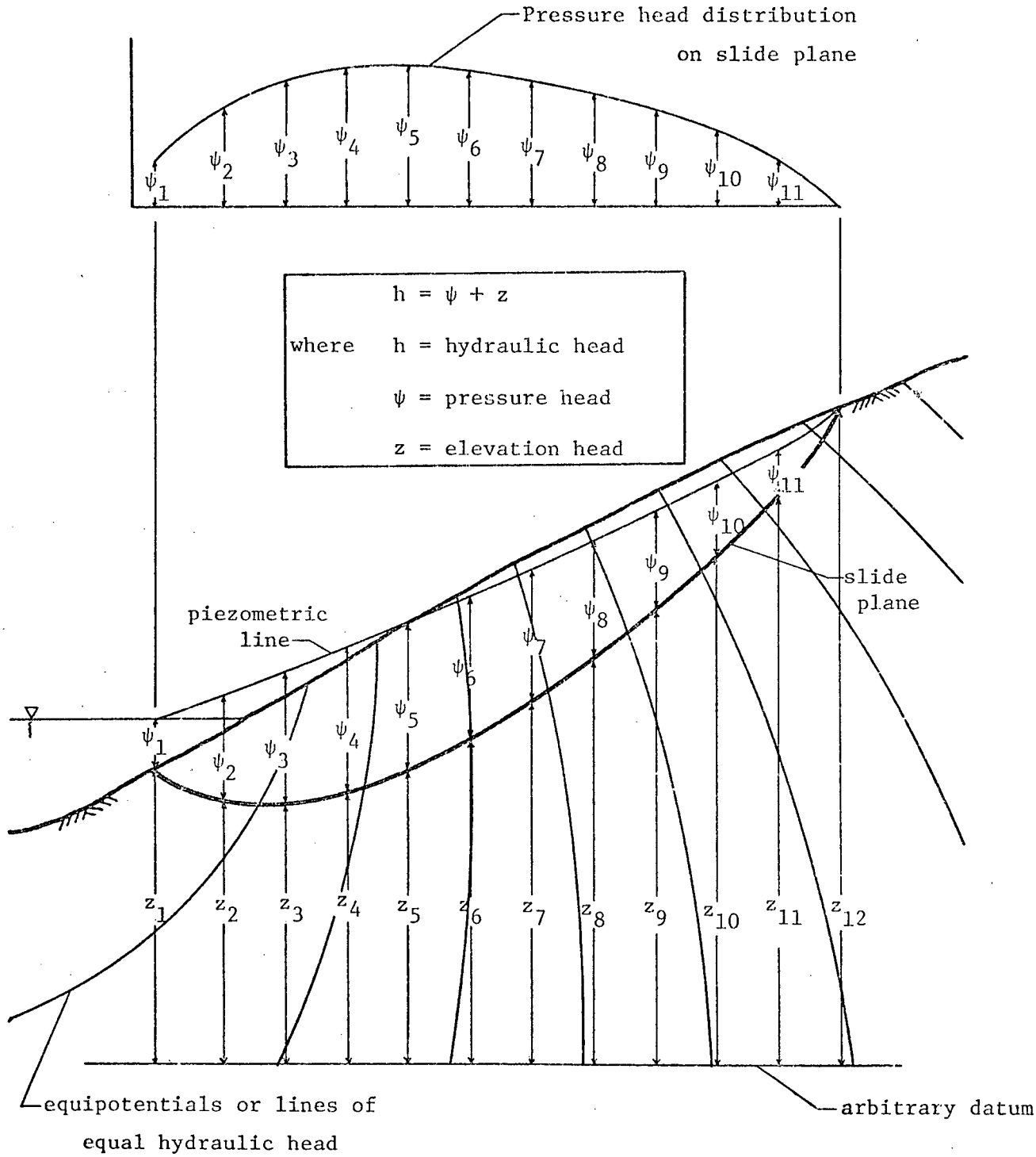

Figure 5-2. Hydraulic head, pressure head and elevation head.

head net. Slope stability formulae can be adapted to process this data directly.

The remaining figures discussed in this chapter are found in APPENDIX II. For reader convenience they should be unfolded and kept handy while reading. The various figures can be considered dimensionless and scale is presented as a multiple of an arbitrary constant. Such models can equally well represent flow patterns for systems covering only a few acres or for those extending over many hundreds of square miles (Freeze and Witherspoon, 1967).

The Effects of Anisotropy

Hydraulic characteristics of both soil and rock are more commonly anisotropic than isotropic. Maasland (1957) gives an extensive discussion of anisotropy. He points out that anisotropy in soils can be caused by stratification. An apparent directional hydraulic conductivity is created in a stratified medium which is identical to that of an anisotropic medium. The stratification may be a result of the shape of mineral grains or alternating layers of different texture. In general, horizontal conductivity is greater than vertical conductivity. He also notes that in many sedimentary rocks there may be a dissemination of very thin shale or micaceous lamination through the porous bed. In common coring techniques these laminations would cause fractures between pieces of core. Testing of the core pieces would miss the thin layers and an erroneous measurement of anisotropy would be obtained. He cites laboratory

and field evidence of anisotropy in soils with horizontal to vertical conductivity ratios ranging from 1 to 42.

Anisotropy resulting from fractures in rock is discussed by Snow (1968). He notes that "anisotropy is the rule; isotropy in fractured rocks is a special circumstance of pressure and fracture geometry."

Figure 5-3 illustrates the effects of anisotropy on the groundwater regime. As will be seen in the next section, the asymmetric topographic profile could represent a variety of cases of dipping geologic units which have been eroded to form flatirons.

The homogeneous, isotropic case is shown in Figure 5-3a, while Figures 5-3b through 5-3e illustrate an anisotropy of one order of magnitude skewed at various angles from the global coordinates. To simulate a decrease of conductivity with depth, two isotropic units underlie the anisotropic region. Note that the equipotentials tend to follow the direction of maximum hydraulic conductivity.

To consider the effect of the different orientations of anisotropy on slope stability, an arbitrary failure surface was drawn beneath the right-hand valley wall. For each figure, the piezometric line representing the hydraulic head at the base of the slide was drawn. These lines are plotted together on Figure 5-4. It can be seen that the highest hydraulic and pressure heads occur when the maximum conductivity is parallel to the dip of the slope, while the lowest occur when the anisotropy is flatlying.

If the difference in elevation between valley floor and the higher, right-hand peak is 1,000 feet, the maximum difference in pressure

head of the two extreme cases (5-3b and 5-3d) is approximately 100 feet. This represents a pore pressure difference of over 6,000 pounds per foot length of slide surface, assuming a one-foot-thick section!

The example vividly illustrates that different orientations of anisotropy can cause very different pore pressure distributions in a slope. It shows, as will the other examples to be discussed, the importance of understanding the geology and hydraulic characteristics of a large area around a slide, not just the slide itself. Interestingly, a dip slope, as well as causing the most adverse groundwater conditions, is also the weakest from a strength of rock perspective.

Thrusts and Interbedded Sedimentary Rocks

A common geologic situation occurs when thick sedimentary units are folded or thrust up from their original horizontal position. With time, the less resistant units are eroded to form valleys, while the more resistant beds form ridges or flatirons. Figure 5-5 (modified from Deere and Patton, 1967, Figure 5) shows six different models of interbedded units with a variety of conductivity contrasts. As discussed in the previous example (Figure 5-3), the dip slope is underlain by the most adverse head distribution. To compare the effects of different conductivity contrasts, piezometric lines have been plotted indicating the hydraulic head at the base of Unit A beneath the dip slope on the right-hand side of the valley.

Figure 5-5a shows what could be interbedded sandstones and shales with the more resistant sandstone occupying the ridges. The

sandstone has a conductivity two orders of magnitude greater than the shale. It is possible that a situation could exist where the more resistant capping unit is also the less conductive unit. For example, such a situation is believed to exist on Saltspring Island in the Strait of Georgia where the shale occupying the valleys has developed a secondary fracture permeability, making it more conductive than the sandstone. The groundwater regime for such an example is shown in Figure 5-5b. For comparison, the piezometric line from 5-5a is plotted on 5-5b. In both examples, high hydraulic heads exist beneath the dip slope, although in 5-5b the piezometric level is somewhat higher because of the thicker confining unit.

With a greater conductivity contrast the results are more startling. This is seen on Figure 5-5c where Unit A has been assigned a conductivity of 10^{-6}, four orders of magnitude lower than the units on either side. The resulting rise in the piezometric line is very great.

Unit A may represent a distinct lithology with low conductivity or it could represent a thrust surface. The thrusting, through production of a fault gorge could have caused the lower conductivity; or a unit of lower conductivity could have caused the high pore pressures which in turn led to the thrust faulting. This latter possibility was proposed by Hubbert and Ruby (1959). In real examples, both mechanisms might be at work and it may not be possible to isolate cause and effect. Figure 5-5c does show, however, the high fluid potentials that could develop beneath a thrust surface. It appears that the stability of enormous thrust blocks is based on the same principles as the stability of much smaller slopes.

No method has yet been developed for successfully measuring anisotropic conductivities in all geologic situations, although Louis and Pernot (1972) describe a detailed field investigation they used to establish anisotropic hydraulic characteristics in metamorphic rocks at a potential damsite. However, such detailed work is expensive and not always possible. For that reason it is often necessary to match model results with a rather scanty amount of field information. If a fit is not obtained, the model is adjusted until a fit is found. Unfortunately, in complex geologies, more than one combination of anisotropic and heterogeneous hydraulic conductivities can result in the same potential net. This problem is illustrated by Figure 5-5d, where Unit A has been assigned an anisotropic conductivity with the major axis (x') 10^{-3} and the minor axis (y'), 10^{-6}. Even with the low conductivity across the unit, the result is a similar but slightly lower piezometric line than in 5-5a, where Unit A has an isotropic conductivity of 10^{-4}. With minor adjustments to the anisotropic conductivities the two could be made the same. This results from the fact that any homogeneous anisotropic medium can be transformed into a fictitious isotropic medium (Maasland, 1957, p. 238). A general example of the transformation of an anisotropic two-layer system is described by Stevens (1936). The reader is referred to these papers for details. The lesson to be learned is that great care must be taken in adjusting models on the basis of scanty field data.

Figures 5-5e and 5-5f show an anisotropic conductivity in Unit A with a contrast of two orders of magnitude. In Figure 5-5f, however, ponded water has been introduced in the valley. Both piezometric

lines are plotted on 5-5f. The ponded water causes a significant rise in the piezometric line. It is particularly worth noting that the effect of the ponded water is felt well above the level of the water on the valley sides.

Faults, Contacts, Dykes and Weathering Profiles

Where there is extensive subsidiary fracturing, faults may take the form of high permeability conduits. Conversely, movement along a fault may cause a gouge zone of very low conductivity. Contacts can also cause a wide variety of effects on the potential distribution depending on the different lithologies in contact, their respective structures, and the nature of the contact itself. Similarly a dyke, although initially much less permeable than the surrounding country rock, may be much more susceptible to weathering and with time become more permeable than the surrounding rock. Deformation of an area intruded by less ductile dyke rocks can cause the dykes to be more permeable through a higher intensity of fracturing. Clearly, careful field investigation is required to establish the significance of any one of these features.

Figure 5-6 illustrates some of the diverse effects described above. For comparison, a plane has been drawn on the section beneath the left-hand valley wall and the piezometric lines representing the hydraulic head on this plane have been drawn for each of 5-6a through 5-6f. All the piezometric lines are drawn together on Figure 5-7.

The homogeneous isotropic case is shown in Figure 5-6a. In Figure 5-6b a less conductive unit is seen overlying another. The contact is simple. The difference is not great but the piezometric line of 5-6b is higher than 5-6a. Presumably if the conductivity contrast was greater or the orientation of the contact different, a more dramatic difference would be apparent.

In Figure 5-6c a fault zone is shown with a conductivity significantly higher than the surrounding rock units. Such a fault acts as a drain and no problems related to slope stability are apparent. In Figures 5-6d and 5-6e the fault zone has been assigned a lower conducvitity than the surrounding rock. The two differ only in that opposite conductivities have been assigned the two major rock units. In both Figures 5--6d and 5-6e the fault zone causes a higher gradient beneath the toe of the slope in the underlying rock unit. A similar situation could result from the intrusion of a less permeable dyke along the contact.

Figure 5-6f shows a situation which combines some of the features of the previous four figures. As well, a weathering profile has been added and the overlying unit has been assigned an anisotropic conductivity. The figure could represent dipping sedimentary rocks thrust against or lying unconformably on a massive intrusive rock of much lower conductivity. A deep weathering profile has developed extending much further down the fault zone or contact between the two units. The situation is reasonable for many non-glaciated areas of the world.

An extensive review of weathering profiles and their effect on flow systems and slope stability is given by Deere and Patton (1971). Table 5-1 gives their description of the parts of a weathering profile for igneous and metamorphic rocks. In many sedimentary rocks the weathering profile is similar but in carbonates the saprolite (I-C) may be absent and the partly weathered rock (II-B) may not be possible to identify. The relative permeabilities and strengths are also listed in Table 5-1. Note that the low-strength residual soils are underlain by a zone of much higher permeability. Inevitably this confining situation will lead to stability problems. The relative permeabilities suggested by Deere and Patton were used as a basis for assigning conductivity values to the various zones shown in Figure 5-6f. The toe of both slopes in the valley shows hydraulic heads detrimental to slope stability. This can be seen in Figure 5-7 by the high piezometric level of 5-6f relative to the other cases.

Layered Colluvium and Buried Weathering Profiles

The recurrence of landslides in areas of old slide debris or colluvium is a fairly common problem. In tropical areas the problem is intensified by the development of weathering profiles both on original ground surface and in subsequent layers of colluvium. The problem of slope stability in layered colluvium is discussed in detail by Deere and Patton (1971) who point out that desiccation or consolidation of the colluvium causes complex layering and that buried weathering profiles can cause examples of the classic confined artesian aquifer situation.

	Zone	Description	Relative Permeability	Relative Strength
I	RESIDUAL SOIL IA	Topsoil, roots, organic material zone of leaching and aluviation. May be porous.	medium to high	low to medium
	IB	Characteristically clay enriched with accumulations of Fe, Al, Si. May be cemented. No relict structures present.	low	commonly low, high if cemented
	IC	Saprolite. Relict rock structures retained. Silty to sandy material with less than 10% core stones. Often micaceous.	medium	low to medium; relict structures very significant
II	WEATHERED ROCK IIA	Transition from saprolite to partly weathered rock. Highly variable, soil-like to rock-like. 10% to 95% core stones with fines commonly fine to coarse sand. Spheroidal weathering common.	high	medium to low where weak structures and relict structures are present
	IIB	Partly weathered rock. Soft to hard rock. Joints stained to altered. Some alteration of feldspars and micas.	medium to high	medium to to high*
III	UNWEATHERED ROCK III	No iron stains are apparent along joints. No weathering of feldspars and micas.	low to medium	very high*

* Considering only intact rock masses with no adversely oriented geologic structures.

Table 5-1. Weathering Profile for Igneous and Metamorphic Rocks after Deere and Patton (1971, p. 92)

Figure 5-8 is an attempt to illustrate the groundwater flow system in such an environment. The basis of the models is Figure 8 of Deere and Patton (1971, p. 108). Figure 5-8a is the homogeneous isotropic case. A single layer of colluvium over a dipping anisotropic rock unit is shown in Figure 5-8b. The colluvium covers a simplified weathering profile. In the weathering profile, conductivities have been adjusted where appropriate, but the anisotropy has been maintained. In Figure 5-8c the single layer of colluvium has been split by Unit A, which represents a partial weathering profile developed on a lower layer of colluvium. Its effect is a zone of lower conductivity. Unit A confines the lower colluvium layer and high pore pressures have developed. For comparison, the piezometric line representing the hydraulic head at the base of Unit A has been plotted for each model. Also plotted is a dashed line representing the weight of overburden above the base of Unit A. A specific weight of 130 pounds per cubic foot has been assumed and the line plotted in terms of an equivalent height of water. If overburden weight becomes less than pore pressures the dashed line will dip below the piezometric line. An example of this is shown in Figure 5-8c and is labelled an area of instability. In real cases, failure would probably occur before such a large discrepancy between the two lines developed. However, the effect of the buried weathering profile has been clearly demonstrated.

Flatlying Weak Rocks, Fractures Due to Stress Relief and the Effects of a Regional Aquifer

Matheson and Thomson (1973) have investigated the occurrence in central Alberta of valley rebound due to stress relief. The rebound was accompanied by interbed slip that would give rise to gouge zones in valley walls. Ferguson (1967, 1974) describes similar rebound phenomena in the Allegheny Plateau region where he found compression faults in the valley bottoms and tension fractures in the valley walls. Patton and Hendron (1974) discuss the above phenomena and further point out the effect of high fluid pressures on valleys in groundwater discharge areas. Figure 5-9 shows three models which illustrate the groundwater regime for an area which exhibits some of these features. The basis for the models is Figure 5 of Patton and Hendron (1974, p. 10).

The models are of a valley cut into flatlying sandstones and shales. The position of the water table below the ground surface has been assumed. For comparison between models, the pressure head distribution on a wedge in the valley wall is shown.

The isotropic homogeneous case is shown in Figure 5-9a. In 5-9b the sandstone and shale units have been introduced with a conductivity contrast of two orders of magnitude. Rebound beneath the valley due to stress relief is indicated by a slight upwarping of the units. Lower conductivity zones, parallel to bedding and somewhat exaggerated from the mylonitic zones described by Patton and Hendron (1974) or the gouge zones of Matheson and Thomson (1973) are seen in the valley walls. Beneath the valley floor are faults due to heaving. Clearly the flow

regime is detrimental to the stability of the valley walls, particularly in the circled areas above the horizontal gouge zones which act to train the groundwater into the valley.

The groundwater regime is even more detrimental to stability in Figure 5-9c where an increased head has been assigned to the left boundary of the thinner sandstone unit, giving it the role of a regional aquifer. Beneath the valley, the increase of hydraulic head with depth is much greater than in the two previous figures. Because of their orientation perpendicular to the equipotentials, the vertical faults in the base of the valley have little effect on the flow system. However, the effect of the horizontal gouge zones is pronounced. Comparison of the pressure head distribution on the wedges from the three models clearly illustrates the influence on slope stability that the various groundwater regimes would have. Also, note the non linear distribution of pressure head on the wedge, different from the commonly assumed linear distributions.

Pleistocene Terraces

In many parts of central British Columbia distinct terraces are found on the sides of present-day river valleys. They are usually a result of glaciofluvial, glaciolacustrine, or alluvial processes and consist of a varying amount of clay, silt, sand and gravel, depending on their origin. Good examples are found in the Fraser Valley,

Thomson Valley and throughout the Okanagan. If water is available for irrigation, they provide ideal farming sites. Roads and railways take advantage of the terraces when possible, but in many places it is necessary for them to traverse a slope beneath a terrace. Stability problems in the unconsolidated terrace sediments are fairly common. Deere and Patton (1967) discuss the stability of varved clay terraces.

The models presented in Figure 5-10 approximate an area adjacent to Trout Creek in Summerland, Southern Okanagan, B.C., where a slide was initiated about 60 years ago and is still moving. This "perpetual landslide" has been studied in detail by Riglin (1976). For Figure 5-10, pre-slide topography was estimated. Although the details of the geology are from the Trout Creek area, the intent is to illustrate a geologic environment and associated groundwater flow system that is similar to many places.

The isotropic, homogeneous case is shown in Figure 5-10a. Simplified versions of the geology are shown in Figures 5-10b and 5-10c. Volcanic rocks (Unit A) overlie less conductive granodiorite (Unit B). The terrace sediments consist of a lowermost group of Tertiary sediments (Unit C), a flatlying layer of less conductive till or silt (Unit D), and an upper zone of sands and gravels (Unit E). In Figure 5-10c the volcanics have been assigned an anisotropic conductivity.

In Figure 5-10d, Units C and D have also been given anisotropic conductivities, the water table in the sands and gravels has been lowered to a more realistic level, and a less conductive unit has been added representing the possible effects of a buried weathering profile on the top of the granodiorite.

This same case is shown in Figure 5-10e except that irrigation of a section of the terrace has been simulated by raising the water table back to the ground surface. In Figure 5-10f the unit representing the weathering profile has been assigned a conductivity higher than the surrounding rocks, perhaps representing a grus developed on the granodiorite. In the same figure, part of Unit C, the Tertiary sediments have also been given a higher conductivity.

To compare the effects of the different flow systems, an arbitrary, initial slide surface was drawn, piezometric lines established, and stability analyses undertaken for the models shown in Figures 5-10a, 5-10c, 5-10d and 5-10f. No attempt was made to find the most critical slide surface although the failure surface used is similar in form to the slide surface that has developed at the Trout Creek locality. Figures 5-10b and 5-10e are exactly the same, in the area of the slide, as 5-10c and 5-10f respectively, rendering analyses unnecessary.

The technique of analysis used is a simplified limit equilibrium method described by Patton and Hendron (1974). The slide is broken into slices and for each slice shearing forces parallel to the base and resisting forces parallel to the base are calculated. For the entire slide, resisting forces are summed and compared to shearing forces to calculate a factor of safety. Interslice forces are considered to sum to zero and moments are not considered. The method is appropriate for a first estimate of the stability. The absolute values of the factors of safety may not be exact but the relative values are useful for comparison.

In calculating factors of safety, it is first necessary to decide on a base model, assign it a factor of safety of one and back-calculate for the angle of internal friction, phi. This phi value is then used in the remaining factor of safety calculations. Another way of comparison is to calculate in each case the phi required for a factor of safety of one. These phi values can then be compared to each other, to laboratory data, or to values reported in the literature. In this way, both the validity of the model can be checked and the significance of the different flow systems can be judged.

Results of the calculations are given in Table 5-2. For the lower water table shown in Figures 5-10e and 5-10f, a phi value of only 10.9 - 11.3^{o} is required, while the saturated cases of Figures 5-10a and 5-10c require phi values of 15.5 - 17.3^{o} for stability. Lab testing by Riglin (1976) of the remoulded material from the slide plane of Trout Creek resulted in a phi value of 18^{o}. This value indicates that a more critical slide surface probably exists for which a higher phi value is required for stability than suggested by my calculations. Nevertheless, 18^{o} is close and with changes in the flow system causing a 55% range in the factor of safety (.89 to 1.44), it is reasonable to conclude that changes in the pressure head due to flow system variations could cause the terrace to fail.

Many similar situations probably exist in British Columbia and other parts of the world. In all cases, the nature of the regional flow system and the position of the terrace in the regional system are critical to understanding and improving stability.

Case	Factor of Safety for PHI = 15.5°	PHI for Factor of Safety = 1.0
Figure 5-10a	1.0	15.5°
Figure 5-10c	.89	17.3°
Figure 5-10d	1.39	11.3°
Figure 5-10f	1.44	10.9°

Table 5-2. Results of Stability Analysis of a Pleistocene Terrace (Figure 5-10). Slice geometry is shown in the figure. A specific weight of 130 pounds per cubic foot was used.

Deformed Metamorphic Rocks and the Effect of a Reservoir on a Deep Rock Slide

The hydraulic characteristics of metamorphic rocks have not, to my knowledge, been studied in great detail. Polyphase deformation can cause complex fold patterns and different lithologies with very different conductivities may be arranged in patterns only understandable after detailed local and regional mapping. In some cases it may not be possible to reasonably model all the complexities. On the other hand, metamorphic rocks often exhibit a surprisingly consistent foliation defined by microfaults or fractures, preferred orientation of inequant minerals, laminar mineral aggregates or a combination of these microstructures (Hobbs et al, 1976). In many cases the foliation is inclined to original bedding. Such a consistent foliation may be much more critical to the groundwater regime than lithologic differences and its

presence may make possible reasonable modelling of a seemingly complex region.

The models shown in Figure 5-11 are intended to illustrate a metamorphic terrain with a consistent foliation that has itself been gently folded in a broad antiform. The groundwater regime of the different models will be compared by considering the piezometric line representing the pressure head at the base of a deep-seated potential rock slide on the dip slope of the valley. Each different geologic situation is shown with and without a reservoir covering a small portion of the toe. Each figure illustrating the reservoir case also includes the piezometric line from the non-reservoir case. Figure 5-12 is a compilation of all the piezometric lines.

Figure 5-11a is the homogeneous isotropic case with no reservoir, while Figure 5-11b is the matching reservoir case. In Figure 5-11c an anisotropy has been introduced to represent the foliation. Davis (1969) notes that reliable field measurement of anisotropy in dense rocks is virtually lacking but goes on to describe a case where permeability was approximately twice as large in the direction of schistocity as it was perpendicular. Lacking better information, this anisotropy was used. The introduction of even this slight anisotropy causes a noticeable rise in the piezometric line. The effect of the reservoir, Figure 5-11d, is more pronounced than in the previous pair.

In Figure 5-11e and 5-11f a more conductive zone has been introduced near the surface, representing a higher fracture frequency due to stress relief and weathering. It has a moderating influence on the piezometric line.

A through-going, less permeable zone is seen in Figure 5-11g. Compared to the surrounding rock, conductivity across the foliation has been reduced by ten, while along the foliation only by four. This zone represents a through-going, more schistose layer, perhaps a thrust surface, that could provide the necessary slide plane for instability to occur. The resulting rise in piezometric surface in both 5-11g and 5-11h, the matching reservoir case is dramatic.

To show the sensitivity of the groundwater flow system to conductivity contrasts, another model was run like 5-11g but with a reduction by ten of the conductivity in the schistose zone. It is shown in Figure 5-11i. The resulting piezometric line is almost twice the height of the previous pair, above the slide plane.

The thrust surface and the more conductive zone representing fractures and weathering near the ground surface are combined in Figures 5-11j and 5-11k. Again, the more conductive surface zone has a moderating influence on the piezometric line.

A zone three times higher in conductivity than the country rock has been added beneath the thrust surface in Figures 5-11ℓ and 5-11m. Such a zone may be due to subsidiary fracturing or perhaps a different lithology. By comparing the piezometric line of 5-11ℓ to that of 5-11j (non-reservoir cases) and 5-11m to that of 5-11k (reservoir cases), on Figure 5-12 it can be seen that the confined, more conductive zone causes a small but measurable rise in the piezometric surface.

To further illustrate the effect of the different groundwater flow regimes on the potential rock slide, a stability analysis was carried out for each case. The procedures outlined in the previous section were used. The results are summarized in Table 5-3.

Case	Factor of Safety for PHI = 31.9°	PHI for Factor of Safety = 1.0
5-11a	1.0	31.9
5-11b	.99	32.1
5-11c	.97	32.8
5-11d	.94	33.6
5-11e	1.04	30.9
5-11f	1.02	31.4
5-11g	.79	38.1
5-11h	.74	40.0
(5-11i)	(.26)	(67.3)
5-11j	.88	35.3
5-11k	.85	36.1
5-11ℓ	.78	38.7
5-11m	.76	39.2

Table 5-3. Results of stability analysis of a potential rock slide in metamorphic terrain. Slice geometry is shown in Figure 5-12. A specific weight of 170 pounds per cubic foot was used.

With the exception of 5-11i, factors of safety vary from .74 to 1.04, a range of 33%. For the same models, conductivity contrasts were less than two orders of magnitude. These contrasts were chosen to be as realistic as possible based on data in the literature and my limited experience. The model shown in Figure 5-11i has a conductivity contrast of about three orders of magnitude. The results of the stability analysis for this case are shown bracketed in Table 5-3 because the situation is completely unrealistic. In order for that slope to stand, the specific weight of the slide material would have to be well over 300 pounds per cubic foot.

Conductivity contrasts of at least twelve orders of magnitude exist in the real world but it can be concluded from the above calculations that variations in geology causing conductivity contrasts of only two orders of magnitude can have a critical effect on the groundwater flow regime of a slope. A fault gouge or geologic unit need not be impermeable or even of exceedingly less conductivity than the surrounding material to adversely affect the flow regime in such a way as to cause instability.

Two important practical points are demonstrated in these models. Firstly, they show that to get useful and accurate field measurements of pressure head in a slope investigation, it is critical that the piezometers penetrate through any less conductive unit that might be acting as a slide plane. The second point is that if a less permeable zone underlies a slide, for drainage to be an effective remedial measure, drain holes must penetrate beneath this less permeable zone.

In all reservoir cases illustrated in Figure 5-11, the effects of the ponded water are felt in the valley slope well above the level of the water surface. As small as the reservoir is, it causes a reduction in the factor of safety of from 1% to 5%. Although this reduction may seem insignificant, if a slope is already close to failure, the change in groundwater regime caused by the introduction of even a small reservoir may be all that is required to cause instability. However, according to Patton (Personal communication, 1976) the detrimental effect on stability shown by my modelling, is not general and cases can be found for which the introduction of a reserovir causes an increase in a slope's stability.

The phi's calculated for a factor of safety of one should be considered to establish the reasonableness of the models. The strength parameters compiled by Deere and Patton (1971, p. 142) include a number of phi values for gneisses, schists, phyllite and granites, weathered to varying degrees, that bracket the 30.9° - 40° range listed in Table 5-3. From this comparison the models appear realistic.

CHAPTER SIX: SUMMARY AND CONCLUSIONS

Slope Stability Analyses

1. There are three distinct aspects in the analysis of the stability of a slope: identifying all the stresses acting, understanding the mechanics which relate the stresses, and determining the natural properties which govern the material behaviour when the stresses are acting.

2. The three categories of analysis, limit equilibrium, elastic-finite element, and Cundall's discrete particle method each have their own advantages and limitations. For any given situation, local conditions and the purpose of the analysis will govern the choice of category.

3. Limit equilibrium techniques have reached the stage where all the laws of static equilibrium can be satisfied. However, the resulting equations are indeterminate without some simplifying assumption. Different limit equilibrium methods utilize different assumptions.

4. Terzaghi's empirical effective stress law is valid for saturated soils but, in some cases of saturated rock, Skempton's modified form may be more appropriate.

5. To undertake a slope stability analysis in terms of effective stress, pore pressures must be known. In practice, these are approximated as a percentage of overburden pressure, approximated with an assumed coefficient, obtained by field measurement or obtained from mathematical models.

6. Difficulties remain in both accurate field measurement and mathematical modelling of flow systems in complex geological environments. The best understanding of the pore pressure distribution in a slope will be obtained if field measurement and modelling are used together. Use of the pore pressure coefficient or the assumption of pore pressures as a percentage of overburden pressure are no longer necessary methods of approximation.

Limiting Assumptions

The following assumptions underlie the theory used to produce the mathematical models developed in this project:

1. The models are fully saturated with the top flow boundary corresponding to the water table.

2. The position of the water table must be known and in most cases is chosen as the ground surface.

3. The models are steady-state.

4. The models are two-dimensional.

5. The model boundaries are either a specified constant head (Dirichlet condition) or constant flux (Neuman condition).

6. The continuous porous media is rigid.

7. Darcy's Law accurately describes the groundwater flow.

8. The geologic case being modelled can be reasonably approximated by an equivalent continuous porous media.

Model Results

1. The models developed in this study serve to rigorously verify many of the possible implications of different flow systems on slope stability, particularly those previously suggested by Deere and Patton (1967, 1971) and Patton and Hendron (1974).

2. Anisotropic hydraulic characteristics are common in both soil and rock. The models completed for this study suggest that for slope stability the worst case is when the principal axis of hydraulic conductivity dips down the slope, while the most stable case is when the principal axis is horizontal.

3. Thick interbedded sedimentary units that have been folded or thrust up, eroded, and now stand as ridges and valleys often have associated complex flow systems. As in the simple anisotropic case, the flow system has a maximum adverse effect on the dip slope.

4. Faults, contacts, and dykes can cause a variety of effects on the groundwater flow system. Careful field investiagtion is required to establish the significance of any one of these features.

5. Weathering profiles can commonly result in a less conductive zone confining another with the resulting flow system extremely detrimental to stability.

6. Layers of colluvium or old landslide debris, particularly if buried weathering profiles are present, can cause complex groundwater flow patterns. Less permeable units are often present and can act as confining layers causing zones of high pore pressures which can lead to instability.

7. Stress relief fractures on valley walls, if accompanied by the production of gouge can adversely influence the effect of the groundwater flow regime on stability.

8. The presence of a regional aquifer beneath a valley can cause anomalously high pore pressure development which can have a detrimental effect on the stability of valley walls.

9. The pressure head distribution on rock wedges can be non-linear and quite different from the commonly assumed linear distribution.

10. The stability of the Pleistocene terraces found throughout British Columbia is in part dependent on the regional groundwater flow system in which the terraces are located. Fluctuations in the groundwater regime causing anomalous increases in the water table could cause a terrace to fail.

11. Modelling of flow systems in highly deformed metamorphic rocks may not be possible because of the complexities of the geology. However, in many cases a through-going foliation exists which may control the flow system and allow reasonable modelling.

12. A more permeable zone near the surface, due to a higher fracture frequency or weathering, has a moderating influence on the groundwater flow regime from a slope stability perspective.

13. The presence of a lithologic unit or thrust surface of lower conductivity than the surrounding rocks can have a major effect on the flow system. Conductivity contrasts of less than two orders of magnitude can cause pore pressure developments critical to stability.

14. The introduction of a reservoir at the toe of the slope can influence the groundwater regime well up the slope from the reservoir surface. If a slope was already close to being unstable, even a low reservoir could provide the change required to cause instability.

15. Piezometers should penetrate through any less conductive unit that might be acting as a slide plane. For drainage to be an effective remedial measure, drainholes must also penetrate beneath such a less permeable zone.

16. All of the results of the modelling illustrate the basic theme of this thesis: to understand the flow system, and therefore pore pressures, that are fundamental to the stability analysis of a slope, it is necessary to understand the regional flow system in which the slope is located. This understanding can only be obtained with a thorough knowledge of the regional geology.

REFERENCES

Bear, J., 1972. Dynamics of Fluids in Porous Media, American Elsevier Publ. Co. Inc., New York, 764 p.

Bell, J.M., 1968. General slope stability analysis, Jour. Soil Mech. and Fdn. Div., A.S.C.E., V. 94, SM 6, 1253-1270.

Bird, C., 1975. UBC Matrix, A Guide to Solving Matrix Problems, University of British Columbia Computing Centre, Vancouver, Canada, 115 p.

Bishop, A.W., 1955. The use of the slip circle in the stability analysis of earth slopes, Geotechnique, V. 5, No. 1, 7-17.

————————, 1967. Progressive failure with special reference to the mechanics causing it, Proceedings, Geotechnical Conference, Oslo, V. 2, 142-150.

————————, 1971. The influence of progressive failure on the method of stability analysis, Geotechnique, V. 21, 168-172.

Bishop, A.W. and N. Morgenstern, 1960. Stability coefficients for earth slopes, Geotechnique, V. 10, 129-150.

Bjerrum, L., 1967. Progressive failure in slopes in overconsolidated plastic clay and clay shales, Jour. Soil Mech. and Fdn. Div., A.S.C.E., V. 93, SM 5, 3-49.

Blight, G.E., 1967. Effective stress evaluation for unsaturated soils, Jour. Soil Mech. and Fdn. Div., A.S.C.E., V. 93, SM 2, 125-148.

Brace, W.F. and R.J. Martin, 1968. A test of the law of effective stress for crystalline rocks of low porosity, Int. Jour. Rock Mech. Min. Sci., V. 5, 415-426.

Castillo, E., 1972. Mathematical model for two dimensional percolation through fissured rock, Proc. of the Symposium on Percolation through Fissured Rock, Stuttgart, T1-D 1-7.

Christian, J.T. and R.V. Whitman, 1969. A one dimensional model for progressive failure, Proc. of the 7th Int'l Conf. on Soil Mech. and Fdn. Eng., V. 2, 541-545.

Collin, A., 1846. Landslides in Clay, Translated by W.R. Schriever, Univ. of Toronto Press, Toronto, 1956.

Coulomb, C.A., 1776. Essai sur une application des règles de maximis et minimis à quelques problèmes de statique, relatifs à l'Architecture, Memoires présentés à l'Académie des Sciences, V. 7, Paris.

Crandall, S.H., 1956. Engineering Analysis, McGraw-Hill Book Company Inc., Toronto, 417 p.

Culmann, K., 1866. Die graphische statik, Zurich.

Cundall, P.A., 1971. A computer model for simulating progressive, large scale movements in blocky rock systems, Symposium of the Int'l. Soc. Rock Mechnics, Nancy, France.

————————, 1974. Rational Design of Tunnel Supports: A Computer Model For Rock Mass Behavior Using Interactive Graphics For the Input and Output of Geometric Data, U.S. Army Corps of Engineers, Technical Report, MRD-2-74.

Cundall, P.A., M.D. Voegele and C. Fairhurst, 1975. Computerized design of rock slopes using interactive graphics for the input and output of geometric data, Preprints, 16th Symposium on Rock Mechanics, Minneapolis, U.S.A., 1-10.

Davis, S.N., 1969. Porosity and permeability of natural materials in Flow Through Porous Media, R. de Wiest ed., Academic Press, London, 54-89.

Deere, D.U. and F.D. Patton, 1967. Effect of pore pressure on the stability of slopes, Paper presented at joint GSA-ASCE Symposium, New Orleans, Nov. 21, 1967.

————————, 1971. Stability of slopes in residual soils, Proc. 4th Pan American Conference on Soil Mech. and Fdn. Eng., San Juan Puerto Rico, 87-170.

Desai, C.S. (editor), 1972. Application of the Finite Element Method in Geotechnical Engineering, V. I, II, III, Soil Mech. Information Analysis Centre, U.S. Army Engineer Waterways Experiment Station, Vicksburg, Missippi, 1227 p.

Duncan, J.M., 1975. Slope stability analysis, Notes prepared for five day short course: Recent Developments in the Design Construction and Performance of Embankment Dams, University of California at Berkeley, 36 p.

Fellenius, W., 1927. Erdstatische Berechnungen mit Reibung und Kohäsion (Adhäsion) und unter Annahme Kreiszylindrischer Gleitflächen, Berlin.

————————, 1936. Calculation of the stability of earth dams, Transactions of the 2nd Int'l. Congress on Large Dams, Washington, V. 4, 445-462.

Ferguson, H.F., 1967. Valley Stress release in the Allegheny Plateau, Engr. Geology., V. 4, No. 1, 63-71.

Forray, M.J., 1968. Variational Calculus in Science and Engineering, McGraw-Hill Book Co., New York, 221 p.

Fredland, D.G., 1974. Slope Stability Analysis, User's Manual CD-4, Transportation and Geotechnical Group, Dept. of Civil Engineering, University of Saskatchewan, Saskatoon, Canada, 103 p.

Freeze, R.A., 1971a. Three-dimensional, transient, saturated - unsaturated flow in a groundwater basin, Water Resource Research, V. 7, No. 2, 347-366.

————————, 1971b. Influence of the unsaturated flow domain on seepage through earth dams, Water Resource Research, V. 7, No. 4, 929-941.

Freeze, R.A. and P.A. Witherspoon, 1966. Theoretical analysis of regional groundwater flow: 1. analysis and numerical solutions to the mathematical model. Water Resource Research, V. 2, No. 4, 641-656.

————————, 1967. Theoretical analysis of regional groundwater flow: 2. effect of water-table configuration and subsurface permability variation, Water Resource Research, V. 3, No. 2, 623-634.

Gale, J.E., 1975. A Numerical Field and Laboratory Study of Flow in Rocks with Deformable Fractures, Ph.D. Thesis, Dept. of Civil Engineering, University of California at Berkeley.

Gillham, R.W. and R.N. Farvolden, 1974. Sensitivity analysis of input parameters in numerical modelling of steady state regional groundwater flow, Water Resource Research, V. 10, No. 3, 529-538.

Goodman, R.E. and Taylor, R.L., 1967. Methods of analysis for rock slopes and abutments: a review of recent developments in Failure and Breakage of Rock, AIME, Chapter 12, 303-320.

Goodman, R.E., R.L. Taylor, and T. Brekke, 1968. A model for the mechanics of jointed rock, Jour. Soil Mech. and Fdn. Div., A.S.C.E., V. 94, SM 3, 637-659.

Haefeli, R., 1965. Creep and progressive failure in snow, soil, rock and ice, Proceedings of the 6th Int'l. Conf. on Soil Mech., Montreal, V. 3, 134-148.

Hendron, A.J., E.J. Cording and A.K. Aieyer, 1971. Analytical and Graphical Methods for the Analysis of Slopes in Rock Masses, NCG Technical Report No. 36, Department of Civil Engineering, University of Illinois, Urbana, 148 p.

Heyman, Jacques, 1972. Coulomb's Memoirs on Statistics, Cambridge at the University Press, Cambridge, England, 212 p.

Hilf, J.W., 1948. Estimating construction pore pressures in rolled earth dams, Proceedings of the 2nd Int'l. Conference on Soil Mech. and Fdn. Eng., Rotterdam, V. III, 234-240.

Hobbs, B.E., W.D. Means, and P.F. Williams, 1976. An Outline of Structural Geology, John Wiley and Sons Inc., New York, 571 p.

Horn, J.A., 1960. Computer analysis of slope stability, Jour. Soil Mech. and Fdn. Div., A.S.C.E., V. 86, SM 3, 1-17.

Hubbert, M.K., 1940. Theory of groundwater motion, Jour. Geology, No. 48, 785-944.

Hubbert, M.K. and W.W. Rubey, 1959. Role of fluid pressure in mechanics of overthrust faulting, Bulletin G.S.A., V. 70, 115-166.

————————, 1960. Role of fluid pressure in mechanics of overthrust faulting - a reply, Bulletin G.S.A., V. 71, 617-628.

Janbu, N., 1954. Stability Analysis of Slopes With Dimensionless Parameters, Harvard Soil Mechanics Series, No. 46, Harvard University, Cambridge, Massachusetts.

————————, 1957. Earth pressure and bearing capacity calculations by generalized procedure of slices, Proceedings of the 4th Int'l. Conference on Soil Mech. and Fdn. Eng., London, V. 2, 207-212.

————————, 1973. Slope stability computations, in Embankment Dam Engineering (Casagrande Volume), ed. by R.C. Hirschfield and S.J. Poulos, John Wiley and Sons, New York, 47-86.

Jennings, J.E., 1960. A revised effective stress law for use in the prediction of the behavior of unsaturated soils, in Pore Pressure and Suction in Soils, Butterworths, London, 151 p.

John, K.W., 1968. Graphical stability analysis of slopes in jointed rock, Jour. Soil Mech. and Fdn. Div., A.S.C.E., V. 94, SM 2, 497-526.

Kantorovich, L.V. and V.I. Krylov, 1964. Approximate Methods in Higher Analysis, translated by C.D. Benster, Interscience, New York, 681 p.

Krey, H., 1936. Erddruck, Erdwiderstand und Tragfähigkeit des Baugrundes, Berlin: Ernst.

Kreysig, E., 1972. Advanced Engineering Mathematics, John Wiley and Sons Inc., New York, 866 p.

Laubscher, H.P., 1960. Role of fluid pressure in mechanics of overthrust faulting - discussion, Bulletin G.S.A., V. 71, 611-616.

Legget, R.F., 1962. Geology and Engineering, McGraw-Hill Book Co. Inc., New York, 884 p.

Little, A.L. and V.E. Price, 1958. The use of an electronic computer for slope stability analysis, Geotechnique, V. 8, 113-120.

Lo, K.Y., 1972. An approach to the problem of progressive failure, Canadian Geotechnical Journal, V. 9, 407-429.

Lo, K.Y. and C.F. Lee, 1973. Analysis of progressive failure in clay slopes, Proceedings of the 8th Int'l. Conference on Soil Mech. and Fdn. Eng., Moscow, V. 1, 251-258.

Londe, P., 1971. The flow of water in rocks, Notes prepared for a summer course on the analysis and design of rock slopes, University of Alberta, Edmonton, Canada, August 23-27, 1971.

Londe, P., G. Vigier and R. Vormeringen, 1969. Stability of rock slopes, a three-dimensional study, Jour. Soil Mech. and Fdn. Div., A.S.C.E., V. 95, SM 1, 235-262.

————, 1970. Stability of rock slopes, graphical methods, Jour. Soil Mech. and Fdn. Div., A.S.C.E., V. 96, SM 4, 1411-1434.

Louis, C., 1969. A study of groundwater flow in jointed rock and its influence on the stability of rock masses, Imperial College, Rock Mechanics Report No. 10, London University.

Louis, C. and M. Pernot, 1972. Three-dimensional investigation of flow conditions of Grand Maison Damsite, Proceedings Symposium of the Int'l. Society of Rock Mechanics, Percolation Through Fissured Rock, Stuttgart, T4-F, 1-16.

Lowe, J. and L. Karafiath, 1960. Stability of earth dams upon drawdown, Proceedings of the 1st Pan American Conference on Soil Mech. and Fdn. Eng., Mexico City, V. 2, 537-552.

Lutton, R.J., 1971. A mechanism for progressive rock mass failure as revealed by loess slumps, Int'l. Jour. Rock Mechanics and Mining Science, V. 8, 143-151.

Maaslan, M., 1957. Soil anistropy and land drainage, in Drainage of Agricultural Lands, ed. by J.M. Luthin, American Society of Agronomy, Monograph VII, 620 p.

Manfredini, G., S. Martinetti and R. Ribachi, 1975. Inadequacy of limiting equilibrium methods for rock slopes design, Proceedings of the 16th Symposium on Rock Mechnics, Design Methods in Rock Mechanics, University of Minnesota, Department of Civil and Mineral Engineering, Minneapolis.

Matheson, D.S. and S. Thomson, 1973. Geological implications of valley rebound, Canadian Journal of Earth Science, V. 10, No. 6, 961-978.

Morgenstern, N.R. and V.E. Price, 1965. The analysis of the stability of general slip surfaces, Geotechnique, V. 15, 79-93.

Nur, A. and J.D. Byerlee, 1971. An exact effective stress law for elastic deformation of rock with fluids, Jour. Geophysical Research, V. 76, No. 26, 6414-6419.

Patton, F.D. and A.J. Hendron, General report on mass movements, Proceedings of the 2nd Int'l. Congress of the Int'l. Assoc. of Eng. Geol., Sao Paulo, Brazil, V. 2, V-Gr, 1-57.

Pinder, G.F. and E.O. Frind, 1972. Application of Galerkin's procedure to aquifer analysis, Water Resource Research, V. 8, No. 1, 108-120.

Remson, I., G.M. Hornberger and F.J. Molz, 1971. Numerical Methods in Subsurface Hydrology, Wiley-Interscience, 389 p.

Rendulic, L., 1935. Ein Beitrag zur Bestimmung der Gleitsicherheit, Der Bauingenier No. 19/20.

Riglin, L., 1976. The Pertual Landlside, Summerland, B.C., Masters of Science Thesis, Dept. of Geology, University of British Columbia.

Romani, F., C.W. Louel and M.E. Harr, 1972. Influence of progressive failure on slope stability, Jour. Soil Mech. and Fdn. Div., A.S.C.E., V. 98, SM 11, 1209-1224.

Sharp, J.C. and Y.N.T. Maini, 1972. Fundamental considerations on the hydraulic characteristics of joints in rocks, Proceedings, Symposium of the Int'l. Society of Rock Mechanics, Percolation Through Fissured Rock, Stuttgart, T1-F, 1-15.

Skempton, A.W., 1948. The $\phi = 0$ analysis of stability and its theoretical basis, Proceedings of the 2nd Int'l. Conferences on Soil Mech. and Fdn. Eng., Rotterdam, V. 1, 72-78.

————————, 1961. Effective stress in soils, concrete and rock in Pore Pressure and Suction in Soils, Butterworths, London, 151 p.

Snow, D.T., 1968. Fracture deformation and changes of permeability and storage upon change of fluid pressure, Quarterly of the Colorado School of Mines, V. 63, No. 1, 201-244.

————————, 1969. Anistropic permeability of fractured media. Water Resource Research, V. 5, No. 6, 1273-1289.

————————, 1972. Fundamentals and in situ determination of permeability, Proceedings, Symposium of the Int'l Society of Rock Mechanics, Percolation Through Fissured Rock, Stuttgart, G1, 1-6.

Spencer, E., 1967. A method of analysis of the stability of embankments assuming parallel interslice forces, Geotechnique, V. 17, 11-26.

Stevens, O.B., 1936. Discussion of paper of Vreedenburgh, Proceedings of the Int'l. Conference on Soil Mech. and Fdn. Eng., V. 3, 165-166.

Taylor, D.W., 1937. The stability of earth slopes, Jour. Boston Soc. of Civil Engineers, Boston, V. 24, No. 3, 337-387.

————, 1948. Fundamentals of Soil Mechanics, John Wiley and Sons Inc., New York, 700 p.

Terzaghi, K., 1923. Die Berechnung der Durchassigkeitsziffer des Tones aus dem Verlauf der Hydrodynamischen Spannungserscheinungen, Sitzungsber. Akad. Wiss Wein Math Naturwiss Kl. Abt. 2A, V. 132, No. 105.

————, 1929. The mechanics of shear failure on clay slopes and creep of retaining walls, Public Roads, V. 10, No. 10, 177-192.

————, 1936a. Simple tests determine hydrostatic uplift, Engineering News Record, V. 116, 872-875.

————, 1936b. The shearing resistance of saturated soils and the angle between the planes of shear, Proceedings of the 1st Int'l. Conference on Soil Mechanics, Cambridge, Massachusetts, V. 1, 54-56.

————, 1936c. Critical height and the factor of safety of slopes against sliding, Proceedings of the 1st Int'l. Conference on Soil Mechanics, Cambridge, Massachusetts, V. 1, 156-161.

Terzaghi, K. and R.B. Peck, 1968. Soil Mechanics in Engineering Practice, John Wiley and Sons Inc., New York, 729 p.

Toth, J.A., 1962. A theory of groundwater motion in small drainage basins in Central Alberta, Canada, Journal Geophysical Research, No. 67, 4375-4387.

————, 1963. A theoretical analysis of groundwater flow in small drainage basins, Journal Geophysical Research, No. 68, 4795-4812.

Turbull, W.J. and M.J. Huorslev, 1967. Special problems in slope stability, Jour. Soil. Mech. and Fdn. Div., A.S.C.E., V. 93, SM 4, 499-528.

Whitman, R.V. and W.A. Bailey, 1967. Use of computers for slope stability analysis, Jour. Soil Mech. and Fdn. Div., A.S.C.E., V. 93, SM 4, 475-498.

Wright, S.G., F.H. Kulhawy and J.M. Duncan, 1973. Accuracy of equilibrium slope stability analysis, Jour. Soil Mech. and Fdn. Div., A.S.C.E., V. 99, SM 10, 783-791.

Weinstock, R., 1952. Calculus of Variations, McGraw-Hill Book Co., New York.

Wittke, W., 1971. Three-dimensional percolation of fissured rock, in Planning Open Pit Mines, ed. by P.W.J. Van Rensburg, South African Institute of Mining and Metallurgy, Johannesburg, 1971.

Wittke, W. and C. Louis, 1966. Determination of the influence of groundwater on the stability of slopes and structures in jointed rock, Proceedings of the 1st Congress on Rock Mechanics, Lisbon, V. 2, 201-206.

Zienkiewicz, O.C., 1971. The Finite Element Method in Engineering Science, McGraw-Hill, London, 521 p.

Zienkiewicz, O.C. and Y.K. Cheung, 1968. The Finite Element Method in Structural and Continuum Mechanics, McGraw-Hill, London, 274 p.

Personal communication. R.A. Freeze, 1976. Dept. of Geological Sciences, University of British Columbia, Vancouver, B.C.

Personal communication. P. Byrne, 1976. Dept. of Civil Engineering, University of British Columbia, Vancouver, B.C.

Personal communication. F.D. Patton, 1976. Consulting Engineering Geologist. West Vancouver, B.C.

APPENDIX I

COMPUTER PROGRAM

APPENDIX I: COMPUTER PROGRAM

Language: Fortran IV

Purpose: To solve, using the finite element method, the steady-state equation of flow for two-dimensional, saturated, heterogeneous, anisotropic porous media.

Listing: A complete listing of the program, sample output, and sample data file, is found at the end of this appendix.

Flow Chart: See Figure I-1.

Subroutines:

1. NOTRAN

   Purpose: To calculate contributions to nodal equations from elements not requiring a cooordinate transformation.

   Availability: Self-contained.

2. TRANS

   Purpose: To calculate contributions to nodal equations from elements requiring a coordinate transformation. After transformation, appropriate contributions are calculated.

   Availability: Self-contained.

3. SLIMP

Purpose: To solve and improve iteratively a system of linear equations of the form

$$[A] \cdot \{x\} = \{B\}$$

Availability: General library, Computing Centre, University of British Columbia.

4. GRAPH 1

Purpose: To set up data appropriately and call SCATCN for plotting.

Availability: Self-contained.

5. GRAPH 2

Purpose: To set up a data file for MPLOT

Availability: Self-contained.

6. SCATCN

Purpose: To produce a contour map from a set of scattered data points.

Availability: General library, Computing Centre, University of British Columbia.

7. MPLOT

Purpose: To produce an equipotential map from the results of a finite element flow program.

Availability: Department of Civil Engineering, University of British Columbia.

Input:

Parameter	Description
NODTOT	Total number of nodes
N	Total number of unknown potential values
LTOT	Total number of elements
MCON	Number of contours to be drawn
MPLOT	If MPLOT = 0, no plot is generated If MPLOT = 1, GRAPH 1 is called and a plot generated with SCATCN If MPLOT = 2, GRAPH 2 is called and a plot generated with MPLOT
IND	Used by SCATCN. Indicates type of plot desired. If IND = 0, scattered data points will be plotted if there are less than 25. If IND = 1, no data points will be plotted, and if IND = 2, all data points will be plotted.
NO	Number of boundary nodes
NIB	Number of the first boundary node
SIZE	Size in inches of the final plot made by SCATCN
SCA	Scale factor used by MPLOT so $y_{max} \leq 9$

Parameter	Description
LDAT (I, J)	Element data. A 2-D array containing the identity of the vertices of the triangular elements. For the jth element, LDAT (1, J) contains the nodal number of the first corner LDAT (2, J) contains the nodal number of the second corner LDAT (3, J) contains the nodal number of the third corner
XCO(I), YCO(I)	One-dimensional arrays containing the x (horizontal) and y (vertical) coordinate of the I nodes.
PERMX(NEL), PERMY(NEL)	One-dimensional arrays containing the x (horizontal) and y (vertical) hydraulic conductivities for each element.
Q(NEL)	One-dimensional array containing the flux into each element per unit length of element boundary.
EL(NEL)	One-dimensional array containing the length of element boundary through which Q(NEL) flows.
THETA(NEL)	One-dimensional array containing the angle which the principal axis of hydraulic conductivity for any given element is skewed from the global coordinates system.
CN(I)	One-dimensional array containing the values of the MCON contours to be drawn.

```
      COMMON LDAT(3,500),XCC(275),YCO(275),PHI(275),G(275),
     1T(275,275),X(275),B(275),IPERM(550),RZ(275),AR(500),C(275),
     2P(275,275),Q(500),EL(500),F(500),THETA(500),ALPHA(275),XCOT(275),
     3YCOT(275),RT(275),PERMX(500),PERMY(500),BX(500),BY(500),CN(50),
     4DATA(3,275),TITLE(20),JCOP(1),I,J,K,NEL,NODTOT,N,NP1,MCON,
     5SIZE,IND,NC,N1B,SCA,LTOT
C
      READ(5,99) TITLE
99    FORMAT(20A4)
      READ(5,1) NODTOT,N,LTOT,MCON,MPLOT,IND,NO,N1B,SIZE,SCA
    1 FORMAT(8I6,2F10.1)
      READ(5,2)((LDAT(I,J),I=1,3),J=1,LTOT)
2     FORMAT(18I4)
      READ(5,4)(YCO(I),XCO(I),I=1,NODTOT)
4     FORMAT(10F8.1)
      READ(5,8)(PERMX(NEL),PERMY(NEL),NEL=1,LTOT)
8     FORMAT(8F10.6)
      READ(5,18)(Q(NEL),NEL=1,LTOT)
18    FORMAT(13F6.1)
      READ(5,29)(EL(NEL),NEL=1,LTOT)
   29 FORMAT(10F8.2)
      READ(5,20)(THETA(NEL),NEL=1,LTOT)
20    FORMAT(16F5.1)
      READ(5,80)(CN(I),I=1,MCON)
80    FORMAT(10F8.1)
C
C     **COMPLETION OF DATA READ IN,WRITE OUT INPUT**
C
      WRITE(6,98) TITLE
98    FORMAT(1H1,20A4)
      WRITE(6,19) NODTOT,LTOT,N
19    FORMAT(1HO,'NODE TOTAL IS',I5,5X,'ELEMENT TOTAL IS',
     1I5,5X,'UNKNOWNS',I5)
      WRITE(6,7)
7     FORMAT(1HO,3X,'ELEMENT NO.',4X,'AREA',11X,'PERMX',5X,'PERMY',9X,
     1'THETA',8X,'Q',9X,'EL',10X,'I',5X,'J',5X,'K'//)
C
C     **SET TOP FLOW BOUNDARY TO THE GROUND SURFACE**
C
```

```
40            NP1=N+1
41            DO 6 J=NP1,NODTOT
42            PHI(J)=YCO(J)
43      6     CONTINUE
44      C
45      C     **INITIALIZE PARAMETERS**
46      C
47            DO 10 I=1,275
48            DO 10 J=1,275
49            P(I,J)=0.000
50            T(I,J)=0.000
51      10    CONTINUE
52            DO 5 J=1,275
53            X(J)=0.000
54            B(J)=0.000
55            RZ(J)=0.000
56      5     CONTINUE
57            DO 3 J=1,550
58            IPERM(J)=0.000
59      3     CONTINUE
60            DO 9 I=1,500
61            F(I)=0.0
62      9     CONTINUE
63      C
64      C     **CONVERT COORDINATE ANGLE TO RADIANS**
65      C
66            DO 31 NEL=1,LTOT
67            THETA(NEL)=(THETA(NEL)/360.0)*2.0*3.14159
68      31    CONTINUE
69      C
70      C     **CALCULATE MATRIX COEFFICIENTS**
71      C
72            DO 11 NEL=1,LTOT
73            I=LDAT(1,NEL)
74            J=LDAT(2,NEL)
75            K=LDAT(3,NEL)
76      C
77            AR(NEL)=(((XCO(J)*YCO(K))-(XCO(K)*YCO(J)))-((XCO(I)*YCO(K))
78           1-(XCO(K)*YCO(I)))+((XCO(I)*YCO(J))-(XCO(J)*YCO(I))))*0.5
```

```
      IF(AR(NEL).LT.0.0) AR(NEL)=-AR(NEL)
C
      WRITE(6,51) NEL,AR(NEL),PERMX(NEL),PERMY(NEL),THETA(NEL),
     1Q(NEL),EL(NEL),I,J,K
   51 FORMAT(1H ,5X,I5,4X,F10.1,5X,2F10.6,5X,F7.4,5X,F6.2,5X,F6.2,
     15X,3I6)
C
      BX(NEL)=PERMX(NEL)/(4.0*AR(NEL))
      BY(NEL)=PERMY(NEL)/(4.0*AR(NEL))
C
C     **CALL APPROPRIATE SUBROUTINE**
C
      IF(THETA(NEL).EQ.0.0) GO TO 42
      CALL TRANS
      GO TO 11
   42 CALL NOTRAN
C
   11 CONTINUE
C
C    **SET SUBROUTINE PARAMETERS AND CALL SLIMP**
C
      M=275
      NDIMAT=M
      ITMAX=14
      EPS=5.E-3
      NRHS=1
C
      DO 14 I=1,N
      DO 14 J=NP1,NODTOT
      P(I,J)=P(I,J)*PHI(J)
      B(I)=B(I)-P(I,J)+F(I)
   14 CONTINUE
C
      DO 12 I=1,N
      DO 12 J=NP1,NODTOT
      P(I,J)=0.000
   12 CONTINUE
      DO 39 I=NP1,NODTOT
      DO 39 J=1,NODTOT
```

```
      P(I,J)=0.000
   39 CONTINUE
C
      CALL SLIMP(P,T,B,X,RZ,IPERM,M,NDIMAT,EPS,NRHS,ITMAX)
C
C  **WRITE OUT RESULTS**
C
      WRITE(6,22)
   22 FORMAT(1H1,6X,'NODE NO.',10X,'XCOORD',9X,'YCOORD',15X,'PHI'//)
      DO 16 I=1,N
      WRITE(6,15) I,XCO(I),YCO(I),X(I)
   15 FORMAT(1H ,5X,I5,10X,F10.1,5X,F10.1,10X,F10.2)
   16 CONTINUE
      DO 17 I=NP1,NODTOT
      WRITE(6,15) I,XCO(I),YCO(I),PHI(I)
   17 CONTINUE
C
C  **CALL PLOTTER IF REQUIRED**
C
      IF(MPLOT.EQ.0) GO TO 21
      IF(MPLOT.EQ.2) GO TO 23
      CALL GRAPH1
      GO TO 21
   23 CALL GRAPH2
   21 CONTINUE
      STOP
      END
      SUBROUTINE NOTRAN
      COMMON LDAT(3,500),XCO(275),YCO(275),PHI(275),G(275),
     1T(275,275),X(275),B(275),IPERM(550),RZ(275),AR(500),C(275),
     2P(275,275),Q(500),EL(500),F(500),THETA(500),ALPHA(275),XCOT(275),
     3YCOT(275),RT(275),PERMX(500),PERMY(500),BX(500),BY(500),CN(50),
     4DATA(3,275),TITLE(20),JCCP(1),I,J,K,NEL,NODTOT,N,NP1,MCON,
     5SIZE,IND,NO,N18,SCA,LTOT
C
C  *****CALCULATION OF MATRIX COEFFICIENTS FOR ELEMENTS NOT
C       REQUIRING COORDINATE TRANSFORMATION*****
C
      P(I,I)=P(I,I)+(BX(NEL)*((YCO(J)-YCO(K))**2)+
```

```
     1BY(NEL)*((XCO(K)-XCO(J))**2))
      P(I,J)=P(I,J)+(BX(NEL)*((YCO(J)-YCO(K))*(YCO(K)-YCO(I)))
     1+BY(NEL)*((XCO(K)-XCO(J))*(XCO(I)-XCO(K))))
      P(I,K)=P(I,K)+(BX(NEL)*((YCO(J)-YCO(K))*(YCO(I)-YCO(J)))
     1+BY(NEL)*((XCO(K)-XCO(J))*(XCO(J)-XCO(I))))
C
      P(J,I)=P(J,I)+(BX(NEL)*((YCO(K)-YCO(I))*(YCO(J)-YCO(K)))
     1+BY(NEL)*((XCO(I)-XCO(K))*(XCO(K)-XCO(J))))
      P(J,J)=P(J,J)+(BX(NEL)*((YCO(K)-YCO(I))**2)+
     1BY(NEL)*((XCO(I)-XCO(K))**2))
      P(J,K)=P(J,K)+(BX(NEL)*((YCO(K)-YCO(I))*(YCO(I)-YCO(J)))
     1+BY(NEL)*((XCO(I)-XCO(K))*(XCO(J)-XCO(I))))
C
      P(K,I)=P(K,I)+(BX(NEL)*((YCO(I)-YCO(J))*(YCO(J)-YCO(K)))
     1+BY(NEL)*((XCO(J)-XCO(I))*(XCO(K)-XCO(J))))
      P(K,J)=P(K,J)+(BX(NEL)*((YCO(I)-YCO(J))*(YCO(K)-YCO(I)))
     1+BY(NEL)*((XCO(J)-XCO(I))*(XCO(I)-XCO(K))))
      P(K,K)=P(K,K)+(BX(NEL)*((YCO(I)-YCO(J))**2)+
     1BY(NEL)*((XCO(J)-XCO(I))**2))
C
      F(I)=F(I)+(0.5*Q(NEL)*EL(NEL))
      F(J)=F(J)+(0.5*Q(NEL)*EL(NEL))
      F(K)=F(K)+(0.5*Q(NEL)*EL(NEL))
C
      RETURN
      END
      SUBROUTINE TRANS
      COMMON LDAT(3,500),XCO(275),YCO(275),PHI(275),G(275),
     1T(275,275),X(275),B(275),IPERM(550),RZ(275),AR(500),C(275),
     2P(275,275),Q(500),EL(500),F(500),THETA(500),ALPHA(275),XCOT(275),
     3YCOT(275),RT(275),PERMX(500),PERMY(500),BX(500),BY(500),CN(50),
     4DATA(3,275),TITLE(20),JCOP(1),I,J,K,NEL,NODTOT,N,NP1,MCON,
     5SIZE,IND,NO,N1B,SCA,LTOT
C
C    ****COORDINATE TRANSFORMATION AND CALCULATION OF MATRIX
C        COEFFICIENTS FOR ELEMENTS HAVING ANISOTROPY SKEWED
C        FROM GLOBAL COORDINATES*****
C
      ALPHA(I)=ATAN(YCO(I)/XCO(I))-THETA(NEL)
```

```
196           ALPHA(J)=ATAN(YCO(J)/XCO(J))-THETA(NEL)
197           ALPHA(K)=ATAN(YCO(K)/XCO(K))-THETA(NEL)
198     C
199           RT(I)=SQRT((XCO(I)**2)+(YCO(I)**2))
200           RT(J)=SQRT((XCO(J)**2)+(YCO(J)**2))
201           RT(K)=SQRT((XCO(K)**2)+(YCO(K)**2))
202     C
203           XCOT(I)=COS(ALPHA(I))*RT(I)
204           XCOT(J)=COS(ALPHA(J))*RT(J)
205           XCOT(K)=COS(ALPHA(K))*RT(K)
206     C
207           YCOT(I)=SIN(ALPHA(I))*RT(I)
208           YCOT(J)=SIN(ALPHA(J))*RT(J)
209           YCOT(K)=SIN(ALPHA(K))*RT(K)
210     C
211            P(I,I)=P(I,I)+(BX(NEL)*((YCOT(J)-YCOT(K))**2)+
212          1BY(NEL)*((XCOT(K)-XCOT(J))**2))
213            P(I,J)=P(I,J)+(BX(NEL)*((YCOT(J)-YCOT(K))*(YCOT(K)-YCOT(I)))
214          1+BY(NEL)*((XCOT(K)-XCOT(J))*(XCOT(I)-XCOT(K))))
215            P(I,K)=P(I,K)+(BX(NEL)*((YCOT(J)-YCOT(K))*(YCOT(I)-YCOT(J)))
216          1+BY(NEL)*((XCOT(K)-XCOT(J))*(XCOT(J)-XCOT(I))))
217     C
218            P(J,I)=P(J,I)+(BX(NEL)*((YCOT(K)-YCOT(I))*(YCOT(J)-YCOT(K)))
219          1+BY(NEL)*((XCOT(I)-XCOT(K))*(XCOT(K)-XCOT(J))))
220            P(J,J)=P(J,J)+(BX(NEL)*((YCOT(K)-YCOT(I))**2)+
221          1BY(NEL)*((XCOT(I)-XCOT(K))**2))
222            P(J,K)=P(J,K)+(BX(NEL)*((YCOT(K)-YCOT(I))*(YCOT(I)-YCOT(J)))
223          1+BY(NEL)*((XCOT(I)-XCOT(K))*(XCOT(J)-XCOT(I))))
224     C
225            P(K,I)=P(K,I)+(BX(NEL)*((YCOT(I)-YCOT(J))*(YCOT(J)-YCOT(K)))
226          1+BY(NEL)*((XCOT(J)-XCOT(I))*(XCOT(K)-XCOT(J))))
227            P(K,J)=P(K,J)+(BX(NEL)*((YCOT(I)-YCOT(J))*(YCOT(K)-YCOT(I)))
228          1+BY(NEL)*((XCOT(J)-XCOT(I))*(XCOT(I)-XCOT(K))))
229            P(K,K)=P(K,K)+(BX(NEL)*((YCOT(I)-YCOT(J))**2)+
230          1BY(NEL)*((XCOT(J)-XCOT(I))**2))
231     C
232           F(I)=F(I)+(0.5*Q(NEL)*EL(NEL))
233           F(J)=F(J)+(0.5*Q(NEL)*EL(NEL))
234           F(K)=F(K)+(0.5*Q(NEL)*EL(NEL))
```

```
      C
            RETURN
            END
            SUBROUTINE GRAPH1
            COMMON LDAT(3,500),XCO(275),YCO(275),PHI(275),G(275),
           1T(275,275),X(275),B(275),IPERM(550),RZ(275),AR(500),C(275),
           2P(275,275),Q(500),EL(500),F(500),THETA(500),ALPHA(275),XCOT(275),
           3YCOT(275),RT(275),PERMX(500),PERMY(500),BX(500),BY(500),CN(50),
           4DATA(3,275),TITLE(20),JCCP(1),I,J,K,NEL,NODTOT,N,NP1,MCON,
           5SIZE,IND,NO,N1B,SCA,LTOT
      C
      C  ****PLOT OF EQUIPOTENTIALS****
      C
            DO 70 I=1,N
            DATA(1,I)=XCO(I)
            DATA(2,I)=YCO(I)
            DATA(3,I)=X(I)
      70    CONTINUE
            DO 71 I=NP1,NODTOT
            DATA(1,I)=XCO(I)
            DATA(2,I)=YCO(I)
            DATA(3,I)=PHI(I)
      71    CONTINUE
      C
            CALL SCATCN(DATA,NODTOT,CN,MCON,SIZE,IND)
            CALL PLOTND
            RETURN
            END
            SUBROUTINE GRAPH2
            COMMON LDAT(3,500),XCO(275),YCO(275),PHI(275),G(275),
           1T(275,275),X(275),B(275),IPERM(550),RZ(275),AR(500),C(275),
           2P(275,275),Q(500),EL(500),F(500),THETA(500),ALPHA(275),XCOT(275),
           3YCOT(275),RT(275),PERMX(500),PERMY(500),BX(500),BY(500),CN(50),
           4DATA(3,275),TITLE(20),JCCP(1),I,J,K,NEL,NODTOT,N,NP1,MCON,
           5SIZE,IND,NO,N1B,SCA,LTOT
      C
      C  ****WRITE DATA IN TEMPORARY FILE IN FORMAT REQUIRED BY MPLOT****
      C
            NE1=1
```

```
      NE2=LTOT
      NN=NODTOT
      NS=1
      NA=10
      XM=1.0
      YM=1.0
      IFLOW=0
      JCCP(1)=1
C
      WRITE(8,81) TITLE
81    FORMAT(20A4)
      WRITE(8,82) LTOT,MCON,NE1,NE2,NN,ND,NS,NA,SCA,XM,YM,IFLOW
82    FORMAT(8I6,3F8.2,I4)
      WRITE(8,82)(JCCP(I),I=1,NS)
      WRITE(8,83)(CN(I),I=1,MCON)
83    FORMAT(6F12.0)
      DO 84 NEL=1,LTOT
      I=LDAT(1,NEL)
      J=LDAT(2,NEL)
      K=LDAT(3,NEL)
      WRITE (8,85) I,J,K,XCO(I),XCO(J),XCO(K),YCO(I),YCO(J),YCO(K)
85    FORMAT(3I6,6F8.1)
84    CONTINUE
      DO 86 I=1,N
      G(I)=X(I)
86    CONTINUE
      DO 90 I=NP1,NODTOT
      G(I)=PHI(I)
90    CONTINUE
      WRITE(8,89)(G(I),I=1,NODTOT)
89    FORMAT(6F12.3)
C
      DO 88 I=N1B,NODTOT
      WRITE(8,87) XCO(I),YCO(I)
87    FORMAT(2F12.2)
88    CONTINUE
C
      RETURN
      END
```

```
SLOPE GROUNDWATER 6
  253   215   446    11     2     2    58   196    21.0   2400.0
215 216   1   1 216 217 217 218   1   1 218  15  15 218 219 219 220  15
 15 220  29  29 220 221 221  29  40  40 221 222 222  40  53  53 222 223
223  53 224 224  53  54  54 224  71  71 224 225 225  71 226 226  71  81
 81 226  80  80 226 227 227  80  90  90 227 228 228  90  91  91 228 103
103 228 229 229 103 230 230 103 101 214 215   1   1 214   2   2   1  15
 15   2  16  16  15  29  29  16  41  41  29  40  40  41  53  53  41  54
 54  41  55  55  54  62  62  54  61  61  54  71  71  61  72  72  71  81
214   2   3   3   2  16  16   3   5   5  16  17  17  16  18  18  16  41
 41  18  30  30  41  42  42  41  43  43  41  55 213 214   3   3 213   4
  4   3   7   7   3   5   5   7   9   9   5  17  17   9  11  11  17  19
 19  17  18  18  19  21  21  18  23  23  18  30  30  23  31  31  30  33
 33  30  42  42  33  35  35  42  44  44  42  43  43  44  45  45  43  48
 48  43  55  55  48  57  57  55  56  56  55  62  62  56  63  63  62  64
 64  62  61  61  64  65  65  61  75  75  61  72  72  75  73  73  72  82
 82  72  81  81  82  83  83  81  84  84  81  80  80  84  95  95  80  90
 90  95  93  93  90  91 101 230 231 231 101 100 100 231 107 107 231 232
100 107 111 111 107 232 232 111 108 108 232 233 108 111 110 110 108 109
109 108 233 233 109 118 118 233 234 109 118 122 118 234 117 117 118 122
117 234 235 235 117 119 119 117 120 120 117 122 119 235 129 129 235 236
236 129 130 130 129 119 130 236 128 128 236 237 237 128 132 132 128 131
131 130 128 132 237 138 138 237 238 238 138 140 140 138 139 139 138 132
140 238 137 137 238 239 239 137 148 148 137 149 149 137 140 149 148 150
148 239 240 240 148 152 152 148 150 152 240 151 151 240 241 241 151 164
164 152 151 164 241 159 159 241 242 242 159 160 160 159 162 162 159 164
160 242 158 158 242 243 243 158 174 174 158 160 174 243 170 170 174 172
172 170 171 171 170 169 169 170 243 243 244 169 169 244 181 181 171 169
181 244 179 179 244 245 245 179 178 178 245 246 246 178 247 212 213   4
  4 212   6   6   4   7   7   6   8   8   7   9   9   8  10  10   9  11
 11  10  12  12  11  19  19  12  20  20  19  21  21  20  22  22  21  23
 23  22  24  24  23  31  31  24  32  32  31  33  33  32  34  34  33  35
 35  34  36  36  35  46  46  35  44  44  46  47  47  44  45  45  47  49
 49  45  48  48  49  59  59  48  57  57  59  58  58  57  56  56  58  66
 66  56  63  63  66  67  67  63  64  64  67  68  68  64  65  65  68  77
 77  65  75  75  77  76  76  75  73  73  76  74  74  73  82  82  74  85
 85  82  83  83  85  86  86  83  84  84  86  87  87  84  95  95  87  96
 96  95  93  93  96  94  94  93  91  91  94  92  92  91 103 103  92 104
104 103 101 101 104 102 102 101 100 100 102 112 112 100 111 111 112 113
```

```
40   113 111 110 110 113 114 114 110 109 109 114 124 124 109 122 122 124 123
41   123 122 120 120 123 121 121 120 119 119 121 133 133 119 130 130 133 134
42   134 130 131 131 134 135 135 131 132 132 135 143 143 132 139 139 143 142
43   142 139 140 140 142 141 141 140 149 149 141 155 155 149 150 150 155 154
44   154 150 152 152 154 153 153 152 164 164 153 165 165 164 162 162 165 163
45   163 162 160 160 163 161 161 160 174 174 161 175 175 174 172 172 175 173
46   173 172 171 171 173 183 183 171 181 181 183 182 182 181 179 179 182 180
47   180 179 178 178 180 187 187 178 247 247 187 248 211 212   6   6 211   8
48     8 211  13  13   8  10  10  13  12  12  13  14  14  12  20  20  14  25
49    25  20  22  22  25  24  24  25  37  37  24  32  32  37  34  34  37  38
50    38  34  36  36  38  46  46  38  50  50  46  47  47  50  49  49  50  60
51    60  49  59  59  60  58  58  60  69  69  58  66  66  67  69  69  67  68
52    68  69  78  78  68  77  77  78  76  76  78  74  74  78  88  88  74  85
53    85  86  88  88  86  87  87  88  97  97  87  96  96  97  94  94  97  92
54    92  97 105 105  92 104 104 105 102 102 105 112 112 105 115 115 112 113
55   113 115 114 114 115 125 125 114 124 124 125 123 123 125 121 121 125 136
56   136 121 133 133 136 134 134 136 135 135 136 144 144 135 143 143 144 142
57   142 144 141 141 144 156 156 141 155 155 156 154 154 156 153 153 156 166
58   166 153 165 165 166 163 163 166 176 176 163 161 161 176 175 175 176 173
59   173 176 184 184 173 183 183 184 182 182 184 185 185 182 180 180 185 188
60   188 180 187 187 188 248 248 188 249 249 188 189 189 188 185 189 249 250
61   250 189 193 193 250 251 251 193 195 195 251 252 252 195 196 196 252 253
62   211 210  13  13 210  14  14 210 209 209  14  26  26  14  25  25  26  39
63    39  25  37  37  39  38  38  39  51  51  38  50  50  51  60  60  51  70
64    70  60  69  69  70  78  78  70  89  89  78  88  88  89  97  97  89 106
65   106  97 105 105 106 115 115 106 126 126 115 125 125 126 136 136 126 145
66   145 136 144 144 145 156 156 145 167 167 156 166 166 167 176 176 167 186
67   186 176 184 184 186 185 185 186 189 189 186 194 194 189 193 193 194 197
68   197 193 195 195 197 196 209  26  27  27  26  39  39  27  52  52  39  51
69    51  52  79  79  51  70  70  79  89  89  79  98  98  89 106 106  98 127
70   127 106 126 126 127 146 146 126 145 145 146 157 157 145 167 167 157 177
71   177 167 186 186 177 190 190 186 194 194 190 198 198 194 197 208 209  27
72    27 208  28  28  27  52  52  28 206 206  52 205 205  52  79  79 205  99
73    99  79  98  98  99 116 116  98 127 127 116 147 147 127 146 146 147 157
74   147 157 168 168 157 177 177 168 191 191 177 190 190 191 199 199 190 198
75   207 208  28  28 207 206 205  99 204 204  99 116 116 204 203 203 116 147
76   147 203 202 202 147 168 168 202 192 192 168 191 191 192 200 200 191 199
77   202 192 201 201 192 200
78   19800.0  3200.0 18000.0  4000.0 16400.0  3200.0 15600.0  2400.0 15600.0  4000.0
```

79	15000.0	2600.0	15000.0	3000.0	14400.0	3200.0	14400.0	3600.0	14000.0	3600.0
80	14000.0	4000.0	13630.0	4000.0	13400.0	3000.0	12000.0	3800.0	19600.0	5000.0
81	17000.0	6000.0	14800.0	4600.0	14200.0	6000.0	13600.0	4750.0	13200.0	4800.0
82	13200.0	5400.0	12800.0	5600.0	12900.0	6000.0	12600.0	6000.0	11600.0	5200.0
83	9600.0	4200.0	7000.0	5000.0	4000.0	5000.0	19000.0	7200.0	13600.0	7000.0
84	12750.0	6600.0	12450.0	6600.0	12600.0	7200.0	12300.0	7400.0	12400.0	8000.0
85	12180.0	8000.0	11600.0	6400.0	11025.0	8000.0	9800.0	6600.0	18800.0	8800.0
86	16000.0	9000.0	13400.0	8200.0	13200.0	9200.0	12400.0	8600.0	12400.0	9200.0
87	12180.0	8600.0	12180.0	9200.0	12400.0	10000.0	12180.0	10000.0	11200.0	9200.0
88	9600.0	10000.0	6000.0	10000.0	17800.0	10400.0	16000.0	12000.0	13600.0	11000.0
89	12800.0	11900.0	12600.0	11000.0	12600.0	11600.0	12400.0	10800.0	11400.0	11000.0
90	14400.0	14000.0	14000.0	12600.0	13000.0	12600.0	13200.0	13400.0	13400.0	14000.0
91	12800.0	12300.0	13000.0	13100.0	13200.0	13800.0	12000.0	13000.0	10000.0	14000.0
92	16000.0	15000.0	14800.0	15400.0	13800.0	15400.0	13800.0	15900.0	13600.0	14800.0
93	13600.0	15200.0	13400.0	14400.0	12600.0	15200.0	7000.0	15000.0	15600.0	18000.0
94	15200.0	16800.0	14000.0	16200.0	14200.0	16850.0	14400.0	17600.0	14000.0	16600.0
95	14200.0	17300.0	14400.0	18000.0	13200.0	17200.0	10600.0	18000.0	15600.0	19000.0
96	15000.0	19600.0	15000.0	20000.0	14800.0	19000.0	14800.0	19400.0	14600.0	18200.0
97	14600.0	18650.0	13800.0	19400.0	8000.0	20000.0	4800.0	18000.0	15600.0	21700.0
98	15400.0	21000.0	15400.0	21500.0	15200.0	20400.0	15200.0	20800.0	14400.0	21400.0
99	12000.0	22000.0	16000.0	22000.0	16400.0	23000.0	16200.0	23800.0	16000.0	23000.0
100	15800.0	22400.0	15600.0	22200.0	15800.0	22820.0	16000.0	23600.0	15000.0	23000.0
101	5600.0	24000.0	17000.0	25000.0	16750.0	24200.0	16800.0	25800.0	16600.0	25200.0
102	16600.0	25620.0	16400.0	24500.0	16400.0	25000.0	16200.0	24300.0	15400.0	25000.0
103	13000.0	26000.0	9400.0	24400.0	17600.0	27400.0	17400.0	26200.0	17000.0	26600.0
104	17200.0	27300.0	17400.0	28000.0	16800.0	26400.0	17000.0	27100.0	17200.0	27800.0
105	16000.0	27000.0	18400.0	29800.0	18200.0	28600.0	17600.0	28600.0	17800.0	29400.0
106	17800.0	29800.0	17600.0	29150.0	17400.0	28500.0	16600.0	29000.0	14000.0	30000.0
107	10400.0	28400.0	6200.0	30000.0	18600.0	30600.0	18000.0	30100.0	18200.0	30800.0
108	19000.0	31800.0	18400.0	31500.0	18400.0	31950.0	18200.0	31200.0	18000.0	30550.0
109	17200.0	31000.0	11200.0	32000.0	19600.0	33800.0	19400.0	32800.0	19000.0	33550.0
110	19000.0	34000.0	18800.0	32800.0	18800.0	33300.0	18600.0	32200.0	18600.0	32600.0
111	17600.0	32800.0	15000.0	34000.0	8000.0	34000.0	20200.0	36000.0	20000.0	35200.0
112	19600.0	35600.0	19400.0	35000.0	19400.0	35600.0	19200.0	34300.0	19200.0	34800.0
113	18200.0	34800.0	12000.0	36000.0	20200.0	37800.0	20000.0	37000.0	20000.0	37600.0
114	19800.0	36350.0	19800.0	36850.0	19600.0	36200.0	18800.0	36400.0	19000.0	37600.0
115	16800.0	38000.0	20200.0	38200.0	19800.0	38600.0	19000.0	39600.0	14000.0	40000.0
116	10000.0	39000.0	6000.0	39000.0	19600.0	41000.0	17000.0	41000.0	20000.0	42600.0
117	20600.0	44000.0	18600.0	44000.0	14600.0	44000.0	12000.0	44000.0	7000.0	44000.0

```
118      2000.0 44000.0  2000.0 36000.0  2000.0 27000.0  2000.0 21000.0  2000.0 14000.0
119      2000.0  8000.0  2000.0  2000.0  6000.0  2000.0  9000.0  2000.0 12000.0  2000.0
120     14000.0  2000.0 15600.0  2000.0 16000.0  2000.0 17600.0  2000.0 20000.0  2000.0
121     21400.0  2000.0 21200.0  3400.0 21000.0  4000.0 20900.0  5800.0 20600.0  7000.0
122     20370.0  8600.0 20000.0  9400.0 19000.0 11200.0 17530.0 14000.0 17170.0 15000.0
123     16750.0 17000.0 16500.0 18000.0 16000.0 20000.0 15900.0 20450.0 15600.0 20800.0
124     16000.0 21260.0 16460.0 22400.0 16800.0 23300.0 17100.0 24000.0 17600.0 25600.0
125     18000.0 26800.0 18360.0 28000.0 18700.0 29200.0 19000.0 30000.0 19360.0 31200.0
126     19730.0 32400.0 20000.0 33260.0 20400.0 34800.0 20550.0 36600.0 20550.0 37200.0
127     20400.0 37800.0 20380.0 38150.0 20310.0 38600.0 20300.0 39000.0 20500.0 40000.0
128     21010.0 41400.0 21450.0 43200.0 21450.0 44000.0
129       .000200   .000100   .000200   .000100   .000200   .000100   .000200   .000100
130       .000200   .000100   .000200   .000100   .000200   .000100   .000200   .000100
131       .000200   .000100   .000200   .000100   .000200   .000100   .000200   .000100
132       .000200   .000100   .000200   .000100   .000200   .000100   .000200   .000100
133       .000200   .000100   .000200   .000100   .000200   .000100   .000200   .000100
134       .000200   .000100   .000200   .000100   .000200   .000100   .000200   .000100
135       .000200   .000100   .000200   .000100   .000200   .000100   .000200   .000100
136       .000200   .000100   .000200   .000100   .000200   .000100   .000200   .000100
137       .000200   .000100   .000200   .000100   .000200   .000100   .000200   .000100
138       .000200   .000100   .000200   .000100   .000200   .000100   .000200   .000100
139       .000200   .000100   .000200   .000100   .000200   .000100   .000200   .000100
140       .000200   .000100   .000200   .000100   .000200   .000100   .000200   .000100
141       .000200   .000100   .000200   .000100   .000200   .000100   .000200   .000100
142       .000200   .000100   .000200   .000100   .000200   .000100   .000200   .000100
143       .000200   .000100   .000200   .000100   .000200   .000100   .000200   .000100
144       .000200   .000100   .000200   .000100   .000200   .000100   .000200   .000100
145       .000200   .000100   .000200   .000100   .000200   .000100   .000200   .000100
146       .000200   .000100   .000200   .000100   .000200   .000100   .000200   .000100
147       .000200   .000100   .000200   .000100   .000200   .000100   .000200   .000100
148       .000200   .000100   .000200   .000100   .000200   .000100   .000200   .000100
149       .000200   .000100   .000200   .000100   .000200   .000100   .000200   .000100
150       .000200   .000100   .000200   .000100   .000200   .000100   .000200   .000100
151       .000200   .000100   .000200   .000100   .000200   .000100   .000200   .000100
152       .000200   .000100   .000200   .000100   .000200   .000100   .000200   .000100
153       .000200   .000100   .000200   .000100   .000200   .000100   .000200   .000100
154       .000200   .000100   .000200   .000100   .000200   .000100   .000200   .000100
155       .000200   .000100   .000200   .000100   .000200   .000100   .000200   .000100
156       .000200   .000100   .000200   .000100   .000200   .000100   .000200   .000100
```

157	.000200	.000100	.000200	.000100	.000200	.000100	.000200	.000100
158	.000200	.000100	.000200	.000100	.000200	.000100	.000200	.000100
159	.000200	.000100	.000200	.000100	.000200	.000100	.000200	.000100
160	.000200	.000100	.000200	.000100	.000200	.000100	.000200	.000100
161	.000200	.000100	.000200	.000100	.000200	.000100	.000200	.000100
162	.000200	.000100	.000200	.000100	.000200	.000100	.000200	.000100
163	.000200	.000100	.000200	.000100	.000200	.000100	.000200	.000100
164	.000200	.000100	.000200	.000100	.000200	.000100	.000200	.000100
165	.000200	.000100	.000200	.000100	.000200	.000100	.000200	.000100
166	.000200	.000100	.000200	.000100	.000200	.000100	.000200	.000100
167	.000200	.000100	.000200	.000100	.000200	.000100	.000200	.000100
168	.000200	.000100	.000200	.000100	.000200	.000100	.000200	.000100
169	.000200	.000100	.000005	.000001	.000005	.000001	.000005	.000001
170	.000005	.000001	.000005	.000001	.000005	.000001	.000005	.000001
171	.000005	.000001	.000005	.000001	.000005	.000001	.000005	.000001
172	.000005	.000001	.000005	.000001	.000005	.000001	.000005	.000001
173	.000005	.000001	.000005	.000001	.000005	.000001	.000005	.000001
174	.000005	.000001	.000005	.000001	.000005	.000001	.000005	.000001
175	.000005	.000001	.000005	.000001	.000005	.000001	.000005	.000001
176	.000005	.000001	.000005	.000001	.000005	.000001	.000005	.000001
177	.000005	.000001	.000005	.000001	.000005	.000001	.000005	.000001
178	.000005	.000001	.000005	.000001	.000005	.000001	.000005	.000001
179	.000005	.000001	.000005	.000001	.000005	.000001	.000005	.000001
180	.000005	.000001	.000005	.000001	.000005	.000001	.000005	.000001
181	.000005	.000001	.000005	.000001	.000005	.000001	.000005	.000001
182	.000005	.000001	.000005	.000001	.000005	.000001	.000005	.000001
183	.000005	.000001	.000005	.000001	.000005	.000001	.000005	.000001
184	.000005	.000001	.000005	.000001	.000005	.000001	.000005	.000001
185	.000005	.000001	.000005	.000001	.000005	.000001	.000005	.000001
186	.000005	.000001	.000005	.000001	.000005	.000001	.000005	.000001
187	.000005	.000001	.000005	.000001	.000005	.000001	.000005	.000001
188	.000005	.000001	.000005	.000001	.000005	.000001	.000005	.000001
189	.000005	.000001	.000005	.000001	.000005	.000001	.000005	.000001
190	.000005	.000001	.000005	.000001	.000005	.000001	.000005	.000001
191	.000005	.000001	.000005	.000001	.000005	.000001	.000005	.000001
192	.000005	.000001	.000005	.000001	.000005	.000001	.000005	.000001
193	.000005	.000001	.000005	.000001	.000005	.000001	.000005	.000001
194	.000005	.000001	.000005	.000001	.000005	.000001	.000005	.000001
195	.000005	.000001	.000005	.000001	.000005	.000001	.000005	.000001

196	.000200	.000100	.000200	.000100	.000200	.000100	.000200	.000100
197	.000200	.000100	.000200	.000100	.000200	.000100	.000200	.000100
198	.000200	.000100	.000200	.000100	.000200	.000100	.000200	.000100
199	.000200	.000100	.000200	.000100	.000200	.000100	.000200	.000100
200	.000200	.000100	.000200	.000100	.000200	.000100	.000200	.000100
201	.000200	.000100	.000200	.000100	.000200	.000100	.000200	.000100
202	.000200	.000100	.000200	.000100	.000200	.000100	.000200	.000100
203	.000200	.000100	.000200	.000100	.000200	.000100	.000200	.000100
204	.000200	.000100	.000200	.000100	.000200	.000100	.000200	.000100
205	.000200	.000100	.000200	.000100	.000200	.000100	.000200	.000100
206	.000200	.000100	.000200	.000100	.000200	.000100	.000200	.000100
207	.000200	.000100	.000200	.000100	.000200	.000100	.000200	.000100
208	.000200	.000100	.000200	.000100	.000200	.000100	.000200	.000100
209	.000200	.000100	.000200	.000100	.000200	.000100	.000200	.000100
210	.000200	.000100	.000200	.000100	.000200	.000100	.000200	.000100
211	.000200	.000100	.000200	.000100	.000200	.000100	.000200	.000100
212	.000200	.000100	.000200	.000100	.000200	.000100	.000200	.000100
213	.000200	.000100	.000200	.000100	.000200	.000100	.000200	.000100
214	.000200	.000100	.000200	.000100	.000200	.000100	.000200	.000100
215	.000200	.000100	.000200	.000100	.000200	.000100	.000200	.000100
216	.000200	.000100	.000200	.000100	.000200	.000100	.000200	.000100
217	.000200	.000100	.000200	.000100	.000200	.000100	.000200	.000100
218	.000200	.000100	.000200	.000100	.000200	.000100	.000200	.000100
219	.000200	.000100	.000200	.000100	.000200	.000100	.000200	.000100
220	.000200	.000100	.000200	.000100	.000200	.000100	.000200	.000100
221	.000200	.000100	.000200	.000100	.000200	.000100	.000200	.000100
222	.000200	.000100	.000200	.000100	.000200	.000100	.000200	.000100
223	.000200	.000100	.000200	.000100	.000200	.000100	.000200	.000100
224	.000200	.000100	.000200	.000100	.000200	.000100	.000200	.000100
225	.000200	.000100	.000200	.000100	.000200	.000100	.000200	.000100
226	.000200	.000100	.000200	.000100	.000200	.000100	.000200	.000100
227	.000200	.000100	.000200	.000100	.000200	.000100	.000200	.000100
228	.000200	.000100	.000200	.000100	.000200	.000100	.000200	.000100
229	.000200	.000100	.000200	.000100	.000200	.000100	.000200	.000100
230	.000200	.000100	.000200	.000100	.000200	.000100	.000200	.000100
231	.000200	.000100	.000200	.000100	.000200	.000100	.000200	.000100
232	.000200	.000100	.000200	.000100	.000200	.000100	.000200	.000100
233	.000200	.000100	.000200	.000100	.000200	.000100	.000200	.000100
234	.000200	.000100	.000200	.000100	.000200	.000100	.000200	.000100

235	.000200	.000100	.000200	.000100	.000200	.000100	.000200	.000100						
236	.000200	.000100	.000200	.000100	.000200	.000100	.000200	.000100						
237	.000200	.000100	.000200	.000100	.000200	.000100	.000200	.000100						
238	.000200	.000100	.000200	.000100	.000200	.000100	.000200	.000100						
239	.000200	.000100	.000200	.000100	.000200	.000100	.000200	.000100						
240	.000200	.000100	.000200	.000100										
241	0.0	0.0	0.0	0.0	0.0	0.0	0.0	0.0	0.0	0.0	0.0	0.0	0.0	0.0
242	0.0	0.0	0.0	0.0	0.0	0.0	0.0	0.0	0.0	0.0	0.0	0.0	0.0	0.0
243	0.0	0.0	0.0	0.0	0.0	0.0	0.0	0.0	0.0	0.0	0.0	0.0	0.0	0.0
244	0.0	0.0	0.0	0.0	0.0	0.0	0.0	0.0	0.0	0.0	0.0	0.0	0.0	0.0
245	0.0	0.0	0.0	0.0	0.0	0.0	0.0	0.0	0.0	0.0	0.0	0.0	0.0	0.0
246	0.0	0.0	0.0	0.0	0.0	0.0	0.0	0.0	0.0	0.0	0.0	0.0	0.0	0.0
247	0.0	0.0	0.0	0.0	0.0	0.0	0.0	0.0	0.0	0.0	0.0	0.0	0.0	0.0
248	0.0	0.0	0.0	0.0	0.0	0.0	0.0	0.0	0.0	0.0	0.0	0.0	0.0	0.0
249	0.0	0.0	0.0	0.0	0.0	0.0	0.0	0.0	0.0	0.0	0.0	0.0	0.0	0.0
250	0.0	0.0	0.0	0.0	0.0	0.0	0.0	0.0	0.0	0.0	0.0	0.0	0.0	0.0
251	0.0	0.0	0.0	0.0	0.0	0.0	0.0	0.0	0.0	0.0	0.0	0.0	0.0	0.0
252	0.0	0.0	0.0	0.0	0.0	0.0	0.0	0.0	0.0	0.0	0.0	0.0	0.0	0.0
253	0.0	0.0	0.0	0.0	0.0	0.0	0.0	0.0	0.0	0.0	0.0	0.0	0.0	0.0
254	0.0	0.0	0.0	0.0	0.0	0.0	0.0	0.0	0.0	0.0	0.0	0.0	0.0	0.0
255	0.0	0.0	0.0	0.0	0.0	0.0	0.0	0.0	0.0	0.0	0.0	0.0	0.0	0.0
256	0.0	0.0	0.0	0.0	0.0	0.0	0.0	0.0	0.0	0.0	0.0	0.0	0.0	0.0
257	0.0	0.0	0.0	0.0	0.0	0.0	0.0	0.0	0.0	0.0	0.0	0.0	0.0	0.0
258	0.0	0.0	0.0	0.0	0.0	0.0	0.0	0.0	0.0	0.0	0.0	0.0	0.0	0.0
259	0.0	0.0	0.0	0.0	0.0	0.0	0.0	0.0	0.0	0.0	0.0	0.0	0.0	0.0
260	0.0	0.0	0.0	0.0	0.0	0.0	0.0	0.0	0.0	0.0	0.0	0.0	0.0	0.0
261	0.0	0.0	0.0	0.0	0.0	0.0	0.0	0.0	0.0	0.0	0.0	0.0	0.0	0.0
262	0.0	0.0	0.0	0.0	0.0	0.0	0.0	0.0	0.0	0.0	0.0	0.0	0.0	0.0
263	0.0	0.0	0.0	0.0	0.0	0.0	0.0	0.0	0.0	0.0	0.0	0.0	0.0	0.0
264	0.0	0.0	0.0	0.0	0.0	0.0	0.0	0.0	0.0	0.0	0.0	0.0	0.0	0.0
265	0.0	0.0	0.0	0.0	0.0	0.0	0.0	0.0	0.0	0.0	0.0	0.0	0.0	0.0
266	0.0	0.0	0.0	0.0	0.0	0.0	0.0	0.0	0.0	0.0	0.0	0.0	0.0	0.0
267	0.0	0.0	0.0	0.0	0.0	0.0	0.0	0.0	0.0	0.0	0.0	0.0	0.0	0.0
268	0.0	0.0	0.0	0.0	0.0	0.0	0.0	0.0	0.0	0.0	0.0	0.0	0.0	0.0
269	0.0	0.0	0.0	0.0	0.0	0.0	0.0	0.0	0.0	0.0	0.0	0.0	0.0	0.0
270	0.0	0.0	0.0	0.0	0.0	0.0	0.0	0.0	0.0	0.0	0.0	0.0	0.0	0.0
271	0.0	0.0	0.0	0.0	0.0	0.0	0.0	0.0	0.0	0.0	0.0	0.0	0.0	0.0
272	0.0	0.0	0.0	0.0	0.0	0.0	0.0	0.0	0.0	0.0	0.0	0.0	0.0	0.0
273	0.0	0.0	0.0	0.0	0.0	0.0	0.0	0.0	0.0	0.0	0.0	0.0	0.0	0.0

274	0.0	0.0	0.0	0.0	0.0	0.0	0.0	0.0	0.0	0.0	0.0	0.0
275	0.0	0.0	0.0	0.0								
276	0.00	0.00	0.00	0.00	0.00	0.00	0.00	0.00	0.00	0.00		
277	0.00	0.00	0.00	0.00	0.00	0.00	0.00	0.00	0.00	0.00		
278	0.00	0.00	0.00	0.00	0.00	0.00	0.00	0.00	0.00	0.00		
279	0.00	0.00	0.00	0.00	0.00	0.00	0.00	0.00	0.00	0.00		
280	0.00	0.00	0.00	0.00	0.00	0.00	0.00	0.00	0.00	0.00		
281	0.00	0.00	0.00	0.00	0.00	0.00	0.00	0.00	0.00	0.00		
282	0.00	0.00	0.00	0.00	0.00	0.00	0.00	0.00	0.00	0.00		
283	0.00	0.00	0.00	0.00	0.00	0.00	0.00	0.00	0.00	0.00		
284	0.00	0.00	0.00	0.00	0.00	0.00	0.00	0.00	0.00	0.00		
285	0.00	0.00	0.00	0.00	0.00	0.00	0.00	0.00	0.00	0.00		
286	0.00	0.00	0.00	0.00	0.00	0.00	0.00	0.00	0.00	0.00		
287	0.00	0.00	0.00	0.00	0.00	0.00	0.00	0.00	0.00	0.00		
288	0.00	0.00	0.00	0.00	0.00	0.00	0.00	0.00	0.00	0.00		
289	0.00	0.00	0.00	0.00	0.00	0.00	0.00	0.00	0.00	0.00		
290	0.00	0.00	0.00	0.00	0.00	0.00	0.00	0.00	0.00	0.00		
291	0.00	0.00	0.00	0.00	0.00	0.00	0.00	0.00	0.00	0.00		
292	0.00	0.00	0.00	0.00	0.00	0.00	0.00	0.00	0.00	0.00		
293	0.00	0.00	0.00	0.00	0.00	0.00	0.00	0.00	0.00	0.00		
294	0.00	0.00	0.00	0.00	0.00	0.00	0.00	0.00	0.00	0.00		
295	0.00	0.00	0.00	0.00	0.00	0.00	0.00	0.00	0.00	0.00		
296	0.00	0.00	0.00	0.00	0.00	0.00	0.00	0.00	0.00	0.00		
297	0.00	0.00	0.00	0.00	0.00	0.00	0.00	0.00	0.00	0.00		
298	0.00	0.00	0.00	0.00	0.00	0.00	0.00	0.00	0.00	0.00		
299	0.00	0.00	0.00	0.00	0.00	0.00	0.00	0.00	0.00	0.00		
300	0.00	0.00	0.00	0.00	0.00	0.00	0.00	0.00	0.00	0.00		
301	0.00	0.00	0.00	0.00	0.00	0.00	0.00	0.00	0.00	0.00		
302	0.00	0.00	0.00	0.00	0.00	0.00	0.00	0.00	0.00	0.00		
303	0.00	0.00	0.00	0.00	0.00	0.00	0.00	0.00	0.00	0.00		
304	0.00	0.00	0.00	0.00	0.00	0.00	0.00	0.00	0.00	0.00		
305	0.00	0.00	0.00	0.00	0.00	0.00	0.00	0.00	0.00	0.00		
306	0.00	0.00	0.00	0.00	0.00	0.00	0.00	0.00	0.00	0.00		
307	0.00	0.00	0.00	0.00	0.00	0.00	0.00	0.00	0.00	0.00		
308	0.00	0.00	0.00	0.00	0.00	0.00	0.00	0.00	0.00	0.00		
309	0.00	0.00	0.00	0.00	0.00	0.00	0.00	0.00	0.00	0.00		
310	0.00	0.00	0.00	0.00	0.00	0.00	0.00	0.00	0.00	0.00		
311	0.00	0.00	0.00	0.00	0.00	0.00	0.00	0.00	0.00	0.00		
312	0.00	0.00	0.00	0.00	0.00	0.00	0.00	0.00	0.00	0.00		

```
313        0.00     0.00     0.00     0.00     0.00     0.00     0.00     0.00     0.00     0.00
314        0.00     0.00     0.00     0.00     0.00     0.00     0.00     0.00     0.00     0.00
315        0.00     0.00     0.00     0.00     0.00     0.00     0.00     0.00     0.00     0.00
316        0.00     0.00     0.00     0.00     0.00     0.00     0.00     0.00     0.00     0.00
317        0.00     0.00     0.00     0.00     0.00     0.00     0.00     0.00     0.00     0.00
318        0.00     0.00     0.00     0.00     0.00     0.00     0.00     0.00     0.00     0.00
319        0.00     0.00     0.00     0.00     0.00     0.00     0.00     0.00     0.00     0.00
320        0.00     0.00     0.00     0.00     0.00     0.00
321  -40.0-40.0-40.0-40.0-40.0-40.0-27.0-27.0-12.0-12.0  0.0 10.0 16.0 16.0 16.0 16.0
322   16.0 16.0 16.0 16.0 16.0 16.0 16.0 16.0 16.0 16.0 16.0-40.0-40.0-40.0-33.0-33.0
323  -23.0-23.0-10.0 13.0 16.0 16.0 16.0 16.0 16.0 16.0-40.0-40.0-40.0-40.0-25.0-15.0
324  -13.0 -5.0  0.0 11.0-40.0-40.0-40.0-40.0-40.0-40.0-26.0-21.0-21.0-20.0-20.0-12.0
325  -12.0-12.0 -8.0 -4.0 -4.0  0.0  0.0  4.0  7.0 16.0 16.0 16.0 16.0 16.0 16.0 16.0
326   16.0 16.0 16.0 16.0 16.0 16.0 16.0 16.0 16.0 16.0 16.0 16.0 16.0 16.0 16.0 16.0
327   16.0 16.0 16.0 16.0 16.0 16.0 16.0 16.0 16.0 16.0 16.0 16.0 16.0 16.0 16.0 16.0
328   16.0 16.0 16.0 16.0 16.0 16.0 16.0 16.0 16.0 16.0 16.0 16.0 16.0 16.0 16.0 16.0
329   16.0 16.0 16.0 16.0 16.0 16.0 16.0 16.0 16.0 16.0 16.0 16.0 16.0 16.0 16.0 16.0
330   16.0 16.0 16.0 16.0 16.0 16.0 16.0 16.0 16.0 16.0 16.0 16.0 16.0 16.0 16.0 16.0
331   16.0-40.0-40.0-40.0-40.0-40.0-40.0-40.0-40.0-27.0-27.0-27.0-27.0-27.0-27.0-12.0
332  -12.0-12.0-12.0-12.0-12.0  0.0  0.0  0.0  0.0  0.0  0.0 16.0 16.0 16.0 16.0 16.0
333   16.0 16.0 16.0 16.0 16.0 16.0 16.0 16.0 16.0 16.0 16.0 16.0 16.0 16.0 16.0 16.0
334   16.0 16.0 16.0 16.0 16.0 16.0 16.0 16.0 16.0 16.0 16.0 16.0 16.0 16.0 16.0 16.0
335   16.0 16.0 16.0 16.0 16.0 16.0 16.0 16.0 16.0 16.0 16.0 16.0 16.0 16.0 16.0 16.0
336   16.0 16.0 16.0 16.0 16.0 16.0 16.0 16.0 16.0 16.0 16.0 16.0 16.0 16.0 16.0 16.0
337   16.0 16.0 16.0 16.0 16.0 16.0 16.0 16.0 16.0 16.0 16.0 16.0-40.0-40.0-40.0-40.0
338  -40.0-40.0-27.0-27.0-27.0-27.0-27.0-12.0-12.0-12.0-12.0  0.0  0.0  0.0  0.0  0.0
339   16.0 16.0 16.0 16.0 16.0 16.0 16.0 16.0 16.0 16.0 16.0 16.0 16.0 16.0 16.0 16.0
340   16.0 16.0 16.0 16.0 16.0 16.0 16.0 16.0 16.0 16.0 16.0 16.0 16.0 16.0 16.0 16.0
341   16.0 16.0 16.0 16.0 16.0 16.0 16.0 16.0 16.0 16.0 16.0 16.0 16.0 16.0 16.0 16.0
342   16.0 16.0 16.0 16.0 16.0 16.0 16.0 16.0 16.0 16.0 16.0 16.0 16.0 16.0 16.0 16.0
343   16.0 16.0-30.0-30.0-30.0-30.0-15.0-15.0-10.0-10.0  0.0  0.0 10.0 16.0 16.0 16.0
344   16.0 16.0 16.0 16.0 16.0 16.0 16.0 16.0 16.0 16.0 16.0 16.0 16.0 16.0 16.0 16.0
345   16.0 16.0 16.0 16.0 16.0 16.0 16.0 16.0-15.0-15.0 -8.0 -8.0  7.0  7.0 16.0 16.0
346   16.0 16.0 16.0 16.0 16.0 16.0 16.0 16.0 16.0 16.0 16.0 16.0 16.0-25.0-25.0-13.0
347   -8.0  0.0  7.0 16.0 16.0 16.0 16.0 16.0 16.0 16.0 16.0 16.0 16.0 16.0 16.0 16.0
348  -25.0-10.0 10.0 16.0 16.0 16.0 16.0 16.0 16.0 16.0 16.0 16.0 16.0 16.0
349   16000.0 16500.0 17000.0 17500.0 18000.0 18500.0 19000.0 19500.0 20000.0 20500.0
350   21000.0
```

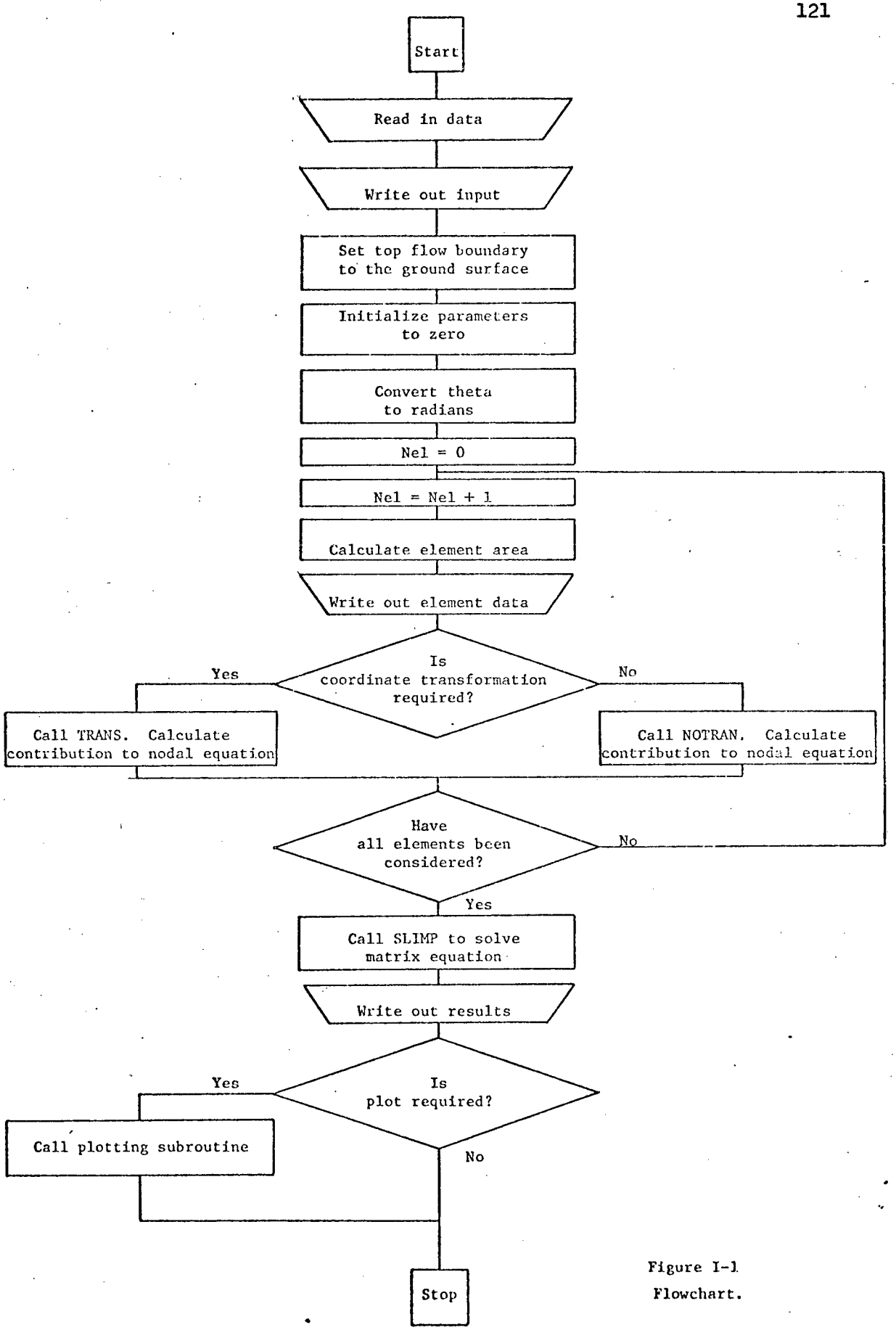

Figure I-1. Flowchart.

APPENDIX II

FIGURES FOR CHAPTER FIVE

(Stored in separate case.)